Conodonts, Reef evolution and Mass extinction across Permian-Triassic Boundary

Wu Ya Sheng

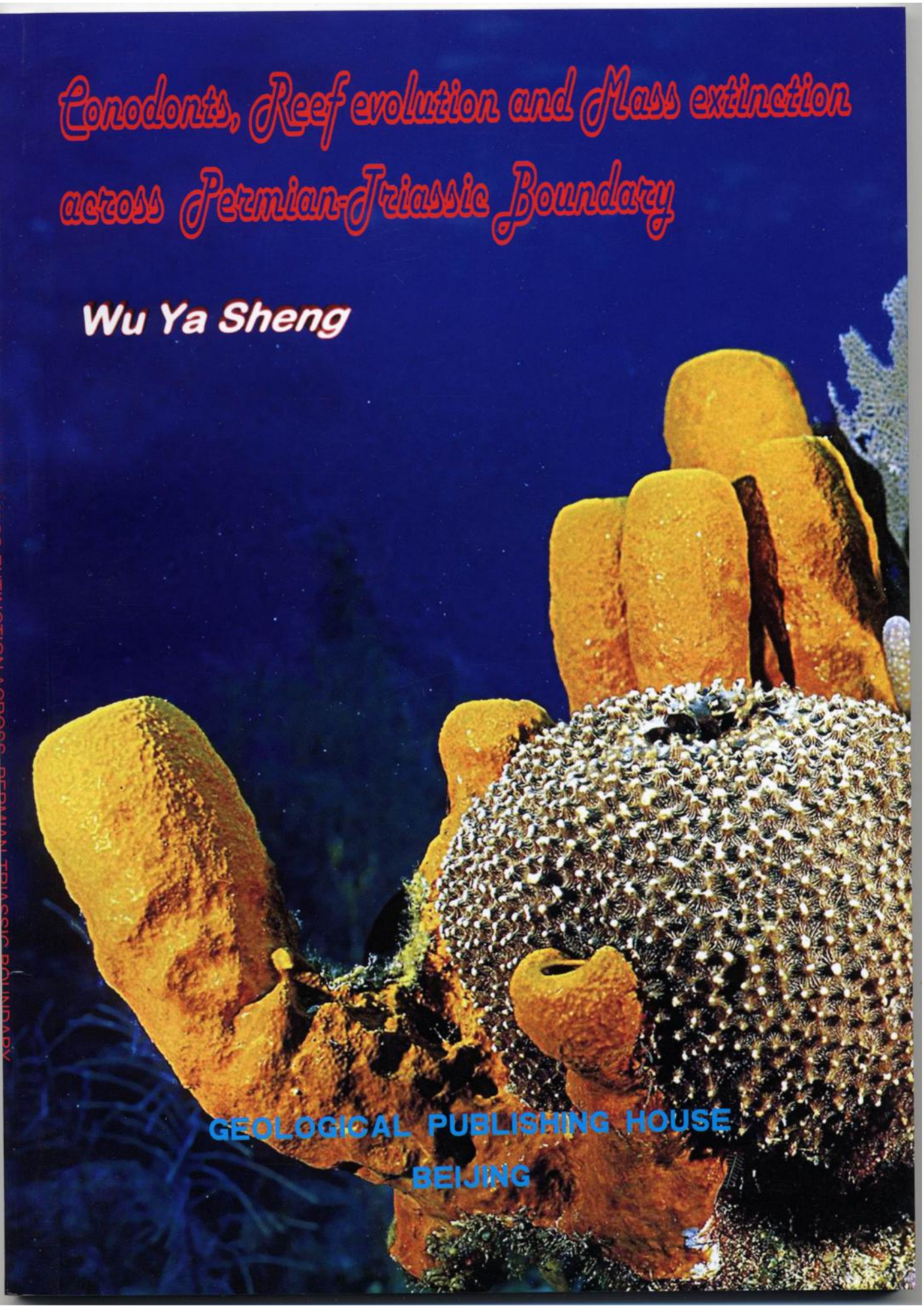

GEOLOGICAL PUBLISHING HOUSE
BEIJING

CONODONTS, REEF EVOLUTION AND MASS EXTINCTION ACROSS PERMIAN-TRIASSIC BOUNDARY

Program Supported by NSF China Grant 40472015

Conodonts, Reef Evolution, and Mass Extinction across Permian-Triassic Boundary

Wu Ya Sheng

Geological Publishing House

Beijing, China

Copy Editor: Sun Yayun

First edition 2005

Cataloging in Publication Data
Conodonts, Reefs, and Mass Extinction across Permian-Triassic Boundary/Wu Yasheng
-Beijing: Geological Publishing House, 2005-5-31
ISBN 7-116-04442-6/Q•24
I. Permian… II. Wu… III. Permian-Triassic-Conodont research IV. Q959.281

Published and distributed by Geological Publishing House

Address: Geological Publishing House, No. 31, Xueyuan Road,
Haidian District, Beijing, P.R. C., 100083
Tel: 86-010-82324573, 86-010-82324508
Fax: 86-010-82310759

Preface

Permian-Triassic transition is a very unusual period of Earth's history, when the largest mass extinction of the Phanerozoic occurred. Many Permian-Triassic boundary (PTB) sections are studied to deal with the biotic evolution and environmental change during this period. Correlation of different PTB sections needs a high-resolution conodont biostratigraphic standard.

Thanks to great work on conodonts of PTB sections such as those on Meishan, Shangsi, Kashmir, and Selong sections by C. Y. Wang, K. X. Zhang, S. L. Mei, Z. S. Li, T. Matsuda, M. J. Orchard, R. S. Nicoll, B. R. Wardlaw, H. Kozur, and others, conodonts of these PTB sections were systematically and profoundly studied, and, due to contribution by H. F. Yin, conodont zones for this period have been established. Due to the contribution of Yin Hongfu, Jin Yugan, and many other researchers, Meishan section has been ratified as the GSSP of the PTB. The conodont zones of Meishan section reasonably become the standard for correlation of PTB sections.

As I made a correlation between a PTB section in Ziyun, Guizhou Province and the Meishan section, I found that some conodonts from the Meishan sections and Kashmir sections are incorrectly identified, which would reduce the reliability of the conodont zone standard, and the accuracy of the correlation. So, a revision on the conodonts from these PTB sections is needed.

As the first part of this work, I checked all conodonts from the PTB sections of Meishan, Shangsi, and Kashmir, and corrected those incorrectly identified. After that, I revised the conodont zones of the P-T transition (Beds 24e to 28 of Meishan section).

An inevitable question about the biotic evolution during the P-T transition is did any Permian reef persist into the Triassic and did any Permian reef-building organism persist into the Triassic. Previous studies on P-T transitional biotic evolution involve almost all marine invertebrate groups but not reef-building calcareous sponges (sponges with calcareous skeleton, including thalamid sponges and inozoans). Permian major reef-building organisms include thalamid sponges, inozoans, and sclerosponges. Of them, thalamid sponges are the most studied, which makes it possible to study the evolution of thalamid sponges across P-T boundary.

In the second part of this work, using an approximate method ("reef representatives"), we determine the distribution areas of reefs in different periods of the Permian and Triassic Periods, and analyzed the evolution of reefs in the Permian and Triassic. In the third part, on the basis of revision of all thalamid sponges from the Permian and Triassic reefs, we compared the thalamid sponges of different periods of the Permian and Triassic at specific level and discussed their evolution. In the last part, we discussed the ecological selection in the end-Permian mass

extinction of marine invertebrate groups and terrestrial plants. On the basis of evidence from different disciplines, especially oxygen isotopic evolution of sea water, global sea-level changes, and ecological selection in the mass extinction, we discussed the possible cause of the end-Permian mass extinctions.

This study was supported by the NSF China Grant 40472015 and 40172007, Academia Sinica Grant K2951-B1-409 (to Jin Yugan), and Mineralogical and Resource Center, Chinese Academy of Science. C. Y. Wang discussed with me about the assignment of each conodont material and gave very helpful ideas. Shen Shuzhong gave much help in collecting documents and a lot of helpful information. J. S. Fan and Y. G. Jin gave me directions as I made study on reef evolution and thalamid sponge evolution. My special thanks are due to them. I sincerely thank J. Y. Rong, H. F. Yin, B. Luan, Y. Wang, W. Wang, Q. H. Shang, W. Z. Li, S. L. Mei, and S. G. Tian for their help in my studies.

Wu, Ya Sheng
Institute of Geology and Geophysics,
Chinese Academy of Science,
Beijing 100029, China
wys@mail.igcas.ac.cn
2004.12.10

Contents

1 Conodonts and Conodont Zones across the Permian-Triassic Boundary: the GSSP and Related Sections

Abstract Conodonts from Meishan sections (the Permian-Triassic boundary GSSP) and previous candidates for GSSP, Shangsi section, Sichuan Province and Guryul Ravine section, Kashmir, were checked and those incorrectly assigned were corrected. The following twenty new species are erected in this study: *Clarkina paradeflecta* sp. nov., *C. elliptica* sp. nov., *C. columnaris* sp. nov., *C. anisomerus* sp. nov., *C. myridentalis* sp. nov., *C. plana* sp. nov., *C. redactus* sp. nov., *Hindeodus amblyodontus* sp. nov., *H. angustus* sp. nov., *H. arcuatus* sp. nov., *H. coalitus* sp. nov., *H. difformis* sp. nov., *H. irregularis* sp. nov., *H. proparvus* sp. nov., *H. scalaris* sp. nov., *H. scutatus* sp. nov., *H. similes* sp. nov., *H. limus* sp. nov., *H. pectinatus* sp. nov., and *H. zhejiangensis* sp. nov. Based on revised taxa, the conodont zones of PTB interval have been revised. After revision, Beds 24e~25, 26, 27a～27b, 27c～27d, and 28 of Meishan sections were defined as *Clarkina yini* zone, *C. meishanensis* zone, *Hindeodus changxingensis* zone, *H. parvus* zone, and *Isarcicella staeschei* zone, respectively.

1.1 Introduction

The time around the Permian-Triassic boundary was a very important epoch of Earth development, when a series of very impressive geological events happened: the mass extinction that has eliminated more than 90% of all marine species and 70% of terrestrial vertebrate genera, the Siberian flood-volcanic event, which has been interpreted as the most voluminous and explosive continental, volcanic event known in the Phanerozoic record, and the worldwide oceanic anoxia, which started in the deep marine areas in the Late Permian and expended to shallow-marine areas in the earliest Triassic. The study of all these events needs a high-resolution conodont biostratigraphic framework.

Well-known Permian-Triassic boundary sections include Meishan sections in Zhejiang Province, southeast China, Shangsi section in Sichuan Province, southwestern China, Guryul Ravine section in Kashmir (Fig. 1.1). Meishan sections include 8 sections located at the hill north to the road from Meishan town to Xinhuai village. In an eastward order, they are named as Sections G, A, B, C, F, D, E, Z, respectively. Besides, Nicoll et al. (2002) named a section 20 m west of Section A as Section AW. Among these sections, Section D is the most well studied, and has been ratified as the GSSP of the Permian-Triassic boundary in March, 2001 by IGU. For this

reason, the conodonts from Section D are the primary basis of conodont zones of PTB interval. In this study, PTB interval is defined as the stratigraphic interval from Bed 24e to Bed 28 of Meishan sections. To increase the applicability of the conodont zone standard, conodonts from other Meishan sections, Shangsi section and Kashmir section are used as supplements to Section D.

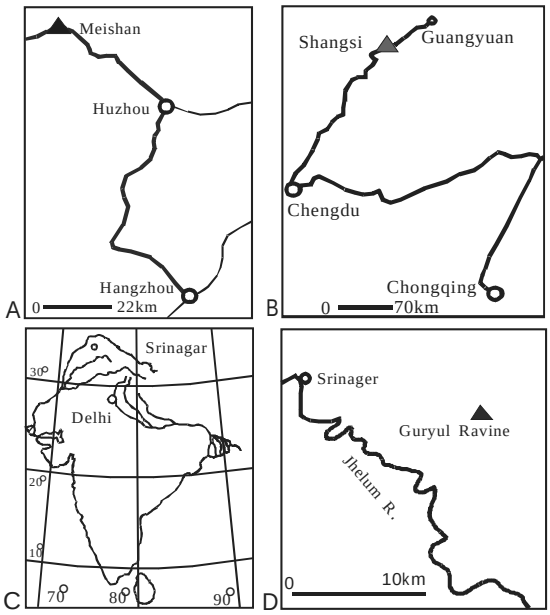

Fig. 1.1 Location PTB sections in Meishan (A), Shangsi (B), and Guryul Ravine(C, D).

Conodonts from these sections have been studied by many researchers (e.g., Matsuda, 1981; Li et al., 1989; Zhang et al., 1995; Wang, 1995; Zhang et al., 1996; Nicoll et al., 2002). Their results comprise the basis of conodont zones for P-T boundary interval. Many researchers contributed to the establishment of conodont zones for PTB interval (e.g., Zhang et al., 1995; Yin et al., 2001). The conodont zone division by Yin et al. (2001) is the latest one and will be focused on in the discussion.

As we identified the conodonts from a PTB section in Guizhou Province, southwestern China, we found that some conodonts from Meishan and Kashmir sections were incorrectly assigned by previous researchers. For example, the materials that were assigned to *Hindeodus typicalis* and *H. latidentatus* by Zhang et al. (1996) should be assigned to other species. Incorrect assignment of conodonts leads to wrong division of conodont zones. So, it is necessary to check the assignment of all conodonts from Meishan, Shangsi, and Kashmir sections, and correct the wrong assignments. After that, conodont zones for PTB interval should be corrected according to revised conodonts.

Disputes on assignment of some conodonts have been present. Some researchers tend to classify conodonts according to carina evolution. However, conodont classification can not be

done based on only one character: all important characters, especially outlines of platform and features of pulp cavity should be considered in identification. Due to very low conodont abundance in PTB interval, the use of carina evolution is limited in classification of PTB conodonts. Anyway, identification of all conodonts from PTB interval should be carried on with the same criteria. Even though the criteria are mainly morphological, the difference between one's materials and the holotype should be carefully evaluated to judge: the difference is intra-species, interspecies, or inter-subspecies?

This study discusses only the conodonts from PTB interval, which include only 4 genera: *Clarkina*, *Hindeodus*, *Isarcicella,* and *Neospathodus*. Most conodonts from PTB interval belong to the former two genera. The criteria for classification of the former two genera in this study include: (1) the outline of the whole element, (2) the features of carina, (3) the features of basal expansion. Generally, distinct differences in more than one aspect are interpreted as inter-species variations. Small differences in one aspect are interpreted as intra-species or inter-subspecies variations.

1.2 General features of the PTB sections and their correlations

At Section D, the uppermost Permian limestone of the Changxing Formation is separated from the Lowest Triassic marl of the Yinkeng Formation by two thin clay beds. In previous studies, the two clay beds were named as Beds 25 and 26. Bed 25 is white, several cm thick, probably of volcanic origin (Clark et al., 1986). The Changxing Formation has been divided as 23 beds, in ascending order, named as Beds 2 to 24. Bed 24 is divided as 5 subdivisions: Beds 24a to 24e, in ascending order. The Yinkeng Formation is divided as 12 beds, in ascending order, named as Beds 27 to 37. Bed 27 is divided as 27a, 27b, 27c, and 27d. The Permian-Triassic boundary has been regarded to lie in the interval from Bed 24e to Bed 28. So, this interval is regarded as the PTB interval.

Sections A, B, C, F, E, and G are all less than 2 km from Section D, all having two clay beds. With clay beds, they can be easily correlated to Section D. Section AW is about 20 m west of section A, and is easy to correlate to sections A and D.

The PTB interval of Section Z has different bed names. At this section, the two clay beds equivalent to Beds 25 and 26 of Section D have been named as 880 and 881, and the interval equivalent to Bed 27 of Section D were divided as 882-1, 882-2, 882-3, and 882-4, in ascending order. Both 882-4 of Section Z and Bed 27d of Section D yield conodont *Hindeodus parvus*, indicating that they are stratigraphically equivalent.

In the Shangsi section, the uppermost Permian (the Dalong Formation) and the overlying lowest Triassic (the Feixianguan Formation) have been divided as 35 litho- beds. In ascending order, they have been named as Beds 18 to 52. This section contains many clay beds. According to the clay beds, Bed 27 of this section is correlated to Bed 26 of Meishan Section D. Bed 31~32

yield *Hindeodus parvus*, and is correlated to Bed 27c-d of Meishan. Beds 29 to 30 are correlated to Beds 27a-b of Meishan. Bed 33 yields *Isarcicella staeschei*, and is correlated to Bed 28 of Meishan.

The PTB interval of Kashmir section has been divided as 10 beds: Beds 52 to 61, in ascending order. Beds 56 and 57 yield *Hindeodus parvus*, and are correlatve to Beds 27c and 27d of Meishan. This interval yields one material belonging to *I. staeschei*, indicating probable sedimentary mixing. The correlation between Meishan sections, Shangsi and Kashmir sections is shown in Table 1.1.

Table 1.1 Correlations between Meishan, Shangsi, and Kashmir sections

Sections G, A, B, C, F, D, E, AW of Meishan (Zhang et al., 1995; Mei et al., 1998; Nicoll et al., 2002)	**Section Z** of Meishan (Wang, 1995)	**Shangsi Section** (Zhang et al., 1984; Li et al., 1989)	**Guryul Ravine Section** of Kashmir (Matsuda, 1981; Murata, 1981)
28 (*I. staeschei*)		Gsc33 (*I. staeschei* and *I. isarcica*)	61 (*I. staeschei*)
27d (*H. parvus*)	882-4 (*H. parvus*)	Gsc32～Gsc31 (*H. parvus*)	56-57 (*H. parvus*)
27c (*H. parvus*)	882-3 (*H*. cf. *parvus*)		
27b	882-2	Gsc 29～Gsc30	55
27a	882-1		
26 (Upper claybed)	881 (Upper claybed)	Gsc27 (claybed)	
25 (Lower claybed)	880 (Lower claybed)		
24e			

1.3 Revisions on the conodonts from the PTB sections

In this section we discuss the features and assignment of all conodonts described from these PTB sections in ascending order of beds. The conodonts from Bed 24e are firstly discussed. Then, those from Beds 25, 26, 27a and 27b, 27c and 27b, and 28 are discussed in turn. When we discuss the conodonts from Bed 24e, those from Section D are discussed first, then those from other Meishan sections, and then those from Shangsi and Kashmir sections. Only the conodonts with figures are considered. For convenient reference to by later researchers, all conodonts are grouped into four plates (Figs.1.2~1.5) according to their occurrence beds. The conodonts from Beds 24e, 25 and 26 of Meishan and the equivalent beds are grouped in Fig. 1.2; those from Bed 27a, 27b and the equivalent beds are grouped in Fig. 1.3; those from Beds 27c, 27d and the equivalent beds are grouped in Fig. 1.4; and those from Bed 28 and the equivalent beds are grouped in Fig. 1.5. Each conodont in these figures is given a name, such as “Z2-11” (Fig. 1.2A, p.37). The following

discussion on the assignments of the conodonts begins with Fig. 1.2A from Bed 24e, and ends with the conodonts of Bed 28 in Fig. 1.5.

1.3.1 Conodonts from Bed 24e of Meishan and the equivalent beds

Zhang et al. (1995) described conodont Z2-11 (Fig. 1.2A) from Bed 24e of Section D, Meishan.

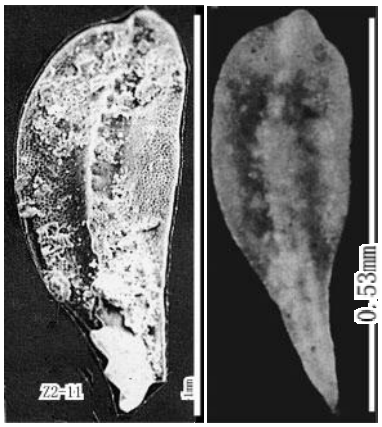

Z2-11: *Clarkina subcarinata* -Zhang et al., 1995, pl. 2, Fig. 11; Bed 24e, Section D. Right: Holotype of *C. subcarinata* (Sweet, 1973) -Teichet, Kummel & Sweet, 1973, pl. 13, Fig. 12. We use Z2-11 as holotype to define ***C. myridentalis* sp. nov**.

Z2-11 was placed in *Clarkina subcarinata* (Sweet). Compared to the holotype of this species, this specimen is larger, and more arched, and has more and bigger denticles, all denticles basally fused, with a proclined rather than reclined cusp, and anterior denticles radially arranged. This material cannot be placed in this species. We use it as holotype to define a new species, C. *myridentalis* sp. nov.

Mei et al. (1998) described conodonts 4L (Fig. 1.2B) and 4J (Fig. 1.2C) from Mc-43 (=Bed 24e) of Section D.

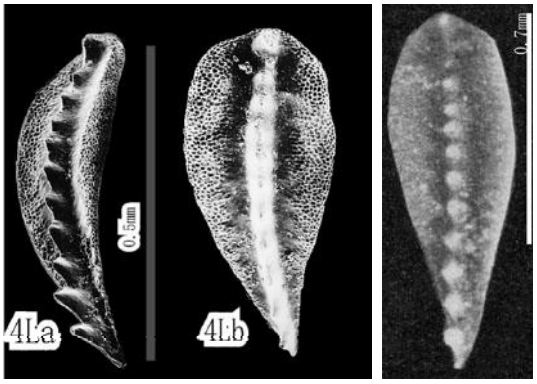

4L: *Clarkina changxingensis yini* Mei et al., 1998 -pl.4, figs.La,b; Bed 24e, Section D. Right: Holotype of *C. changxingensis* (Wang et Wang, 1981) -Wang & Wang, 1981, pl. 1, figs. 13, 16. We regard 4L as a species, ***C. yini*** Mei et al., 1998

4L was placed in *C. changxingensis yini* Mei et al. (1998). Compared to the holotype of *C.*

changxingensis, 4L is more arched, with reclined denticles in the same form and decreasing in size posteriorward, while in the holotype, the denticles are all erect. So, 4L cannot be placed in this species and this subspecies is promoted to a species: *C. yini* Mei et al. (1998) (grad nov.).

4J was placed in *C. deflecta* (Wang et Wang, 1981). 4J differs from the holotype of this species in the linguiform rather than rhombic posterior end of the platform. The carina in the latter abruptly turns right at the posterior end and is terminated at the posterior right angle. 4J cannot be placed in this species. 4J resembles the holotype of *C. parasubcarinata* Mei et al. (1998) very much in denticle pattern and platform outline. Thus, 4J is assigned to *C. parasubcarinata*.

4Ja,b: *C. deflecta* (Wang and Wang, 1981) - Mei et al., 1998, pl. 4, figs.Ja, Jb; Bed 24e, Section D; bar 0.5mm. 4Ia: Holotype of *C. parasubcarinata* Mei et al., 1998 -pl. 4, fig. Ia; bar 0.5mm. Right: Holotype of *C. deflecta* (Wang et Wang, 1981) –Wang & Wang, 1981, pl. 2, fig. 9. We think 4J belongs to ***C. parasubcarinata***.

Zhang et al. (1996) described conodont Y1-1 (Fig. 1.2D) from Bed 24e of Section G.

Y1-1 was placed in *Hindeodus typicalis* (Sweet). Y1-1 differs from the holotype of this species in its smaller cusp and different denticle pattern. The four posterior denticles in the former are much wider than the anterior denticles. Besides, the anterior face of the former is steeper. So, Y1-1 cannot be placed in this species. It resembles the holotype of *Hindeodus inflatus* Nicoll et al. (2002) (Fig. 1.2E) very much in blade shape, denticle pattern, and basal expansion shape, and is assigned to *Hindeodus inflatus*.

Y1-1: *H. typicalis* (Sweet) -Zhang et al., 1996, pl. 1, Fig. 1; Bed 24e, Section G; bar 0.2mm. Middle: Holotype of *H. inflatus* Nicoll et al., 2002 -pl. 10, Fig. 1; beds 25-26, Section D; bar 0.25mm. Right: Holotype of *H. typicalis* (Sweet, 1970); bar 0.26mm. We think Y1-1 belongs to ***H. inflatus***.

1.3.2 Conodonts from Bed 25 of Meishan and the equivalent beds

Nicoll et al. (2002) described conodont N10-1 (Fig. 1.2E) from Bed 25-26 of Section D.

N10-1 was used as holotype to define the species *Hindeodus inflatus* Nicoll et al. (2002). This species differs from *Hindeodus latidentatus* (Kozur, Mostler et Rahimi-Yazd, 1975) in that the cusp in the latter is less prominent, and basal expansion seems not to develop.

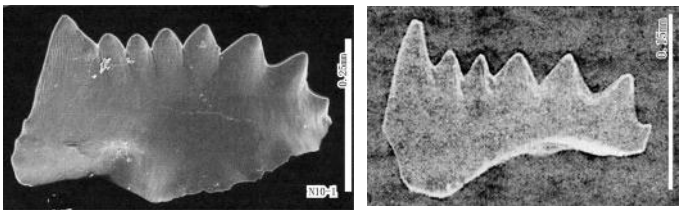

N10-1: Holotype of ***H. inflatus*** Nicoll et al., 2002 -pl. 10, Fig. 1, Bed 25-26, Section D; bar 0.25mm. Right: Holotype of *H. latidentatus* (Kozur, Mostler et Rahimi-Yazd, 1975).

Zhang et al. (1996) described conodont Zh7-3 (Fig. 1.2F) from Bed 25 of Section D.

Zh7-3 was placed in *C. changxingensis*. Zh7-3 differs from the holotype of this species in that the former has strongly upturned platform side edges, while the platform of the latter is relatively flat. Besides, they have different denticles. So, Zh7-3 cannot be assigned to this species. It seems to belong to a new species, and here is regarded as ***C.* sp. 1.**

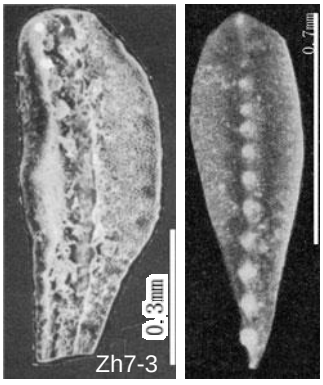

Zh7-3: *Clarkina changxingensis* -Zhang et al., 1996, pl.II.7, fig. 3; Bed 25, Section D. Right: Holotype of *C. changxingensis* (Wang & Wang, 1981), pl. 1, figs. 13, 16. We regard Zh7-3 as ***C.* sp.1.**

Zhang et al. (1995) described conodont Z2-3 (Fig. 1.2G) from Bed 25 of Section F.

Z2-3 was placed in *C. carinata* (Clark, 1959). The holotype of this species has a shrink at the posterior of the platform, while Z2-3 doesn't have. The platform is evenly arched in Z2-3, while the latter has a relatively flat platform posterior but an abruptly arched platform anterior. So, Z2-3 cannot be assigned to this species. Z2-3 resembles the holotype of *C. yini* (Fig. 1.2B) very much in platform shape and denticle pattern, and is placed in *C. yini*.

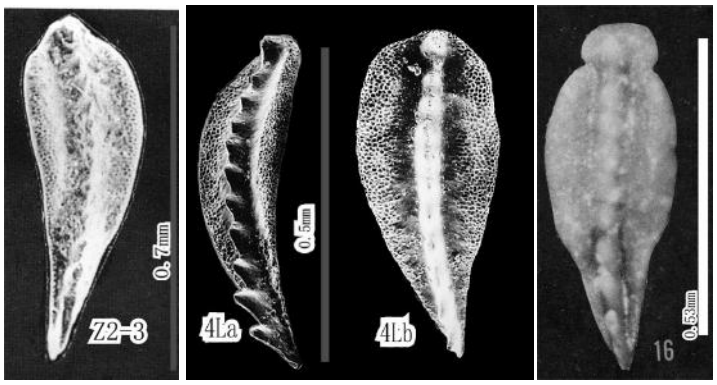

Z2-3: *C. carinata* (Clark) -Zhang et al., 1995, pl. 2, fig. 3; Bed 25, Section F. 4La,b: Holotype of *C. yini* Mei et al., 1998 -pl.4, figs.La,b. Right: Holotype of *C. carinata* （Clark, 1959） -pl. 44, figs 16-17, 19. We think Z2-3 belongs to ***C. yini***.

Zhang et al. (1995) described conodonts Z2-1 (Fig. 1.2H), Z2-4 (Fig. 1.2I), and Z2-7 (Fig. 1.2J) from Bed 25 of Section A.

Z2-1 was placed in *C. changxingensis* (Wang et Wang, 1981). Z2-1 differs from the holotype of this species in platform shape and denticle pattern, and cannot be placed in this species. Z2-1 resembles the holotype of *C. myridentalis* sp. nov. (Fig. 1.2A) very much in platform shape and denticle pattern, and is placed in *C. myridentalis* sp. nov.

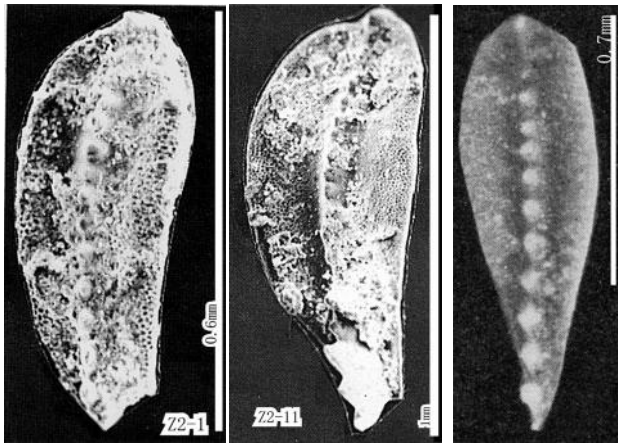

Z2-1: *Clarkina changxingensis* (wang et Wang, 1981) -Zhang et al., 1995, pl. 2, Fig. 1; Bed 25, Section A. Z2-11: Holotype of *C. myridentalis* sp. nov. Right: Holotype of *C. changxingensis* (Wang et Wang, 1981), pl. 1, figs. 13, 16. We think Z2-1 belongs to ***C. myridentalis*** sp. nov.

Z2-4 was placed in *Clarkina meishanensis* Zhang et al. (1995). Two different specimens, Z2-4 and Z2-6 (Fig. 1.2V), were placed in this species by Zhang et al. When this species was defined, no holotype was designated. Z2-4 has a flat platform, while the platform of Z2-6 abruptly arched at the anterior part. Besides, they have different denticle patterns, and different cusps. We think that such difference makes them to be assigned to different species. We designate Z2-6 as the holotype of *Clarkina meishanensis*. Z2-4 is used as holotype to define a new species: *C. plana* sp. nov.

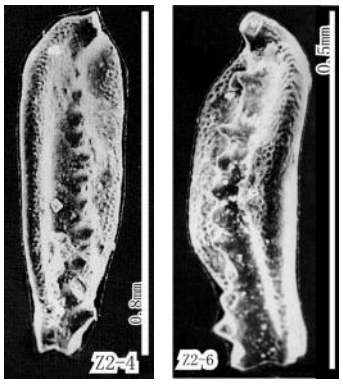

Z2-4: *C. meishanensis* Zhang et al., 1995 -Zhang et al., 1995, pl. 2, fig. 4; Bed 25, Section A. Right: Holotype of *C. meishanensis* Zhang et al., 1995 -pl. 2, fig. 6; Bed 26, Section F. We use Z2-4 as holotype to define ***C. plana* sp. nov.**

Z2-7 was placed in *C. deflecta* (Wang et Wang, 1981). Z2-7 doesn't has a rhombic platform posterior end, or a carina turning right at its posterior end, but has a arched rather than flat platform, and cannot be assigned to this species. The posterior end of Z2-7 seems to be damaged. It seems to belong to a new species, and is regarded as ***C.* sp. 2**.

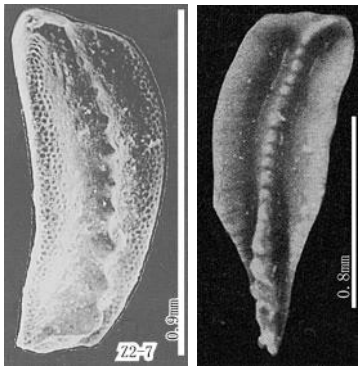

Z2-7: *Clarkina deflecta* (Wang et Wang, 1981) -Zhang et al., 1995, pl. 2, fig. 7; Bed 25, Section A. Right: Holotype of *C. deflecta* (Wang et Wang, 1981) –Wang & Wang, 1981, pl. 2, fig. 9. We regard Z2-7 as ***C.* sp. 2.**

Zhang et al. (1996) described conodonts Zh7-17 (Fig. 1.2K) and Zh7-6 (Fig. 1.2L) from Bed 25 of Section A, and Zh7-8 (Fig. 1.2M) from Bed 25 of Section E.

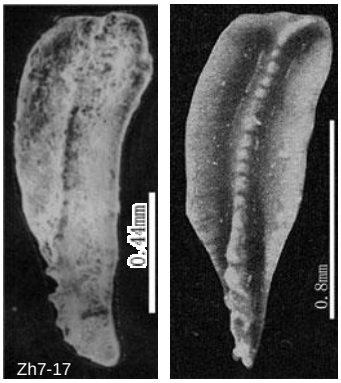

Zh7-17: *C. deflecta* -Zhang et al., 1996, pl.II.7, Fig. 17; Bed 25, Section A. Right: Holotype of *C. deflecta* (Wang et Wang, 1981) –Wang & Wang, 1981, pl. 2, fig. 9. We use Zh7-17 as holotype to define ***C. anisomerus* sp. nov.**

Zh7-17 was placed in *C. deflecta* (Wang et Wang, 1981). Zh7-17 has a subround rather than rhombic posterior platform end. Besides, the carina in Zh7-17 is different from that of the holotype of *C. deflecta*. Thus, Zh7-17 cannot be placed in this species. Zh7-17 is used as holotype to define a new species, *C. anisomerus* sp. nov.

Zh7-6 was placed in *C. deflecta* (Wang et Wang, 1981), too. Zh7-6 has a subround platform end, and denticles fused as a ridge, and cannot be assigned to this species. It is used as holotype to define a new species, *C. redactus* sp. nov.

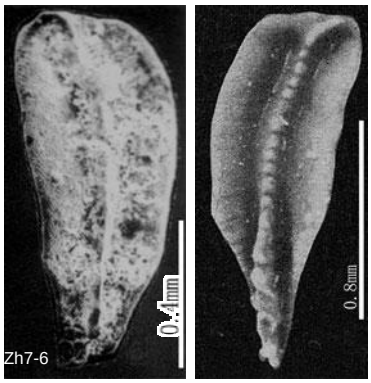

Zh7-6: *Clarkina deflecta* -Zhang et al., 1996, pl.II.7, fig. 6; Bed 25, Section A. Right: Holotype of *C. deflecta* (Wang et Wang, 1981) –Wang & Wang, 1981, pl. 2, fig. 9. We use Zh7-6 as holotype to define ***C. redactus* sp. nov.**

Zh7-8 was placed in *C. carinata*. Zh7-8 differs from the holotype of this species in that the

former does not has a shrink at its posterior platform end, but has a big reclined cusp terminally located. Their denticle patterns are very different. So, Zh7-8 cannot be placed in this species. It seems to belong to a new species, and is regarded as **C. sp. 3**.

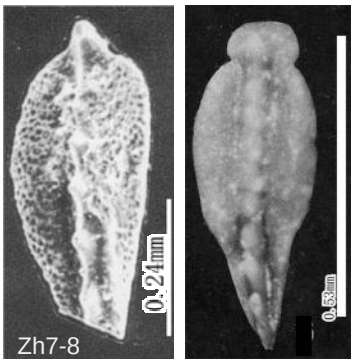

Zh7-8: *C. carinata* -Zhang et al., 1996, pl.II.7, fig. 8; Bed 25, Section E. Right: Holotype of *C. carinata* (Clark, 1959) -Clark, 1959, pl. 44, figs.16-17, 19. We regard Zh7-8 as ***C.* sp. 3.**

Wang (1995) described conodonts W1-3 (Fig. 1.2N) from 880 of Section Z (=Bed 25 of Section D).

W1-3 was placed in *C.* sp. W1-3 resembles Z2-4 (Fig. 1.2I: *C. plana* sp. nov.). W1-3 is an incomplete specimen, and is regarded to belong to *C. plana* sp. nov.

Zhang et al. (1996) described conodont Y1-7 (Fig. 1.2O) from Bed 25 of Section C.

Y1-7 was placed in *H. latidentatus (*Kozur, Mostler et Rahimi-Yazd, 1975). Y1-7 has a big cusp. As we know, *Hindeodus* elements with big cusp did not occur until Bed 27c. So, we suspect that there is a mistake about the occurrence horizon of Y1-7. Y1-7 has a very big cusp and very expanded base. We use Y1-7 as holotype to define a new species, *H. humilis* sp. nov.

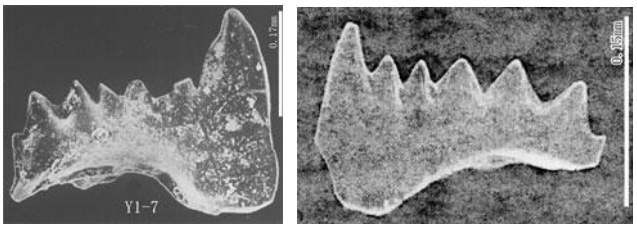

Y1-7: *H. latidentatus* -Zhang et al., 1996, pl. 1, fig. 7; Bed 25(?), Section C; bar 0.17mm. Right: Holotype of *H. latidentatus* (Kozur, Mostler et Rahimi-Yazd, 1975); bar 0.15mm. We use Y1-7 as holotype to define ***H. humilis* sp. nov.**

1.3.3 Conodonts from Bed 26 of Meishan and the equivalent beds

Zhang et al. (1996) described conodonts Zh6-22 (Fig. 1.2Q), Zh7-16 (Fig. 1.2R), Zh7-4 (Fig. 1.2S), and Zh7-18 (Fig. 1.2T) from Bed 26 of Section D.

Zh6-22 was placed in *C. changxingensis*. Compared to the holotype of this species, Zh6-22 has different platform shape and carina, and cannot be placed in this species. It can be a new species, and is regarded as ***C.* sp. 4**.

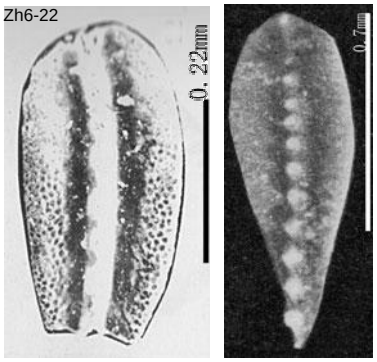

Zh6-22: *Clarkina changxingensis* -Zhang et al., 1996, pl.II.6, fig. 22; Bed 26, section D. Right: Holotype of *C. changxingensis* (Wang et Wang, 1981) -Wang & Wang, 1981, pl. 1, figs. 13, 16. We regard Zh6-22 as ***C.* sp. 4.**

Zh7-16 was placed in *C. deflecta*. Zh7-16 differs from the holotype of this species in the round posterior angles of the platform. Besides, they have different carinas. So, Zh7-16 cannot be assigned to this species. It can be a new species, and is regarded as ***C.* sp. 5**.

Zh7-4 was placed in *C.* sp. It has a nephroid platform, and strong, thick denticles. We use it as holotype to define a new species, ***C. columnaris* sp. nov.**

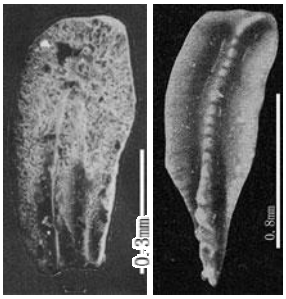

Zh7-16: *C. deflecta* -Zhang et al., 1996, pl. II.7, Fig. 16; Bed 26, Section D. Right: Holotype of *C. deflecta* (Wang et Wang, 1981) -Wang & Wang, 1981, pl. 2, fig. 9. We regard Zh7-16 as ***C.* sp. 5.**

Zh7-18 was placed in *C. deflecta*. It has a quadrate rather than rhombic posterior end of platform. So, it cannot be assign to this species. It seems to belong to a new species, and is regarded as ***C.* sp. 6**.

Zhang et al. (1995) described conodonts Z2-2 (Fig. 1.2U), Z2-6 (Fig. 1.2V), and Z2-8 (Fig. 1.2W) from Bed 26 of Section F.

Z2-2 was placed in *C. changxingensis* (Wang et Wang, 1981). It differs from the holotype of this species in its wider platform, more or less fused carina, and bigger cusp at the posterior end. It cannot be assigned to this species. It seems to belong to a new species, and is regarded as ***C.* sp. 7**.

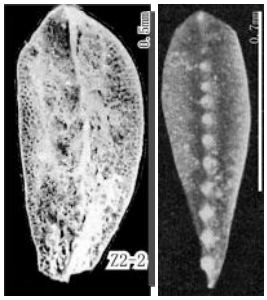

Z2-2: *C. changxingensis* (Wang et Wang, 1981) -Zhang et al., 1995, pl. 2, fig. 2; Bed 26, Section F. Right: Holotype of *C. changxingensis* (Wang et Wang, 1981) -Wang & Wang, 1981, pl. 1, figs. 13,16. We regard Z2-2 as ***C.* sp. 7.**

Z2-6 was placed in *Clarkina meishanensis* Zhang (1995). It has a flat platform posterior, while the anterior of its platform abruptly turns aborally, with a big, erect, conical cusp terminally located. Anterior denticles are basally fused. This specimen is designated as the holotype of this species.

Z2-8 was placed in *C. deflecta* (Wang et Wang, 1981). Z2-8 has a more or less rhombic posterior platform end, and two deep adcarina grooves. It differs from the holotype of this species in that the latter has two parallel platform side margins, while in the former the two platform side margins are not parallel. Z2-8 is regarded as a new subspecies, *C. deflecta* subsp. 1.

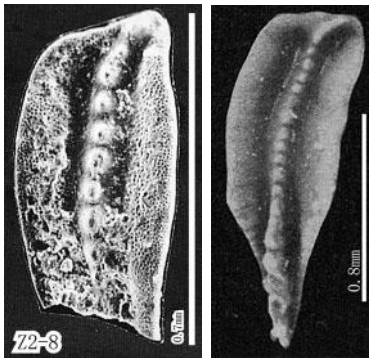

Z2-8: *Clarkina deflecta* (Wang et Wang, 1981) -Zhang et al., 1995, pl. 2, fig. 8, Bed 26, Section F. Right: Holotype of *C. deflecta* (Wang et Wang, 1981) -Wang & Wang, 1981, pl. 2, fig. 9. We regard Z2-8 as a new subspecies of this species：***C. deflecta* subsp. 1**.

Zhang et al. (1995) described conodont Z2-5 (Fig. 1.2X) from Bed 26 of Section A.

Z2-5 was placed in *C. meishanensis* Zhang (1995). Z2-5 differs from the holotype of this species in platform shape and denticle pattern, and cannot be assigned to this species. It resembles 4L (Fig. 1.2B: *C. yini* Mei et al., 1998) in platform shape and denticle pattern, and is regarded as *C.* cf. *yini*.

Z2-5: *Clarkina meishanensis* -Zhang et al., 1995, pl. 2, fig. 5; Bed 26, Section A. 4L: Holotype of *C. yini* Mei et al., 1998. Z2-6: Holotype of *C. meishanensis* Zhang et al., 1995. We regard Z2-5 as ***C.* cf. *yini***.

Zhang et al. (1996) described conodonts Zh6-19, Zh6-21 (Fig. 1.2Y) from Bed 26 of Section F.

Zh6-19 was placed in *C. changxingensis*. Z6-19 has a flat platform posterior but an abruptly and aborally turned platform anterior, and unclear denticles. It differs from this species, but resembles Z2-6 (Fig. 1.2V: *C. meishanensis*), and is regarded as *C.* cf. *meishanensis*.

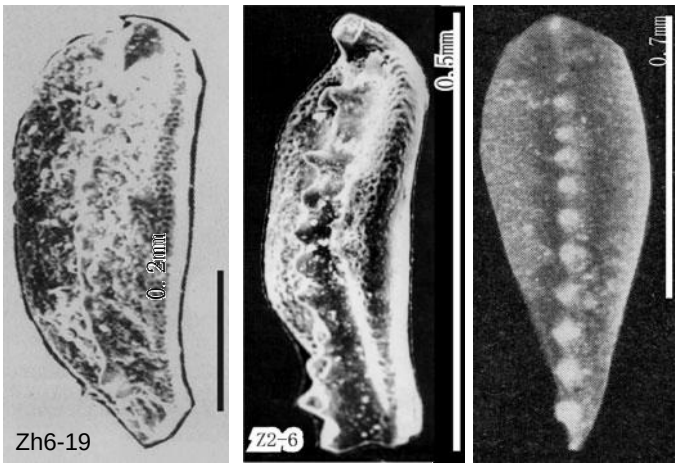

Zh6-19: *C. changxingensis* -Zhang et al., 1996, pl.II.6, Fig. 19; Bed 26, section F. Z2-6: Holotype of *C. meishanensis* Zhang et al., 1995. Right: Holotype of *C. changxingensis*（Wang et Wang, 1981）-Wang & Wang, 1981, pl. 1, figs. 13, 16. We regard Zh6-19 as ***C. cf. meishanensis.***

Zh6-21 was placed in *C. deflecta*. Its posterior platform end is linguiform, instead of rhombic, with a denticle pattern different from that of *C. deflecta*. So, Zh6-21 cannot be assigned to this species. It resembles W1-8 (Fig. 1.4H: *C. paradeflecta* sp. nov.) in platform shape and denticle pattern, and is assigned to *C. paradeflecta* sp. nov.

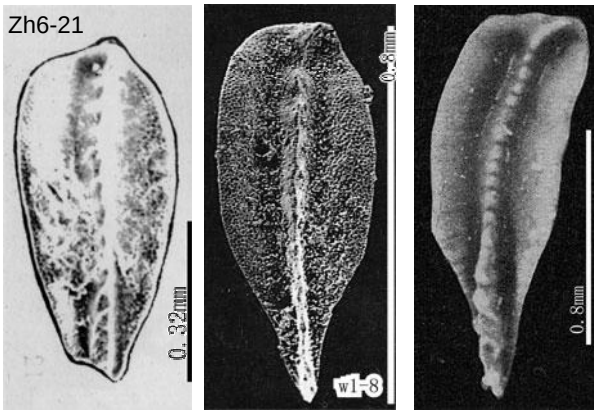

Zh6-21: *Clarkina deflecta* -Zhang et al., 1996, pl.II.6, fig. 21; Bed 26, Section F. W1-8: Holotype of *C. paradeflecta* sp. nov. Right: Holotype of *C. deflecta* (Wang et Wang, 1981) -Wang & Wang, 1981, pl. 2, fig. 9. We think Zh6-21 belongs to ***C. paradeflecta* sp. nov.**

Wang et al. (1995) described conodonts W1-5, W1-6, W1-7 (Fig. 1.2Z), W1-10, and W1-12 (Fig. 1.2P) from 881 of Section Z (=Bed 26 of Section D).

W1-5 was placed in *C. changxingensis* (Wang et Wang, 1981). This specimen is damaged, and is difficult to identify.

W1-6 and W1-7 were placed in *C. deflecta* (Wang et Wang, 1981). These two specimens resemble the holotype of this species in that both of them have rhombic platform ends and carinas that turn right at their posterior ends. So, they belong to the same species. Even so, the former have two platform side margins not parallel, while the latter has two parallel platform side margins. So, W1-6 and W1-7 are regarded as new subspecies of this species, *C. deflecta* subsp. 2, and *C. deflecta* subsp. 3.

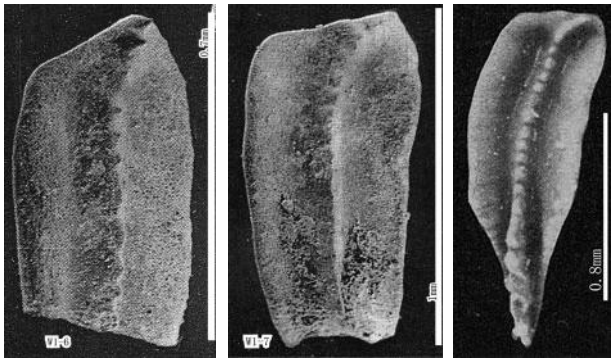

W1-6: *C. deflecta* (Wang et Wang, 1981) -Wang, 1995, pl. 1, fig. 6; bar 0.7mm. We regard it as ***C. deflecta* subsp. 2**. W1-7: *C. deflecta* (Wang et Wang, 1981) -Wang, 1995, pl. 1, fig. 7; bar 1mm. We regard it as ***C. deflecta* subsp. 3**. Right: Holotype of *C. deflecta* (Wang et Wang, 1981) -Wang & Wang, 1981, pl. 2, fig. 9.

W1-10 was regarded as *C.* sp. Since the specimen is damaged, it is difficult to identify.

W1-12 was placed in *C. dicerocarinata* (Wang et Wang, 1981). It resembles the holotype of this species in its cordiform platform end and a carina bifurcating at the posterior end. It differs from the latter in its completely fused carina. So, it is regarded as a new subspecies of this species, *C. dicerocarinata* subsp. 1.

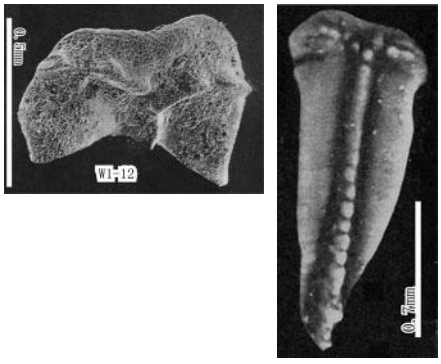

W1-12: *Clarkina dicerocarinata* (Wang et Wang, 1981) –Wang, 1995, pl. 1, Fig. 12. Right: Holotype of *C. dicerocarinata* (Wang et Wang, 1981) -Wang & Wang, 1981, pl. 2, fig. 14. We regard W1-12 as ***C. dicerocarinata* subsp. 1**.

Li et al. (1989) described conodont L43-10 (Fig. 1.2AA) from Bed 27 of Shangsi section (=Bed 26 of Section D). It was placed in *C. tulongensis*. The holotype of *C. tulongensis* has a middle concavity in one side, while L43-10 does not have. The outline of platform, cordiform posterior end of the platform, and bifurcating posterior end of the carina of L43-10 resemble *C. dicerocarinata* (Wang et Wang, 1981). We regard L43-10 as *C.* cf. *dicerocarinata* (Wang et Wang, 1981).

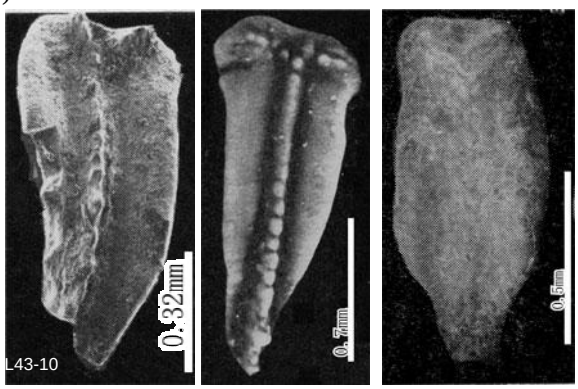

L43-10: *C. tulongensis* Tian -Li et al., 1989, pl. 43, Fig. 10; Gsc27-1, Shangsi Section. Middle: Holotype of *C. dicerocarinata* (Wang et Wang, 1981) -Wang &Wang, 1981, pl. 2, Fig. 14. Right: Holotype of *C. tulongensis* (Tian, 1982) -Tian, 1982, pl. 1, Fig. 17. We regard L43-10 as ***C.* cf. *dicerocarinata***.

1.3.4 Conodonts from Bed 27a~27b of Meishan and the equivalent beds

1.3.4.1 Conodonts from Bed 27a of Meishan and the equivalent beds

No conodonts have been reported from Bed 27a of Section D.

Wang (1995) described conodonts W2-12 (Fig. 1.3A), W2-16 (Fig. 1.3B), W2-15 (Fig. 1.3C), W1-13 (Fig. 1.3D) from 882-1 of Section Z (=27a of Section D).

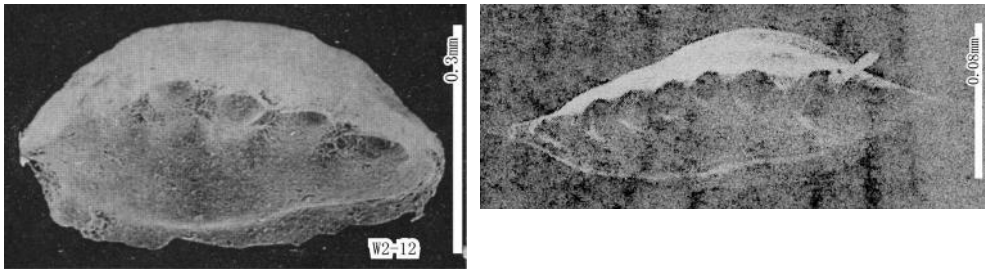

W2-12: *Hindeodus* cf. *turgidus* (Kozur, Mostler et Rahimi-Yazd, 1975) -Wang, 1995，pl. 2, Fig. 12. Right: Holotype of *H. turgidus* (Kozur, Mostler et Rahimi-Yazd, 1975)-pl. 7, fig 11-12. We use W2-12 as holotype to define ***H. turgidus brevis* subsp. nov.** and holotype of this species to define ***H. turgidus minutus* subsp. nov.**

W2-12 was regarded as *H.* cf. *turgidus* (Kozur, Mostler et Rahimi-Yazd, 1975). Compared to the holotype of this species, W2-12 is bigger and wider. Both of them are hat-like in oral view, and have lower denticles. W2-12 is assigned to this species, and is used as holotype to defined a new subspecies, *H. turgidus brevis* subsp. nov. The holotype of this species is used to define another new subspecies, *H. turgidus minutus* subsp. nov.

W2-16 was used as holotype to define *H. changxingensis* Wang (1995). It is characterized by its big cusp, falciform basal expansion, and a flat, adenticulate top face. There seems to be undeveloped denticles at posterior face and the transition between cusp and top face. It resembles the holotype of *H. julfensis* (Sweet, 1973) (Teicher, Kummel and Sweet, 1973, pl. 11, fig. 12) in blade shape. But, there are radiate grooves on the middle and anterior blade of the latter. Y1-2 (Fig. 1.3J) from Bed 27b of Section D resembles W2-16. However, the former has no denticles, except for the cusp. We use Y1-2 to define a new subspecies, *H. changxingensis levis* subsp. nov., and W2-16 to define another new subspecies, *H. changxingensis flatus* subsp. nov. It is noted that Perri et al. (2003) placed *Hindeodus changxingensis* to *Isarcicella*. In my opinion, however, the blade shape of this species is greatly different from that of *Isarcicella*. Hence, I disagree with Perri et al. in the change in the placement of this species. The specimen (Pl. 1, figs.17-19) Perri et al. assigned to "*Isarcicella changxingensis*" differs from the holotype of *Hindeodus changxingensis* in the denticulate top face in the former, and cannot be placed in this species.

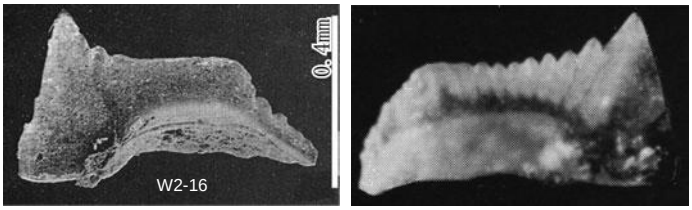

W2-16: Holotype of *Hindeodus changxingensis* -Wang, 1995, pl. 2, Fig. 16. Right: Holotype of *H. julfensis* (Sweet, 1973) -Teichert, Kummel and Sweet, 1973, pl. 11, Fig. 12.

W2-15 was placed in *Hindeodus changxingensis* Wang (1995). It differs from the holotype of this species (Fig. 1.3C) in its erect, rather than anteriorly declined anterior face. W2-15 seems to have wider basal expansion. So, it is regarded as *H.* cf. *changxingensis*.

W1-13 was placed in *Clarkina* cf. *planata* (Clark, 1959). It greatly differs from the holotype of this species. Its elliptic shape of platform and low and wide denticles are characteristic. It cannot be assigned to this species. We use W1-13 to define a new species, *C. elliptica* sp. nov.

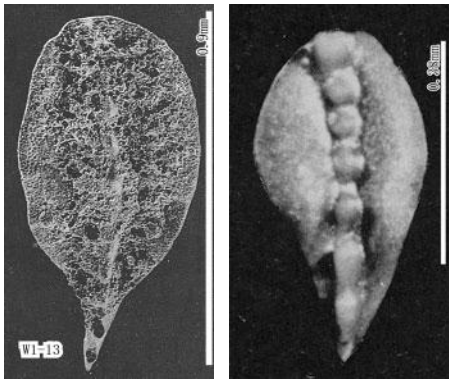

W1-13: *Clarkina* cf. *planata* (Clark, 1959) -Wang, 1995，pl. 1, fig. 13. Right: Holotype of *C. planata* (Clark, 1959) –Clark, 1959, pl. 44, fig. 9; bar 0.38mm. We use W1-13 as holotype to define ***C. elliptica* sp. nov.**

Nicoll et al. (2002) described conodonts N18-1 (Fig. 1.3E), N18-2 (Fig. 1.3F), and N19-1 (Fig. 1.3G) from Bed 27a of Section AW.

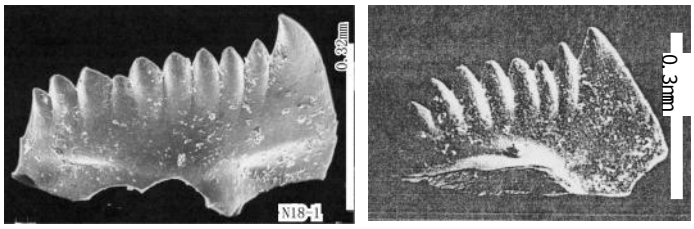

N18-1: *Hindeodus priscus* (Kozur, 1995) -Nicoll et al., 2002, pl. 18, Fig. 1; Bed 27a, Section AW. Right: Holotype of *H. pricus*. We use N18-1 as holotype to define ***H. limus* sp. nov.**

N18-1 was placed in *H. priscus* (Kozur, 1995). This species was defined by Kozur (1995) using the fig. 1 of plate 3 by Perri (1991). N18-1 differs from the holotype of this species in that the denticle prongs in the former are arranged in a straight line, instead of a S-shape line in the latter. So, N18-1 cannot be assigned to this species. We use N18-1 as holotype to define a new species, *H. limus* sp. nov.

N18-2 was placed in *H. priscus* (Kozur, 1995), too. It differs from the holotype of this species in its fused columnar denticles radially arranged. We use N18-2 as holotype to define a new species, *H. pectinatus* sp. nov.

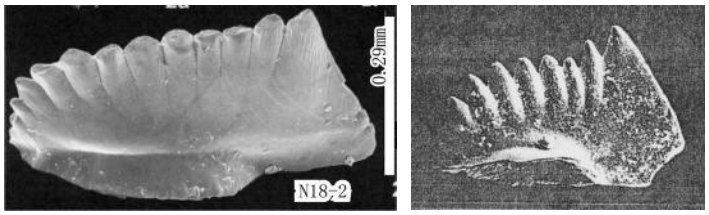

N18-2: *H. priscus* -Nicoll et al., 2002, pl. 18, fig. 2; Bed 27a, Section AW. Right: Holotype of *H. pricus* (Kozur, 1995). We use N18-2 as holotype to define ***H. pectinatus* sp. nov.**

N19-1 was regarded as *H.* n. sp. A. It resembles the holotype of *H. inflatus* Nicoll et al. (2002), and is assigned to this species.

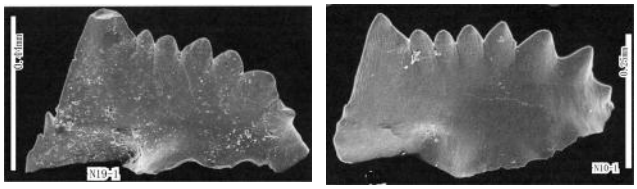

N19-1: *H*. n sp A -Nicoll et al., 2002, pl. 19, Fig. 1; Bed 27a, Section AW; bar 0.44mm. N10-1: Holotype of *H. inflatus* (Nicoll et al., 2002), -pl. 10, fig. 1; bar 0.25mm. We think N19-1 belongs to ***H. inflatus***.

Zhang et al. (1995) described conodont Z2-15 (Fig. 1.3I) from Bed 27a of Section A.

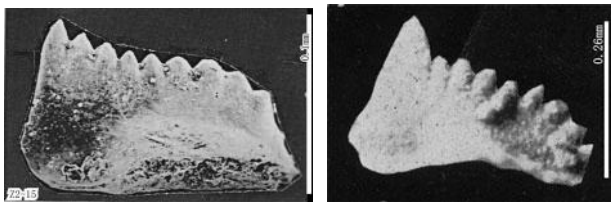

Z2-15: *Hindeodus typicalis* (Sweet) -Zhang, 1995; Bed 27a, Section A. Right: Holotype of *H. typicalis* (Sweet, 1970) –Sweet, 1970b, pl. 1, fig. 22. We use Z2-15 as holotype to define ***H. zhejiangensis* sp. nov.**

Z2-15 was placed in *Hindeodus typicalis* (Sweet), and designated as index fossil of a conodont zone. The specimen (Sweet, 1970a: pl. 1, figs.13, 22) designated as the holotype of this species by Sweet (1970a) for the first time have a very prominent cusp and conical denticles more or less irregularly arranged. In a later paper in the same year, Sweet (1970b) designated a specimen without cusp (Sweet, 1970b: pl. 1, figs. 13, 20) as the holotype of this species. We regard the holotype he designated earlier to be acceptable. Z2-15 has no prominent cusp, and cannot be placed in this species. Z2-15 resembles the holotype of *H. latidentatus* (Kozur, Mostler et Rahimi-Yazd, 1975) in that the denticle tips in the former are arranged in a S-shape line. But, the basal expansion in the former is much more prominent than in the latter. So, Z2-15 cannot be assigned to this species. We use Z2-15 as holotype to define a new species, *Hindeodus zhejiangensis* sp. nov., and pl. 1, fig. 20 of Sweet (1970b) as holotype to define another new species, ***Hindeodus kozuri* sp. nov.**

1.3.4.2 Conodonts from Bed 27b of Meishan and the equivalent beds

Zhang et al. (1996) described conodonts Y1-2 (Fig. 1.3J), Y1-3 (Fig. 1.3K) from Bed 27b of Section D.

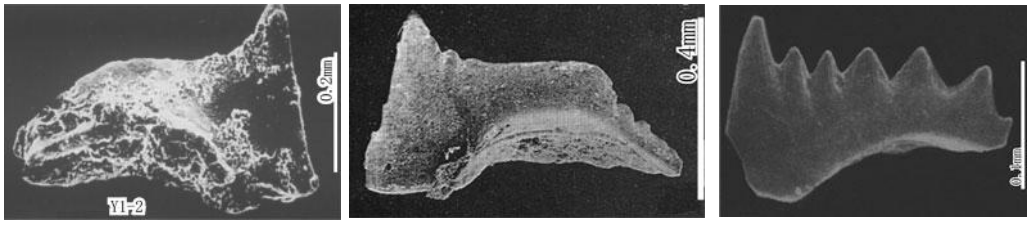

Y1-2: *H. latidentatus* (Kozur, Mostler et Rahimi-Yazd) -Zhang et al., 1996, pl. 1, fig. 2; Bed 27b, Section D. Middle: Holotype of *H. changxingensis* - Wang, 1995, pl. 2, Fig. 16; 882-1, Section Z. Right: Holotype of *H. latidentatus* (Kozur, Mostler et Rahimi-Yazd, 1975) -Kozur, Mostler and Rahimi-Yazd, 1975, pl. 2, fig. 6. We use Y1-2 to define ***H. changxingensis levis* subsp. nov.**

Y1-2 was placed in *H. latidentatus*. Y1-2 differs from the holotype of this species in its big cusp and totally absence of denticles. It cannot be assigned to this species. It resembles W2-16 (Fig. 1.3B: *H. changxingensis*) in blade shape and denticle pattern. W2-16 has some undeveloped denticles on posterior face and the transition between cusp and top face. We use Y1-2 as holotype to define a new subspecies, *H. changxingensis levis* subsp. nov.

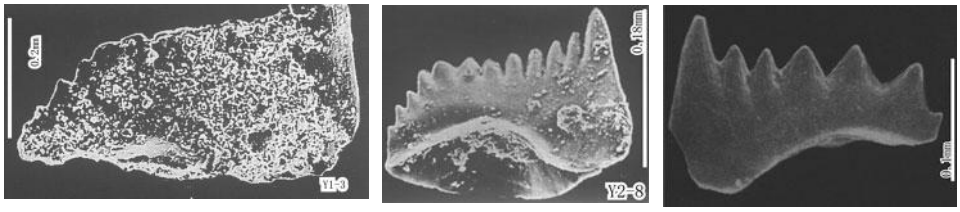

Y1-3: *H. latidentatus* (Kozur, Mostler et Rahimi-Yazd)-Zhang et al., 1996, pl. 1, fig. 3; Bed 27b, Section D. Y2-8: Holotype of *H. difformis* sp. nov. Right: Holotype of *H. latidentatus* (Kozur, Mostler et Rahimi-Yazd, 1975) -pl. 2, fig. 6. We think Y1-3 belongs to ***H. difformis* sp. nov.**

Y1-3 was placed in *H. latidentatus*. It differs from the holotype of this species in blade shape and denticle pattern, and cannot be assigned to this species. It resembles Y2-8 (Fig. 1.4C: *H. difformis*). Denticles seem to be less developed in Y1-3. Y1-3 is assigned to *H. difformis* sp. nov.

Nicoll et al. (2002) described conodont N9-1 (Fig. 1.3L) from Bed 27b of Section D.

N9-1 was used as holotype to define *Hindeodus eurypyge* Nicoll et al. (2002). The cusp of N9-1 was damaged, and probably as thick as other denticles. N9-1 resembles N18-1 (Fig. 1.3E: *Hindeodus limus* sp. nov.) in blade shape and basal expansion. However, N18-1 has a thicker and

reclined cusp.

Wang (1995) described conodonts W1-8 (Fig. 1.3H) and W2-6 (Fig. 1.3M) from 882-2 of Section Z (=27b of Section D).

W1-8 was placed in C. *deflecta* (Wang et Wang, 1981). W1-8 has an asymmetric linguiform, rather than rhombic posterior platform end, and cannot be assigned to this species. Its denticles are more or less fused. The carina turns right at the posterior end and reaches the terminal end of the platform. We use W1-8 as holotype to define a new species, *C. paradeflecta* sp. nov. Zh6-21 (Fig. 1.2Y) is assigned to this new species, too.

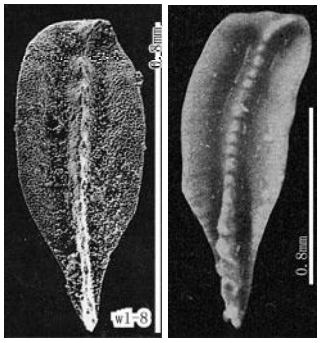

W1-8: *Clarkina deflecta* (Wang et Wang, 1981) -Wang, 1995, pl. 1, fig. 8. Right: Holotype of *C. deflecta* (Wang et Wang, 1981) –Wang & Wang, 1981, pl. 2, fig. 9. We use W1-8 as holotype to define ***C. paradeflecta* sp. nov.**

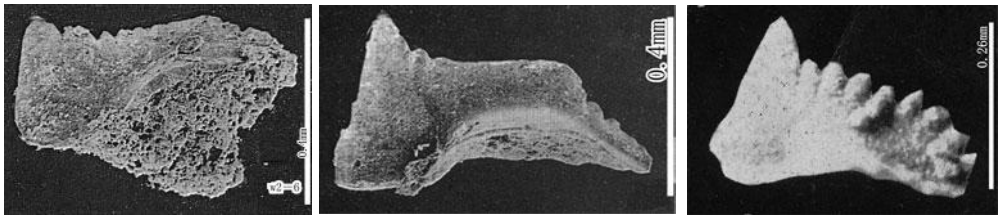

W2-6: *H. typicalis* (Sweet, 1970) -Wang, 1995, pl. 2, fig. 6; bar 0.4mm. Middle: Holotype of *H. changxingensis* Wang, 1995 -pl. 2, fig. 16. Right: Holotype of *H. typicalis* (Sweet, 1970) –Sweet, 1970b, pl. 1, fig. 22. We use W2-6 to define ***H. changxingensis rotundus* subsp. nov.**

W2-6 was placed in *Hindeodus typicalis* (Sweet, 1970). It differs from the holotype of this species in blade shape and denticle pattern, and cannot be assigned to this species. It resembles W2-16 (Fig. 1.3B: *H. changxingensis*) in blade shape and denticle pattern. In the former, however, there are more prominent denticles at the transition between cusp and top face, and the top face is not flat but slightly reclined. We use W2-6 to define *H. changxingensis rotundus* subsp. nov.

1.3.4.3 Conodonts from Bed 27a-27b of Meishan and the equivalent beds

Li et al. (1989) described conodonts L39-13 (Fig. 1.3N) and L39-11 (Fig. 1.3O) from Bed 29 of Shangsi section (=Bed 27a-b of Section D).

L39-13 was placed in *H. decrescens* (Dai et Zhang, 1989). L39-13 has characteristic blade shape. Its basal expansion is belt-like. It differs from the holotype of *Hindeodus parvus* in its smaller cusp and blade shape.

L39-11 was placed in *H. decrescens* (Dai et Zhang, 1989), too. However, it has no denticles. It resembles Y1-2 (Fig. 1.3J: *Hindeodus changxingensis levis* subsp. nov.) in blade shape and absence of denticles except for cusp. They are slightly different in basal expansion. L39-11 was assigned to *Hindeodus changxingensis levis* subsp. nov.

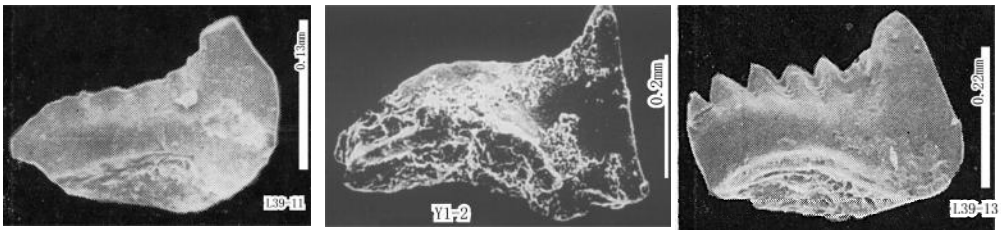

L39-11: *H. decrescens* (Dai et Zhang, 1989) –Li et al., 1989, pl.39, Fig. 11; Bed 29, Shangsi Section. Y1-2: Holotype of *H. changxingensis levis* subsp. nov. L39-13: Holotype of *H. decrescens* (Dai et Zhang, 1989) –Li et al., 1989, pl.39, Fig. 13. We think L39-11 belongs to ***H. changxingensis levis* subsp. nov.**

1.3.5 Conodonts from Bed 27c and 27d of Meishan and the equivalent beds

1.3.5.1 Conodonts from Bed 27c of Meishan and the equivalent beds

Zhang et al. (1995) described conodont Z2-14 (Fig. 1.4A) from Bed 27c of Section D.

Z2-14 was placed in *Isarcicella parva* (Kozur et Pjatakova). It differs from the holotype of this species in that there are denticles at the posterior face in the former, while there is no one in the latter. Basal expansion is lunate in the former, but belt-like in the latter. So, Z2-14 cannot be assigned to this species. We use Z2-14 as holotype to define a new species, *Hindeodus irregularis* sp. nov.

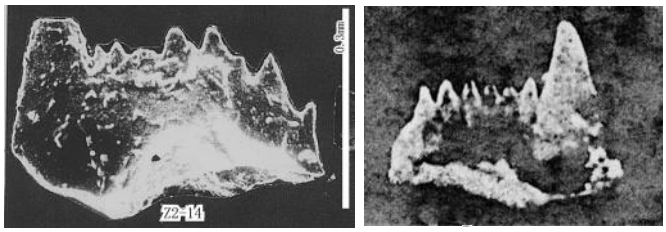

Z2-14: *Isarcicella parva* -Zhang et al., 1995, pl. 2, Fig. 14; Bed 27c, Section D. Right: Holotype of *H. parvus* (Kozur et Pjatakova, 1975) -Kozur, 1975, Taf. 1, Fig. 17. We use Z2-14 as holotype to define ***H. irregularis* sp. nov.**

Zhang et al. (1996) described conodonts Y2-5 (Fig. 1.4B) from Bed 27c of Section D, Y2-8 (Fig. 1.4C) from Bed 27c of Section E, Y2-2 (Fig. 1.4D) from Bed 27c of a section between B and C.

Y2-5 was placed in *H. parvus*. It resembles the holotype of this species in the large and reclined cusp, blade shape, and denticle pattern, and belongs to this species.

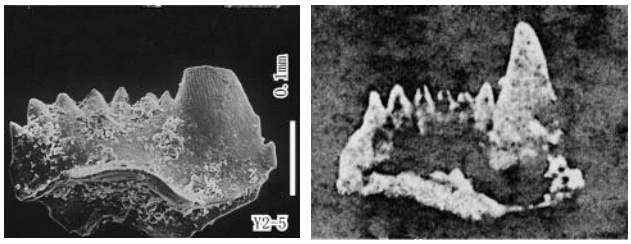

Y2-5: *Hindeodus parvus* -Zhang et al., 1996, pl. 2, fig. 5; Bed 27c, Section D. Right: Holotype of *H. parvus* (Kozur et Pjatakova) -Kozur, 1975, pl. 1, Fig. 17. Y2-5 belongs to ***H. parvus***.

Y2-8 was placed in *H. parvus*, too. However, the cusp in Y2-8 is not as big as that of this species (more than 2~3 times wider than denticles). Besides, they have different denticle patterns. So, Y2-8 cannot be assigned to this species. We use this specimen as holotype to define a new species, *H. differmis* sp. nov. It is characterized by: (1) a cusp 2 times wider than denticles, (2) denticle tips arranged in a S-shape line, (3) wider and lower denticles at the transition between the top face and posterior face, and (4) belt-like basal expansion.

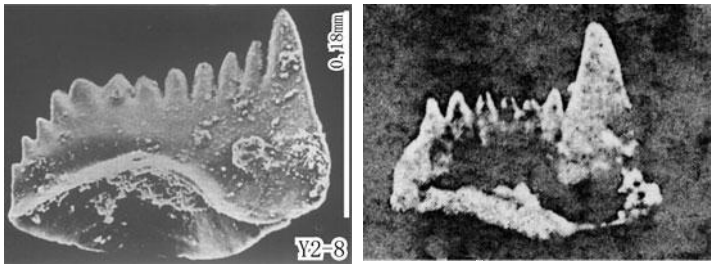

Y2-8: *H. parvus* -Zhang et al., 1996, pl. 2, fig. 8; Bed 27c, Section E. Right: Holotype of *H. parvus* (Kozur et Pjatakova) -Kozur, 1975, taf.1, Fig. 17. We use Y2-8 as holotype to define ***H. differmis* sp. nov.**

Y2-2 was placed in *H. latidentatus* (Kozur, Mostler et Rahimi-Yazd, 1975). Y2-2 differs from the holotype of this species in that the former has a very prominent cusp, while the latter does not have; the basal expansion in the former is very wide, while basal expansion in the latter is not prominent. So, Y2-2 cannot be assigned to this species. We use it as holotype to define a new species, *H. scutatus* sp. nov.

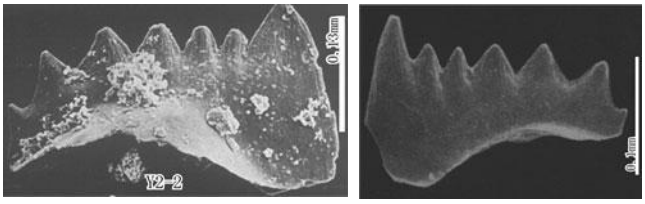

Y2-2: *H. latidentatus* (Kozur, Mostler et Rahimi-Yazd)-Zhang et al., 1996, pl. 2, fig. 2; Bed 27c, a section between Sections B and C. Right: Holotype of *H. latidentatus* (Kozur, Mostler et Rahimi-Yazd, 1975) -pl. 2, fig. 6. We use Y2-2 as holotype to define ***H. scutatus* sp. nov.**

Wang (1995) described conodonts W2-3 (Fig. 1.4E) , W2-9 (Fig. 1.4F), W2-2 (Fig. 1.4G), W2-5 (Fig. 1.4H), W2-4 (Fig. 1.4I), W2-8 (Fig. 1.4J), W2-1 (Fig. 1.4K), W1-1 (Fig. 1.4L), and W3-6 (Fig. 1.4M) from 882-3 of Section Z (=Bed 27c of Section D).

W2-3 was placed in *H.* cf. *turgidus* (Kozur, Mostler et Rahimi-Yazd). W2-3 greatly differs

from the holotype of this species in blade shape and denticle pattern, and cannot be assigned to this species. It resembles the holotype of *H. parvus* in blade shape and denticle pattern. It differs from the latter in the fused columnar denticles in the former. So, W2-3 is regarded as *H.* cf. *parvus*.

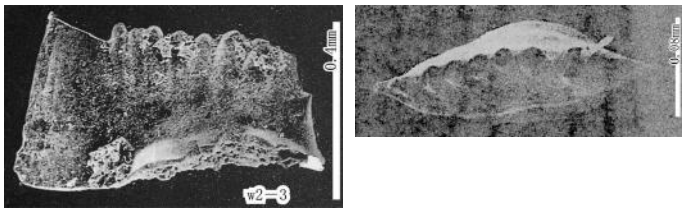

W2-3: *H*. cf *turgidus* (Kozur, Mostler et Rahimi-Yazd, 1975) -Wang, 1995, pl. 2, fig. 3. Right: Holotype of *H*. *turgidus* -Kozur, Mostler and Rahimi-Yazd, 1975, pl. 7, Fig. 12. We regard W2-3 as ***H*. cf. *parvus*.**

W2-9 was placed in *Hindeodus* cf. *turgidus* (Kozur, Mostler et Rahimi-Yazd, 1975), too. It differs from the holotype of this species in blade shape and denticle pattern, and cannot be assigned to this species. It is characterized by (1) denticles all erect and similar in shape and size, (2) denticle tips in S-shape line, (3) no prominent cusp, and (4) belt-like basal expansion. We use W2-9 as holotype to define a new species, *Hindeodus similes* sp. nov.

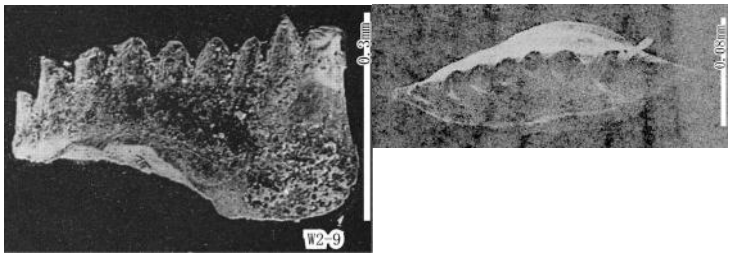

W2-9: *H*. cf *turgidus* (Kozur, Mostler et Rahimi-Yazd, 1975) -Wang, 1995, pl. 2, fig. 9. Right: Holotype of *H*. *turgidus* (Kozur, Mostler et Rahimi-Yazd, 1975) -pl. 7, Fig. 12. We use W2-9 to define ***H. similes* sp. nov.**

W2-2 was placed in *H. parvus*. W2-2 has a very large cusp. However, it differs from the holotype of this species in blade shape, denticle pattern, and basal expansion, and cannot be assigned to this species. It resembles *H. typicalis* (Sweet, 1970) in its large cusp and radially arranged but more or less irregular denticles. It differs from the latter in its spherical basal expansion. We regarded it as *H.* cf. *typicalis.*

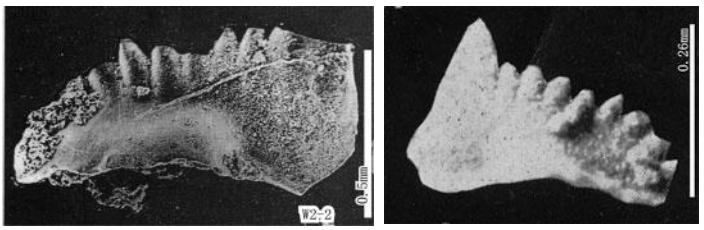

W2-2: *H*. *parvus* morphotype 2 -Wang, 1995, pl. 2, fig. 2. Right: Holotype of *H*. *typicalis* (Sweet, 1970) –Sweet, 1970b, pl. 1, fig. 22. We regard W2-2 as ***H*. cf. *typicalis***.

W2-5 was placed in *H. latidentatus* (Kozur, Mostler et Rahimi-Yazd, 1975). It differs from the holotype of this species in its basally fused thicker and blunt denticles, and more prominent basal expansion. Basal expansion seems to be undeveloped in the latter. But, they are similar in that denticles become wider and lower at their posterior ends. W2-5 cannot be assigned to this species. We use it as holotype to define a new species, *H. amblyodontus* sp. nov.

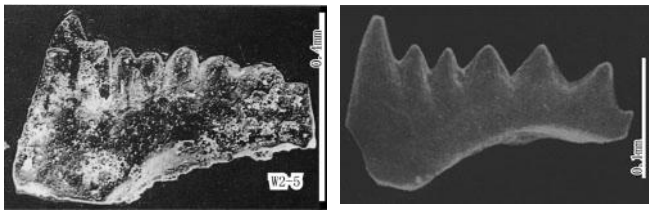

W2-5: *H. latidentatus* (Kozur, Mostler et Rahimi–Yazd, 1975) -Wang, 1995, pl. 2, fig. 5. Right: Holotype of *H. latidentatus* (Kozur, Mostler et Rahimi-Yazd, 1975). We use W2-5 as holotype to define ***H. amblyodontus* sp. nov.**

W2-4 was placed in *H. latidentatus* (Kozur, Mostler et Rahimi-Yazd, 1975). It differs from the holotype of this species in its blade shape, denticle pattern, big cusp, and prominent basal expansion, and cannot be assigned to this species. We use it as holotype to define a new species, *H. proparvus* sp. nov.

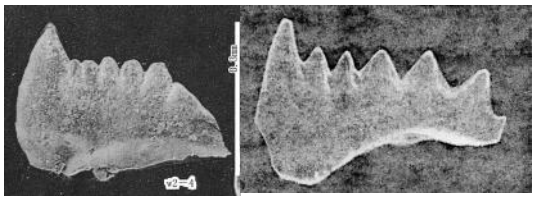

W2-4: *Hindeodus latidentatus* (Kozur, Mostler et Rahimi –Yazd, 1975) -Wang, 1995, pl. 2, fig. 4; bar 0.3mm. Right: Holotype of *H. latidentatus* (Kozur, Mostler et Rahimi-Yazd, 1975) -pl. 2, fig. 6. We use W2-4 as holotype to define ***H. proparvus* sp. nov.**

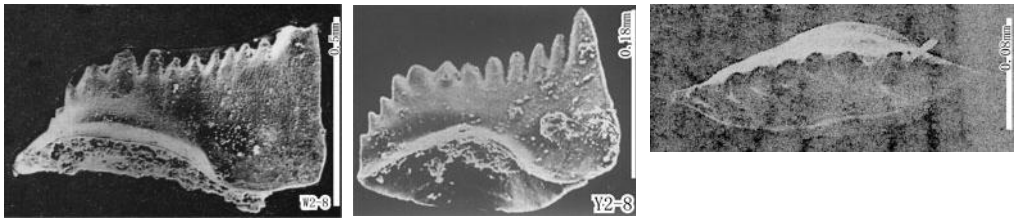

W2-8: *H*. cf *turgidus* (Kozur, Mostler et Rahimi-Yazd, 1975) -Wang, 1995, pl. 2, fig. 8. Y2-8: Holotype of *H. difformis* sp. nov. Right: Holotype of *H. turgidus* (Kozur, Mostler et Rahimi-Yazd, 1975) -pl. 7, Fig. 12. We think W2-8 belongs to ***H. difformis* sp. nov.**

W2-8 was placed in *H.* cf. *turgidus* (Kozur, Mostler et Rahimi-Yazd, 1975). It differs from the holotype of this species in blade shape and denticle pattern, and cannot be assigned to this species. It resembles Y2-8 (Fig. 1.4C: *H. difformis* sp. nov.) in blade shape and denticle pattern. They are different in that the denticles in the latter are not in the same direction, and basal

expansion extends posteriorly in the former. These are probably intra-species variations. W2-8 is assigned to *H. difformis* sp. nov.

W2-1 was placed in *H. parvus* (Kozur et Pjatakova, 1975). It differs from the holotype of this species in that in the former the transition between top face and posterior face is gradual, and there are denticles at the posterior face. So, W2-1 cannot be assigned to this species. It has a big cusp and falciform basal expansion, and seems to belong to a new species. It is regarded as ***H.* sp. 1**.

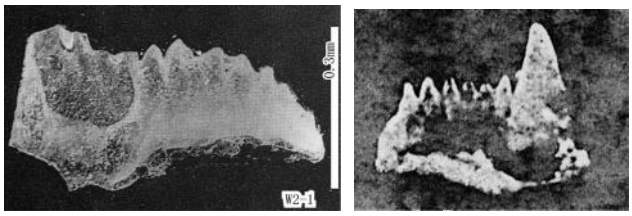

W2-1: *Hindeodus parvus* morphotype 2 -Wang, 1995, pl. 2, Fig. 1. Right: Holotype of *H. parvus* (Kozur et Pjatakova, 1975) -Kozur, 1975, pl. 1, Fig. 17. We regard W2-1 as ***H.* sp. 1**.

W1-1 was placed in *C. changxingensis* (Wang et Wang, 1981). It differs from the holotype of this species in its asymmetric linguiform platform and denticles fused as a ridge, and cannot be assigned to this species. It resembles to W1-8 (Fig. 1.3H: *C. paradeflecta* sp. nov.) in platform shape and denticle pattern. The difference is that the platform of W1-8 is wider. This is probably intra-species variation. So, W1-1 is assigned to *C. paradeflecta* sp. nov.

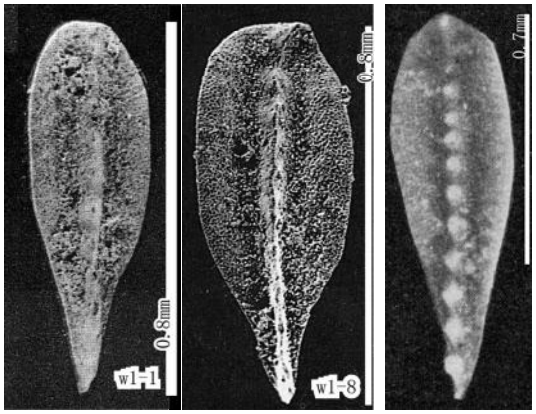

W1-1: *Clarkina changxingensis* (Wang et Wang, 1981) -Wang, 1995, pl. 1, Fig. 1. W1-8: holotype of *C. paradeflecta* sp. nov. Right: Holotype of *C. changxingensis* (Wang et Wang, 1981) –pl. 1, Fig. 13. We think W1-1 belongs to ***C. paradeflecta* sp. nov.**

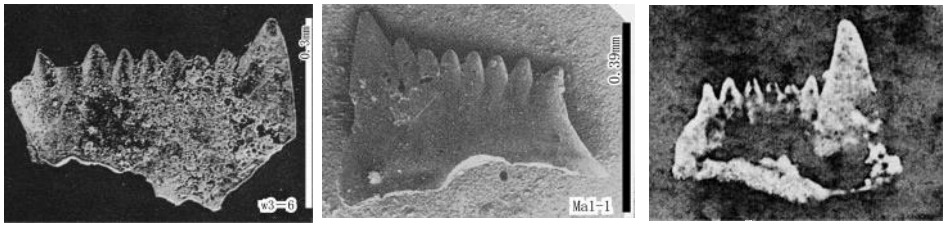

W3-6: *H. parvus* Mophotype1 –Wang, 1995, pl.3, fig. 6; bar 0.3mm. Ma1-1: holotype of *H. scalaris* sp. nov. Right: Holotype of *H. parvus* (Kozur et Pjatakova) -Kozur, 1975, pl. 1, Fig. 17. We think W3-6 belongs to ***H. scalaris* sp. nov.**

W3-6 was placed in *Hindeodus parvus*. It does not have so large (more than 2~3 times wider than other denticles) a cusp as the holotype of this species, and cannot be assigned to this species. W3-6 resembles Ma1-1 (Fig. 1.4W: *H. scalaris* sp. nov.) in blade shape and denticle pattern, and is assigned to the same species, *H. scalaris* sp. nov.

1.3.5.2 Conodonts from Bed 27d of Meishan and the equivalent beds

Zhang et al. (1996) described conodont Y2-4 (Fig. 1.4N) from bed 27d of Section D.

Y2-4 was placed in *Hindeodus parvus*. It resembles the holotype of this species in a very prominent cusp wider by 3~4 times than denticles, denticles distributed at only top face, and belt-like basal expansion. It is a typical *Hindeodus parvus*.

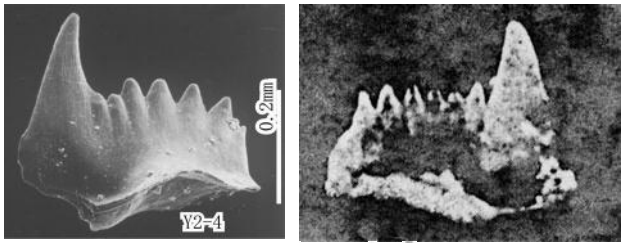

Y2-4: *Hindeodus parvus* -Zhang et al., 1996, pl. 2, fig. 4; Bed 27d, Section D. Right: Holotype of *H. parvus* (Kozur et Pjatakova) -Kozur, 1975, pl. 1, Fig. 17. Y2-4 belongs to ***H. parvus***.

Wang (1995) described conodonts W3-3 (Fig. 1.4O), W3-8 (Fig. 1.4P), W3-5 (Fig. 1.4Q), W2-7 (Fig. 1.4R), and W1-11 (Fig. 1.4S) from 882-4 of Section Z (=27d of Section D).

W3-3 was placed in *Hindeodus parvus*. It does not have so large a cusp as the holotype of this species. There are denticles at posterior face and the transition between cusp and top face. These make it to be excluded from this species. W3-3 resembles Y2-8 (Fig. 1.4C: *H. differmis* sp. nov.) in: (1) denticle tips arranged in a S-shaped line, (2) cusp not so wider as in *H. parvus*, (3) wider denticles at the transition between top face and posterior face. The basal expansion in W3-3 is lunate rather than belt-like, which can be an intra-species variation. W3-3 is assigned to *H. differmis* sp. nov.

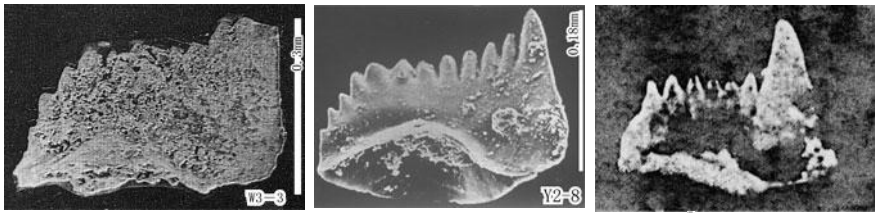

W3-3: *H. parvus* Mophotype 2 –Wang, 1995, pl. 3, fig. 3; 882-4, Section Z. Y2-8: Holotype of *H. differmis* sp. nov. Right: Holotype of *H. parvus* (Kozur et Pjatakova) -Kozur, 1975, pl. 1, Fig. 17. We think W3-3 belongs to ***H. differmis* sp. nov.**

W3-8 was placed in *Hindeodus parvus*. It differs from the holotype of this species in blade shape, denticle pattern, and especially basal expansion, and cannot be assigned to this species. It

is characterized by a very large cusp, a laterally extended basal expansion like shield, direct contact between denticles and basal expansion, and wider denticles at the posterior end. It resembles Y2-2 (Fig. 1.4D: *H. scutatus* sp. nov.) in blade shape and denticle pattern and is assigned to the same species, *H. scutatus* sp. nov.

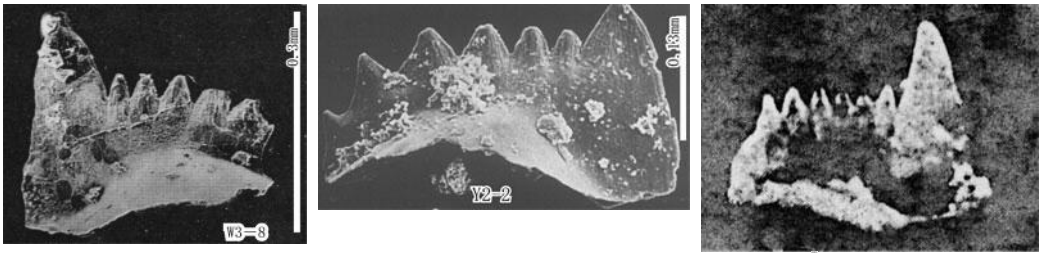

W3-8: *Hindeodus parvus* Mophotype1 –Wang, 1995, pl. 3, fig. 8. Y2-2: Holotype of *H. scutatus* sp. nov. Right: Holotype of *H. parvus* (Kozur et Pjatakova, 1975) -Kozur, 1975, pl. 1, Fig. 17. We think W3-8 belongs to ***H. scutatus* sp. nov.**

W3-5 was placed in *H. turgidus* (Kozur, Mostler et Rahimi-Yazd, 1975). It differs from the holotype of this species in blade shape and denticle pattern, and cannot be assigned to this species. It is characterized by a relatively small cusp, fused but thick and blunt denticles, spherical basal expansion, and S-shaped oral margin. We use it as holotype to define a new species, *Hindeodus coalitus* sp. nov.

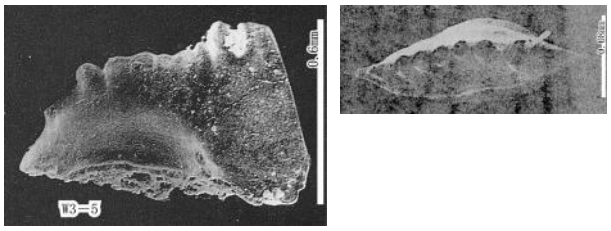

W3-5: *H. turgidus* (Kozur, Mostler et Rahimi-Yazd, 1975) -Wang, 1995, pl. 3, fig. 5. Right: Holotype of *H. turgidus* (Kozur, Mostler et Rahimi -Yazd, 1975) -pl. 7, Fig. 12. We use W3-5 as holotype to define ***H. coalitus* sp. nov.**

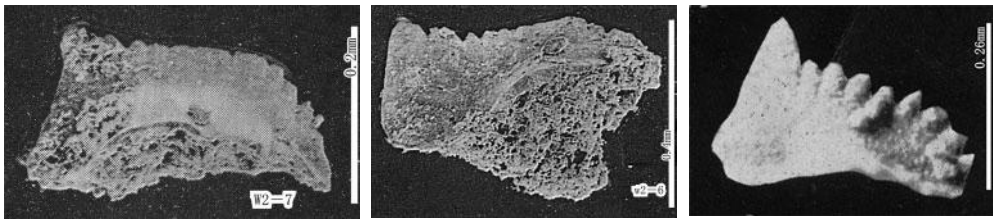

W2-7: *H. typicalis* (Sweet, 1970) -Wang, 1995, pl. 2, fig. 7. W2-6: Holotype of *H. changxingensis rotundus* subsp. nov. Right: Holotype of *H. typicalis* (Sweet, 1970) -Sweet, 1970b, pl. 1, fig. 22. We think W2-7 belongs to ***H. changxingensis rotundus* subsp. nov.**

W2-7 was placed in *H. typicalis* (Sweet, 1970). It differs from the holotype of this species in relatively smaller cusp and denticles, and much more prominent basal expansion. It cannot be

assigned to this species. It resembles W2-6 (Fig. 1.3M: *H. changxingensis rotundus* subsp. nov.) in blade shape and denticle pattern, and is assigned to the same subspecies, *H. changxingensis rotundus* subsp. nov.

W1-11 was placed in *C.* sp. It has a thick carina of fused denticles and a subround posterior platform end, but no cusp. It seems to belong to a new species, and is regarded as ***C.* sp. 8.**

Li et al. (1989) described many materials assigned to *H. parvus* from Bed 31 to 32 of Shangsi section (=27c~27d of Section D). All these specimens have parvus-type cusp, but are different from the holotype of this species in less regular denticles and not flat top face. Besides, they described conodont L45-14 (Fig. 1.4T).

L45-14 was used as holotype to define *H. anterodentata* (Dai et Tian, 1989). This specimen has a belt-like depression along its posterior base, with a basal cavity posteriorly located, and cannot be assigned to *Hindeodus*. It seems to belong to *Neospathodus*. It is characterized by a cusp. It is regarded as *Neospathodus anterodentata* (Dai et Tian, 1989).

Matsuda (1981) described conodonts Ma1-11 (Fig. 1.4U), Ma1-12 (Fig. 1.4V), and Ma1-1 (Fig. 1.4W) from Beds 56~57 of Guryul Ravine section, Kashmir (=27c-d of Section D).

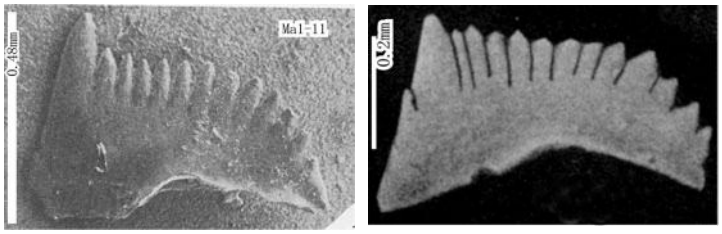

Ma1-11: *H. minitue* (Ellison, 1941) –Matsuda, 1981, pl. 1, Fig. 11, Bed 56, Kashmir. Right: Holotype of *H. minutus* (Ellison, 1941). We use Ma1-11 as holotype to define ***H. angustus* sp. nov.**

Ma1-11 was placed in *H. minutus*. It greatly differs from the holotype of this species in blade shape and denticle pattern, and cannot be assigned to this species. It is characterized by: (1) a cusp two times wider than denticles, (2) denticle tips arranged in a S-shaped line, (3) all denticles in the same shape, and (4) falciform basal expansion. We use it as holotype to define a new species, *H. angustus* sp. nov.

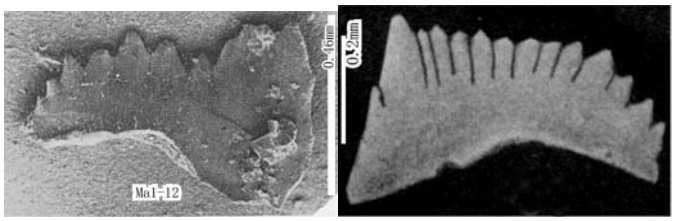

Ma1-12: *H. minutus* (Ellison, 1941) Pa element -Matsuda, 1981, pl. 1, Fig. 12. Right: Holotype of *H. minutus* (Ellison, 1941). We use Ma1-12 as holotype to define ***H. arcuatus* sp. nov.**

Ma1-12 was placed in *H. minutus*. It greatly differs from the holotype of this species in blade

shape and denticle pattern, and cannot be assigned to this species. It is characterized by (1) relatively small cusp, (2) denticle tips arranged in a S-shaped line, (3) low denticles at top face and posterior face, (4) flat side surface and not prominent basal expansion, and (5) rounded anterior basal angle. We use Ma1-12 as holotype to define a new species, *H. arcuatus* sp. nov.

Ma1-1 was placed in *H. minutus* (Ellison, 1941). It greatly differs from the holotype of this species in blade shape and denticle pattern, and cannot be assigned to this species. It is characterized by: (1) a cusp two times wider than denticles, (2) denticle tips in a straight line, (3) all denticles same in shape and distributed only at top face, and (4) belt-like basal expansion. We use it as holotype to define a new species, *H. scalaris* sp. nov. W3-6 (Fig. 1.4M) is assigned to this new species.

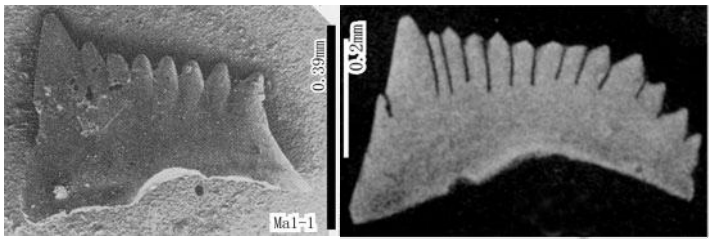

Ma1-1: *H. minutus* (Ellison, 1941) -Matsuda, 1981, pl. 1, Fig. 1. Right: Holotype of *H. minutus* (Ellison, 1941). We use Ma1-1 as holotype to define ***H. scalaris* sp. nov.**

1.3.6 Conodonts from Bed 28 of Meishan and the equivalent beds

Zhang et al. (1996) described conodonts Zh8-8 (Fig. 1.5A) and Zh8-12 (Fig. 1.5B) from Bed 28 of Section D, and Zh8-15 (Fig. 1.5C) from Bed 28 of Section C.

Zh8-8 was placed in *Isarcicella* sp. It has no prominent cusp, but more or less regular, thick denticles. It seems to belong to a new species, and is regarded as ***H.* sp. 2.**

Zh8-12 was placed in *H. parvus.* It has a large cusp most probably of parvus-type. However, its denticles are much bigger than those in the holotype of this species. Besides, the part between denticles and basal expansion is much smaller. It seems to belong to a new species similar to this species, and is regarded as *H.* cf. *parvus*.

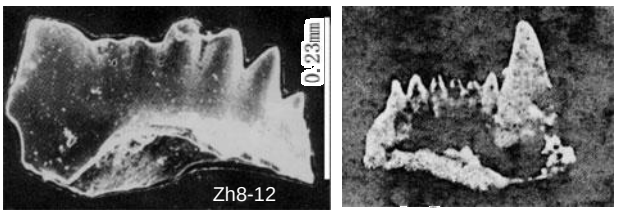

Zh8-12： *Hindeodus parvus* -Zhang et al., 1996, pl.II.8, Fig. 12; Bed 28, Section D. Right: Holotype of *H. parvus* (Kozur et Pjatakova, 1975) -Kozur, 1975, pl. 1, Fig. 17. We regard Zh8-12 as ***H.* cf. *parvus***.

Zh8-15 was placed in *H. parvus*, too. It has a very large and reclined cusp (parvus-type). But, its denticles are radially arranged. It seems to belong to a new species similar to this species, and is regarded as *H.* cf. *parvus*.

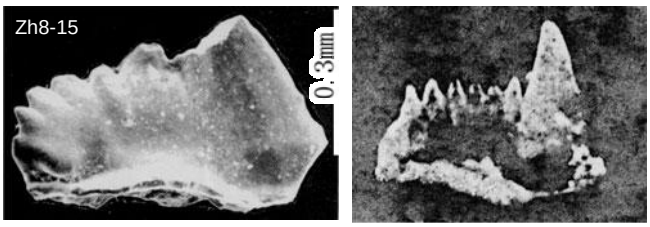

Zh8-15: *H. parvus* -Zhang et al., 1996, pl.II.8, Fig. 15; Bed 28, Section C. Right: Holotype of *H. parvus* (Kozur et Pjatakova, 1975) -Kozur, 1975, pl. 1, Fig. 17. We regard Zh8-15 as ***H.* cf. *parvus***.

Zhang et al. (1995) described conodont Z2-13 (Fig. 1.5D) from Bed 28 of Section A.

Z2-13 was placed in *Isarcicella isarcica* (Huckriede, 1958). It differs from the holotype of this species in that in the latter there is one or more than one denticle at the basal expansion on two sides, while in the former there is one denticle at the basal expansion on only one side. Dai and Zhang (1989) defined the materials with denticle at the basal expansion on only one side as *I. staeschei*. Z2-13 resembles the holotype of this species, and is assigned to *I. staeschei* Dai et Zhang (1989).

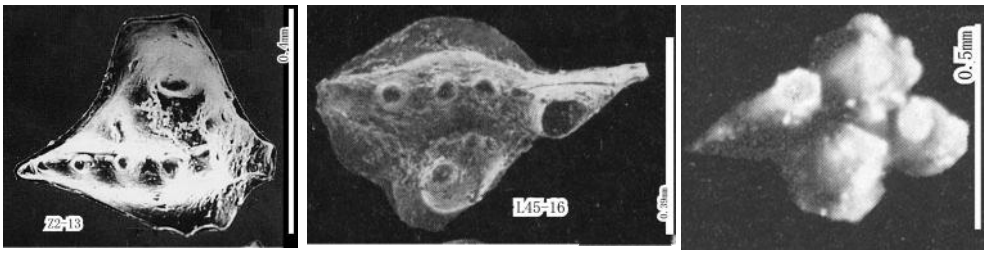

Z2-13: *Isarcicella isarcica* (Huckriede) -Zhang et al., 1995, pl. 2, Fig. 13; Bed 28, Section A. L45-16: Holotype of *I. staeschei* Dai et Zhang -Li et al., 1989, pl. 45, Fig. 16; Gsc33-2, Shangsi Section. Right: Holotype of *I. isarcica* (Huckriede, 1958) -pl. 10，fig. 7. We think Z2-13 belongs to ***I. staeschei*** Dai et Zhang.

Li et al. (1989) described conodont L45-18 (Fig. 1.5E) from Bed 33 ("Gsc33-2") of Shangsi section (probably equivalent to Bed 28 of Section D).

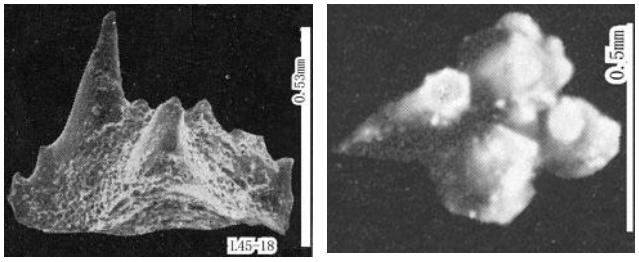

L45-18: *I. isarcica* (Huckriede) -Li et al., 1989, pl. 45, Fig. 18. Right: Holotype of *I. isarcica* (Huckriede, 1958). L45-18 belongs to ***I. isarcica***.

L45-18 was placed in *I. isarcica* (Huckriede). It resembles to the holotype of this species in that it has denticles at the basal expansions on both sides.

Matsuda (1981) described conodonts Ma1-6 (Fig. 1.5F) and Ma1-5 (Fig. 1.5G) from Bed 61 of Kashmir section (=Bed 28 of Section D).

Ma1-6 was placed in *H. minutus*. Ma1-6 greatly differs from the holotype of this species in blade shape and denticle pattern, and cannot be assigned to this species. It is characterized by very strong, conical denticles and undeveloped basal expansion. It seems to belong to a new species, and is regarded as ***H.* sp. 3**.

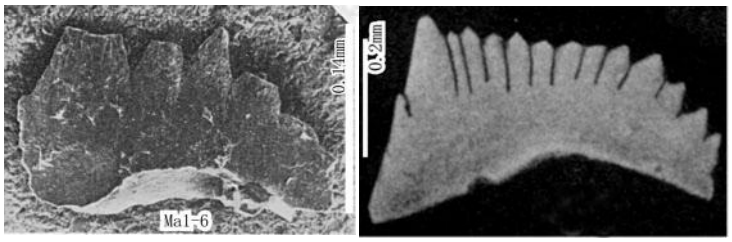

Ma1-6: *H. minutus* (Ellison, 1941) –Matsuda, 1981, pl. 1, fig. 6. Right: Holotype of *H. minutus* (Ellison, 1941). We regard Ma1-6 as ***H.* sp. 3**.

Ma1-5 was placed in *H. minutus* (Ellison, 1941), too. It has depressed basal margin, instead of basal expansion, and lateral costae, and cannot be assign to this genus. It belongs to *Neospathodus*. All denticles are reclined, same in shape, and similar in size. It seems to belong to a new species, and is regarded as ***Neospathodus* sp. 1**.

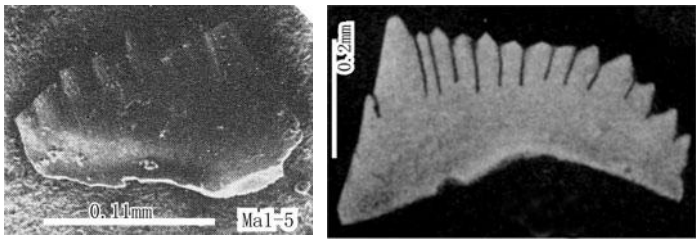

Ma1-5: *H. minutus* (Ellison, 1941) -Matsuda, 1981, pl. 1, fig. 5. Right: Holotype of *H. minutus* (Ellison, 1941). We regard Ma1-5 as ***Neospathodus* sp. 1.**

1.4 Revision on the conodont zones of PTB interval

Changes in conodont assignments lead to changes in the geological ranges of the related taxa. Correspondingly, some conodont zones previously defined and the occurrences of some evolutionary events need to revise. Many researchers have studied the conodont zone division for the PTB interval. The latest and most important scheme (Table 1.2) is that by Yin et al. (2001).

Previous researchers defined the conodonts of Bed 24e as *C. changxingensis yini* zone, with the first appearance of *C. changxingensis yini* as the base of this zone. As discussed above, *C. changxingensis yini* should be *C. yini*. It is present not only in Bed 24e, but also in Bed 25 and

even Bed 26. Previous researchers stated that there were 12 conodont species in Bed 24e. Actually, there are only 4 (see Table 1.3) species. Of them, *H. inflatus* lasted into Bed 27a. *C. myridentalis* is present in Beds 24e to 25. Since both *C. yini* and *C. myridentalis* are present in Beds 24e and 25, we regard the conodonts in these two beds as one fauna, named as *C. yini* zone or *C. myridentalis* zone. This zone is characterized by the presence of *C. yini* and/or *C. myridentalis*. *C. parasubcarinata* is also an important component of this zone, though it also appeared in below Bed 24.

Table 1.2 Conodont zones of PTB interval proposed by Yin et al. (2001)

	Beds	Conodonts	Subdivision	Conodont zone
Yinkeng Formation	28	*Isarcicella isarcica* (Section A)		*I. isarcica* zone
		H. parvus		*H. parvus* zone
	27c	*H. parvus*		
	27b	*H. latidentatus*	*H. typicalis* Fauna	*H. latidentatus-C. meishanensis* zone
	27a	*H. typicalis*		
	26	*C. changxingensis* (Section F), *C. deflecta, C. meishanensis, C. carinata, C.* sp., *typicalis*	*C. meishan-ensis* Fauna	
	25	*C. changxingensis, C. carinata, C. deflecta, C. meishanensis, H. typicalis, H. latidentatus*		
Changxing Formation	24e	*C. changxingensis yini*，*C. subcarinata, C. changxingensis, C. deflecta, C. carinata, H. typicalis* (Section G)		*C. changxingensis yini* zone

Previous researchers defined Beds 25 to 27b as *H. latidentatus-C. meishanensis* zone. It is divided as two faunas: *C. meishanensis* fauna in Beds 25 to 26, and *H. typicalis* fauna in Beds 27a to 27b. Yin et al. believed that *C. meishanensis* occurred in Beds 25 and 26. This study shows that it actually occurs only in Bed 26.

According to previous researches, *H. typicalis* occurs in Beds Bed 24a to 29. Actually, however, the specimens from Bed 27a (Fig. 1.3I) assigned to this species by Zhang et al. (1995) belongs to a new species, *H. zhejiangensis* sp. nov.; the specimen from Bed 27b (Fig. 1.3M) assigned to this species by Wang (1995) actually belongs to *H. changxingensis*; the specimen from Bed 24e (Fig. 1.1D) assigned to this species by Zhang et al. (1996) actually belongs to *H. inflatus* Nicoll et al. (2002). So, Bed 27a and 27b cannot be defined as *H. typicalis* fauna.

Table 1.3 Conodont zone division for PTB interval suggested in this work

Beds	Conodonts	Conodont zones
28	***H.* cf. *parvus* 1**, ***H.* cf. *parvus* 2**, ***H.* sp. 2**, ***H.* sp. 3**, *I isarcica*, *I. staeschei*, ***Neospathodus* sp.1**.	*I. staeschei* zone
27d	***C. paradeflecta***, ***C.* sp. 8**, ***H. amblyodontus***, ***H. angustus***, ***H. arcuatus***, ***H.* cf. *parvus***, ***H.* cf. *typicalis***, ***H. changxingensis rotundus***, ***H. coalitus***, ***H. difformis***, ***H. irregularis***, *H. parvus*, ***H. proparvus***, ***H. scalaris***, ***H. scutatus***, ***H. similes***, ***H.* sp. 1**, *Neospathodus anterodentata*	*H. parvus* zone
27c		
27b	***C. elliptica***, ***C. paradeflecta***, *H.* cf. *changxingensis*, ***H. changxingensis flatus***, ***H. changxingensis levis***, ***H. changxingensis rotundus***, *H. decrescens*, ***H. difformis***, *H. eurypyge*, *H. inflatus*, ***H. limus***, ***H. pectinatus***, ***H. turgidus brevis***, ***H. zhejiangensis***	*H. changxing-ensis levis* zone
27a		
26	***C.* cf. *yini***, ***C. columnaris***, ***C. deflecta* subsp.1**, ***C. deflecta* subsp. 2**, ***C. deflecta* subsp. 3**, ***C. dicerocarinata* subsp. 1**, ***C.* cf. *dicerocarinata***, *C. meishanensis*, ***C.* cf. *meishanensis***, ***C. paradeflecta***, ***C.* sp. 4**, ***C.* sp. 5**, ***C.* sp. 6**, ***C.* sp. 7**	*C. meishan-ensis* zone
25	***C. anisomerus***, ***C. myridentalis***, ***C. plana***, ***C. redactus***, ***C.* sp. 1**, ***C.* sp. 2**, ***C.* sp. 3**, *C. yini*, ***H. humilis*** (wrong horizon?), *H. inflatus*	*C. yini* zone
24e	***C. myridentalis***, *C. parasubcarinata*, *C. yini*, *H. inflatus*	

According to previous researches, *H. latidentatus* occurs in Beds 24a to 29. Actually, the specimen from Bed 25 (Fig. 1.2O) assigned to this species by Zhang et al. (1996) belongs to *H. humilis* sp. nov. The specimen from Bed 27b (Fig. 1.3J) assigned to this species by Zhang et al. (1996) actually belongs to *H. changxingensis*. Another specimen from Bed 27b (Fig. 1.3K) assigned to this species by Zhang et al. (1996) actually belongs to *H. difformis*. So, *H. latidentatus* cannot be used to define the conodont zone of Beds 25 to 27b.

An important fact is that the conodonts of Bed 26 are almost all components of *Clarkina*, while the conodonts of Bed 27a and the above beds are almost all components of *Hindeodus*. That is, the boundary between Beds 26 and 27a is an important biotic evolutionary boundary. For this reason, the conodonts of Beds 26 and 27a cannot be put into one conodont fauna.

As shown above, the occurrence of revised *C. meishanensis* is limited to Bed 26. Beside, Bed 26 yields two subspecies of *C. deflecta*. Previous researchers (Mei et al., 1998; Zhang et al.,

1995; Zhang et al., 1996) reported *C. deflecta* from Beds 24e and 25. The current study denies the occurrence of this species in these two beds. So, the two new subspecies of *C. deflecta* are distributed only in bed 26. The conodont fauna of Bed 26 is different from those of Bed 24e and 27a, and should be defined as an independent conodont zone. The holotype of *C. deflecta* is from Bed 24d (Wang, C., Shen, S., personal comm.), and different from the two subspecies in Bed 26. We define the conodont fauna of Bed 26 as *C. meishanensis* Zone. Even so, the two subspecies of *C. deflecta* have wider distribution, and are more effective index fossil of this zone.

In Beds 27a and 27b, components of *Hindeodus* abruptly became dominant. The conodonts of these two beds have no parvus-type cusp (more than two times wider than other denticles and reclined). The most characteristic component of Beds 27a and 27b is *H. changxingensis*, which has an adenticulate top face. This species has wide distribution in Sections D, Z and Shangsi section. We define the conodonts of Beds 27a and 27b as *H. changxingensis* zone. *H. turgidus* is an impressive component of this zone.

The conodonts of Beds 27c and 27d were defined as *H. parvus* zone by Yin et al. (2001). In these two beds, *Hindeodus* components with parvus-type cusp abruptly flourished (including 5 species). The conodonts were still dominated by *Hindeodus* components, and are different from those of Bed 28. So, they belong to an independent conodont fauna. *H. parvus* is the most widely distributed component of this fauna (Wang, 1995; Zhang et al., 1996; Li et al., 1989; Matsuda, 1981; Yang et al., 1999; Yao et al., 1987; Perri, 1991). So, to define the conodonts of Beds 27c and 27d as *H. parvus* zone is proper. This zone is characterized by the presence of *H. parvus* and the absence of *I. staeschei*. Besides, *H. scutatus* and *H. difformis* are two other important index fossils of this zone.

Conodonts of Beds 28 and 29 are previously defined as *Isarcicella isarcica* zone. Here we discuss only the conodonts of Bed 28. In Beds 28, the conodont diversity abruptly decreased to several species (there are about 19 species in Beds 27c and 27d), and has different composition. *H. parvus* was believed to last into Beds 28 and 29. But, those in Beds 28 and 29 are different from typical *H. parvus* (Fig. 1.4N). Other conodonts are new components of *Isarcicella*, *Neospathodus*, and probably *Hindeodus*. *I. staeschei* is the most common conodont of Bed 28. It has been reported from Meishan, Shangsi and Kashmir sections (Zhang et al., 1995; Li et al., 1989; Matsuda, 1981).

Only one specimen of *Isarcicella* has been found from Meishan sections (Section A). It was wrongly assigned to *I. isarcica* by Zhang et al. (1995), and the conodont fauna of Bed 28 was named as *I. isarcica* zone by them. Actually, this specimen belongs to *I. staeschei*. Yang et al. (1999) found that in many sections in South China *I. staeschei* appeared early than *I. isarcica*. Its late presence was accompanied by *I. isarcica*. For this reason, Yang et al. (1999) established two conodont zones: *I. staeschei* zone and *I. isarcica* zone. In Meishan and Kashmir sections, *I. staeschei* occurred in the absence of *I. isarcica*. Thus, we define Bed 28 as *I. staeschei* zone. In Shangsi section, *I. staeschei* occurs together with *I. isarcica* in the deposits overlying the *H. parvus* zone, which probably indicates the absence of *I. staeschei* zone.

1.5 Descriptions of new taxa

Clarkina myridentalis sp. nov. (Fig. 1.2A, H)

Diagnosis. A *Clarkina* with an ovate platform strongly and evenly arched up, denticles small, basally fused, similar in size and shape, anterior denticles basally fused, posterior cusp small, cone-like, slightly proclined. Fig. 1.2A is the holotype.

Clarkina yin Mei et al., 1998 (Fig. 1.2B)

Diagnosis. A *Clarkina* with a strongly and evenly arched platform, reclined denticles similar in form and posteriorward decreasing in size.

Clarkina plana sp. nov. (Fig. 1.2I)

Diagnosis. A *Clarkina* with a flat platform with two sides nearly parallel, denticles discrete, high, cone-like, and decrease in size from anterior to posterior, a large cusp slightly reclined and with an elongate cross section.

Clarkina anisomerus sp. nov. (Fig. 1.2K)

Diagnosis. A *Clarkina* with an arched-up platform with a subround, but slightly asymmetric posterior end, denticles very small, basally fused, anterior denticles fused into a par, with a undeveloped posterior cusp.

Clarkina redactus sp. nov. (Fig. 1.2L)

Diagnosis. A *Clarkina* with an arched-up platform with a asymmetric subround posterior end, all denticles fused into a ridge, posterior cusp undeveloped.

Clarkina columnaris sp. nov. (Fig. 1.2S)

Diagnosis. A *Clarkina* with a nephroid platform, strong, thick denticles densely arranged, two deep adcarina grooves, and a small posterior cusp.

Clarkina elliptica sp. nov. (Fig. 1.3D)

Diagnosis. A *Clarkina* with an elliptic platform, which sharply pass into the anterior bar, 7 to 8 denticles very low and wide, ridge-like, top surface with reticulate accouterment, which is irregular near the carina, and some round holes, no obvious cusp.

Clarkina paradeflecta sp. nov. (Fig. 1.3H, 1.4L)

Diagnosis. A *Clarkina* with an asymmetric linguiform, rather than rhombic posterior platform end, denticles more or less fused, carina turns right at the posterior end and reaches the terminal end of the platform, cusp not prominent. Fig.1.3H is the holotype.

Hindeodus humilis sp. nov. (Fig. 1.2O)

Diagnosis. A *Hindeodus* with a very large cusp, denticles at top face as well as posterior face, and developed basal expansion laterally extending.

Hindeodus turgidus brevis subsp. nov. (Fig. 1.3A)

Diagnosis. A *Hindeodus turgidus* with larger blade, no prominent cusp, but 4 low denticles at top face. In oral view, its length is about two times of its width.

Hindeodus turgidus minutus subsp. nov.

Diagnosis. A *Hindeodus turgidus* with small blade, no prominent cusp, but 6-8 low denticles at top face. In oral view, its length is more than two times of its width. The holotype of this species is used as the holotype of this subspecies.

Hindeodus changxingensis flatus subsp. nov. (Fig. 1.3B)

Diagnosis. A *Hindeodus changxingensis* with a flat adenticulate top face, an anterior face reclined at about 70 degrees, some undeveloped denticles at posterior face and between the cusp and top face, basal expansion falciform.

Hindeodus limus sp. nov. (Fig. 1.3E)

Diagnosis. A *Hindeodus* with a cusp about 2 times wider than denticles and slightly reclined, denticles at only top face erect and similar in shape and size, denticle tips arranged in a straight line, basal expansion belt-like.

Hindeodus pectinatus sp. nov. (Fig. 1.3F)

Diagnosis. A *Hindeodus* with a cusp similar to denticles in size and shape, denticles pillar-like, blunt, basally fused, radially arranged at top face and posterior face, basal expansion belt-like.

Hindeodus zhejiangensis sp. nov. (Fig. 1.3I)

Diagnosis. A *Hindeodus* with a cusp similar to denticles in shape and size, denticles at top face and posterior face, in low conical shape, posterior denticles wider, denticle tips arranged in S-shape line, basal expansion lunular in shape.

Hindeodus changxingensis levis subsp. nov. (Fig. 1.3J)

Diagnosis. A *Hindeodus changxingensis* with no denticle.

Hindeodus changxingensis rotundus subsp. nov. (Fig. 1.3M, 1.4R)

Diagnosis. A *H. changxingensis* with more denticles at between the cusp and top face, top face not flat but declined posteriorly. Fig. 1.3M is the holotype.

Hindeodus irregularis sp. nov. (Fig. 1.4A)

Diagnosis. A *Hindeodus* with a very big cusp (more than 2 times wider than denticles), denticles conical in shape, more or less irregular in size and arrangement at top face and posterior face, basal expansion lunate in shape.

Hindeodus difformis sp. nov. (Fig. 1.4C, J, O)

Diagnosis. A *Hindeodus* with a cusp 3 times wider than denticles, denticles at top face, posterior face, as well as between cusp and top face, different in height and width, denticles at between top face and posterior face much wider, tips of denticles and cusp arranged in S-shape line, basal expansion belt-like. Fig. 1.4C is the holotype.

Hindeodus scutatus sp. nov. (Fig. 1.4D, P)

Diagnosis. A *Hindeodus* with a big cusp about two times wider than denticles, denticles conical in shape, increasing in size posteriorly, basal expansion very wide, laterally extending. Fig. 1.4D is the holotype.

Hindeodus similes sp. nov. (Fig. 1.4F)

Diagnosis. A *Hindeodus* with a cusp similar to denticles in shape and size, denticles at top face and posterior face all erect, similar in shape and size, basal expansion belt-like.

Hindeodus amblyodontus sp. nov. (Fig. 1.4H)

Diagnosis. A *Hindeodus* with a cusp slightly higher than denticles, denticles pillar-like, basally fused, posterior denticles lower but wider, no denticles at posterior face, basal expansion belt-like.

Hindeodus proparvus sp. nov. (Fig. 1.4I)

Diagnosis. A *Hindeodus* with a cusp 2~3 times wider than denticles and slightly reclined, denticles at only top face, increasing in width posteriorly, anterior face arcual, basal expansion belt-like.

Hindeodus coalitus sp. nov. (Fig. 1.4Q)

Diagnosis. A *Hindeodus* with a cusp similar to denticles in shape and size, denticles very blunt, at only top face, all fused, tips of denticles and cusp arranged in S-shape line, basal expansion spherical.

Hindeodus angustus sp. nov. (Fig. 1.4U)

Diagnosis. A *Hindeodus* with a cusp 2 times wider than denticles, denticles all high conical in shape, radially arranged at top face and posterior face, tips of denticles and cusp arranged in S-shape line, basal expansion belt-like.

Hindeodus arcuatus sp. nov. (Fig. 1.4V)

Diagnosis. A *Hindeodus* with a cusp similar to denticles in shape and size, denticles at top face, posterior face, as well as between the cusp and top face, small, conical, anterior base rounded, basal expansion not prominent.

Hindeodus scalaris sp. nov. (Fig. 1.4W, M)

Diagnosis. A *Hindeodus* with a cusp 2 times wider than denticles, denticles at only top face, all erect, conical in shape, similar in size, tips of denticles arranged in a straight line, basal expansion belt-like. Fig. 1.4W is the holotype.

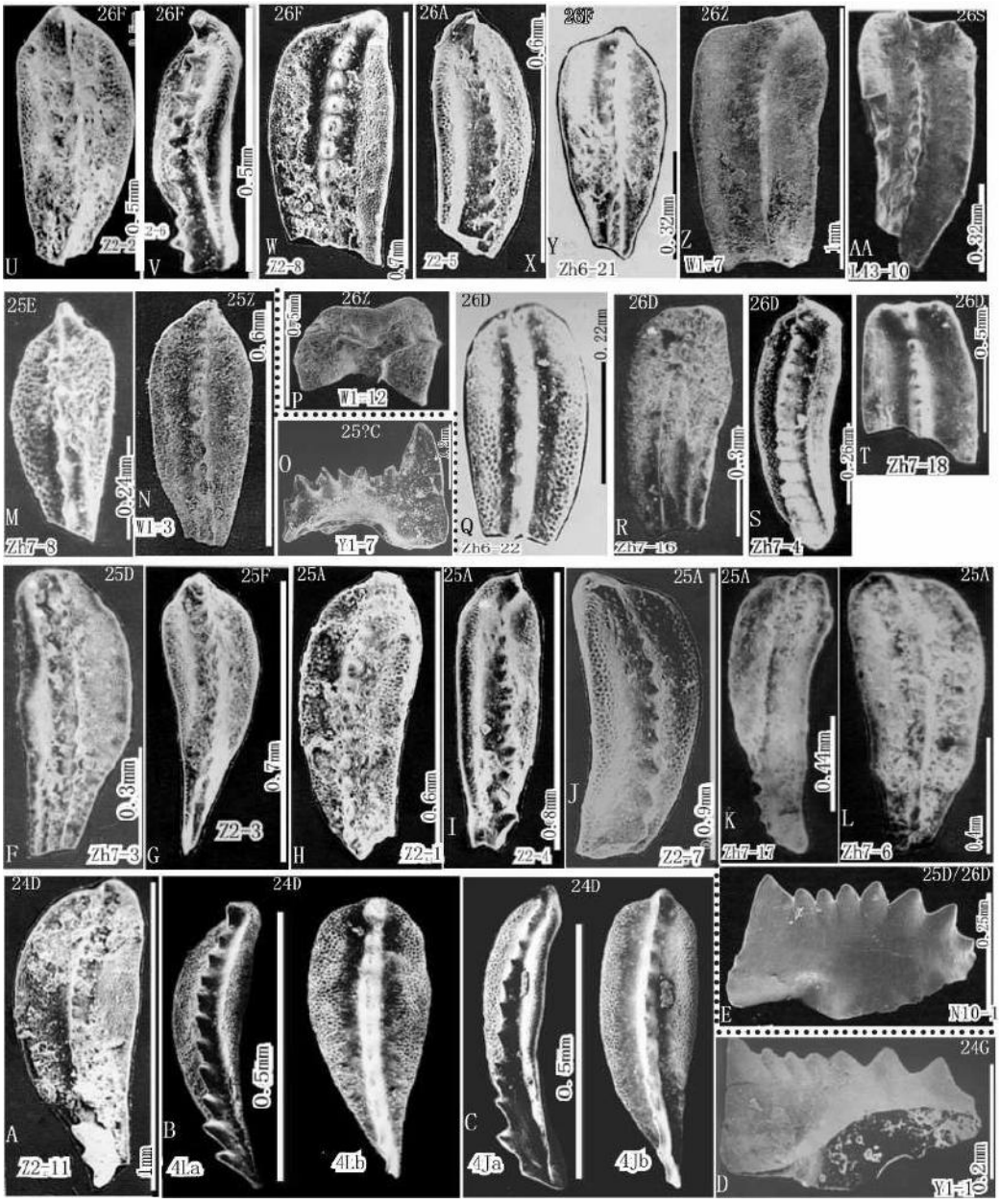

Fig. 1.2**A -Z, AA**. Conodonts from Beds 24e, 25 and 26. (*C.* =*Clarkina*, *H.* =*Hindeodus*, D/24e=Bed 24e of Section D, others contractions in similar way). ***A -D.*** Conodonts from Bed 24e. **A**, *C. myridentalis* sp. nov. (Holotype), =*C. subcarinata* (Sweet) -Zhang et al., 1995, pl. 2, Fig. 11, from D/24e. **B**, *C. yini* Mei et al., 1998 (Holotype), ＝*C. changxingensis yini* - Mei et al., 1998, pl. 4, figs. La, Lb, from D/Mc -43. **C**, *C. parasubcarinata* Mei et al., 1998, ＝*C. deflecta* (Wang et Wang, 1981) - Mei et al. 1998, pl. 4, figs.Ja, Jb, from D/Mc -43. **D**, *H. inflatus* Nicoll et al., 2002, =*H. typicalis* (Sweet) -Zhang et al., 1996, pl. 1, Fig. 1, from G/24e. ***E -O***. Conodonts from Bed 25. **E**, *H. inflatus* Nicoll et al., 2002, =*H. inflatus* (Holotype) -Nicoll et al. 2002, Fig. 10 -1, from D/25~26. **F**, *C.* sp. 1, ＝*C. changxingensis* - Zhang et al., 1996, pl. II.7, fig. 3, from D/25. **G**, *C. yini* Mei et al., 1998, =*C. carinata* (Clark) -Zhang et al., 1995, pl. 2, fig. 3, from F/25. **H**, *C. myridentalis* sp. nov., =*C. changxingensis* (Wang et Wang, 1981) -Zhang et al., 1995, pl. 2, Fig. 1, from A/25. **I**, *C. plana* sp. nov. (Holotype), =*C. meishanensis* – Zhang et al., 1995, pl. 2, fig. 4, from A/25. **J**, *C.* sp. 2, ＝*C. deflecta* (Wang et Wang, 1981) -Zhang et al. 1995, pl. 2, fig. 7, from A/25. **K**, *C. anisomerus* sp. nov. (Holotype),＝*C. deflecta* -Zhang et al., 1996, pl. II.7, Fig. 17, from A/25. **L**, *C. redactus* sp. nov. (Holotype), = *C. deflecta* -Zhang et al., 1996, pl. II.7, fig. 6, from A/25. **M**, *C.* sp. 3, = *C. carinata* -Zhang et al., 1996, pl. II.7, fig. 8, from E/25. **N**, *C. plana* sp. nov., =*C.* sp. -Wang, 1995, pl. 1, fig. 3, from Z/880 (=D/25). **O**, *H. humilis* sp. nov. (Holotype), =*H. latidentatus* -Zhang et al., 1996, pl. 1, fig. 7, from C/25 (wrong horizon?). ***P -Z, AA.*** Conodonts from Bed 26. **P**, *C. dicerocarinata* subsp. 1, =*C. dicerocarinata*? (Wang et Wang, 1981) -Wang, 1995, pl. 1, Fig. 12, from Z/881 (=D/26). **Q**, *C.* sp. 4, = *C. changxingensi*s -Zhang et al., 1996, pl. II.6, fig. 22, from D/26. **R**, *C.* sp. 5, = *C. deflecta* -Zhang et al., 1996, pl. II.7, Fig. 16, from D/26. **S**, *C. columnaris* sp. nov. (Holotype), = *C.* sp. -Zhang et al., 1996, pl. II.7, fig. 4, from D/26. **T**, *C.* sp. 6, = *C. deflecta* -Zhang et al., 1996, pl. II.7, Fig. 18, from D/26. **U**, *C.* sp. 7, =*C. changxingensis* (Wang et Wang, 1981) -Zhang et al., 1995, pl. 2, fig2, from F/26. **V**, *C. meishanensis* Zhang et al., 1995, (here designated as holotype), =*C. meishanensis* (No designation of holotype) -Zhang et al., 1995, from F/26. **W**, *C. deflecta* subsp. 1, =*C. deflecta* (Wang et Wang, 1981) - Zhang et al., 1995, pl. 2, fig. 8, from F/26. **X**, *C.* cf. *yini* Mei et al., 1998, =*C. meishanensis* - Zhang et al., 1995, pl. 2, fig. 5, from A/26. **Y**, *C. paradeflecta* sp. nov., = *C. deflecta* -Zhang et al., 1996, pl. II.6, fig. 21, from F/26. **Z**, *C. deflecta* subsp. 3, =*C. deflecta* (Wang et Wang, 1981) -Wang, 1995, pl. 1, fig. 7, from Z/881 (=D/26). **AA**, *C.* cf. *dicerocarinata*, =*Neogondolella tulongensis* Tian -Li et al., 1989, pl. 43, figs.10, 11, from Shangsi/27 (=D/26).

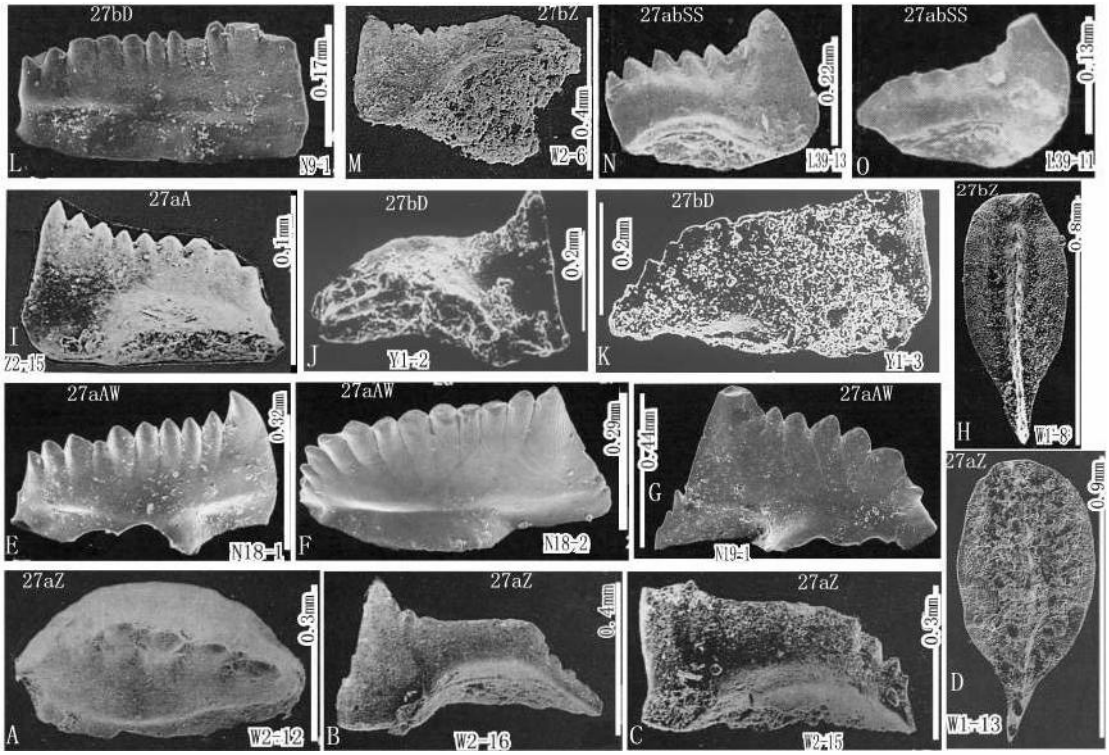

Fig. 1.3**A -O**. Conodonts from Beds 27a and 27b. (*C.* =*Clarkina*, *H.* =*Hindeodus*, D/27a=Bed 27a of Section D, others contractions in similar way). **A**, *H. turgidus brevis* subsp. nov., = *H.* cf. *turgidus* (Kozur, Mostler et Rahimi -Yazd, 1975) -Wang, 1995, pl. 2, figs.12, 13, from Z/882-1 (=D/27a). **B**, *H. changxingensis flatus* subsp. nov., = *H. changxingensis* (Holotype) -Wang, 1995, pl. 2, Fig. 16, from Z/882 -1 (=D/27a). **C**, *H.* cf. *changxingensis*, = *H. changxingensis* –Wang, 1995, pl. 2, fig. 15, from Z/882-1 (=D/27a). **D**, *C. elliptica* sp. nov. (Holotype), = *C.* cf. *planata* (Clark, 1959) -Wang, 1995, pl. 1, Fig. 13, from Z/882-1 (=D/27a). **E**, *H. limus* sp. nov. (Holotype), = *H. priscus* (Kozur, 1995) -Nicoll et al., 2002, pl. 18, fig. 1, from AW/27a. **F**, *H. pectinatus* sp. nov. (Holotype), = *H. priscus* (Kozur, 1995) - Nicoll et al., 2002, pl. 18, fig. 2, from AW/27a. **G**, *H. inflatus* Nicoll et al., 2002, = *H.* n. sp. A -Nicoll et al., 2002, pl. 19, fig. 1, from AW/27a. **H**, *C. paradeflecta* sp. nov. (Holotype), = *C. deflecta* (Wang et Wang, 1981) -Wang, 1995, pl. 1, fig. 8, from Z/882-2 (=D/27b). **I**, *H. zhejiangensis* sp. nov. (Holotype), ＝*H. typicalis* (Sweet) -Zhang et al., 1995, pl. 2, fig. 15, from A/27a. **J**, *H. changxingensis levis* subsp. nov. (Holotype), = *H. latidentatus* (Kozur, Mostler et Rahimi-Yazd) -Zhang et al., 1996, pl. 1, fig. 2, from D/27b. **K**, *H. difformis* sp. nov., =*H. latidentatus* (Kozur, Mostler et Rahimi-Yazd) -Zhang et al., 1996, pl. 1, fig. 3, from D/27b. **L**, *H. eurypyge* Nicoll et al., 2002, = *H. eurypyge* -Nicoll et al., 2002, pl. 9, fig. 1, from D/27b. **M**, *H. changxingensis rotundus* subsp. nov., = *H. typicalis* (Sweet, 1970) -Wang, 1995, pl. 2, fig. 6, from Z/882-2 (=D/27b). **N**, *H. decrescens* (Dai et Zhang, 1989) = *H. decrescens* (Dai et Zhang, 1989) (Holotype) -Li et al., 1989, pl. 39, fig. 13, from Shangsi/29 (=D/27a-b). **O**, *H. changxingensis levis* subsp. nov., = *H. decrescens* (Dai et Zhang, 1989) –Li et al., 1989, pl. 39, Fig. 11, from Shangsi/29 (=D/27a-b).

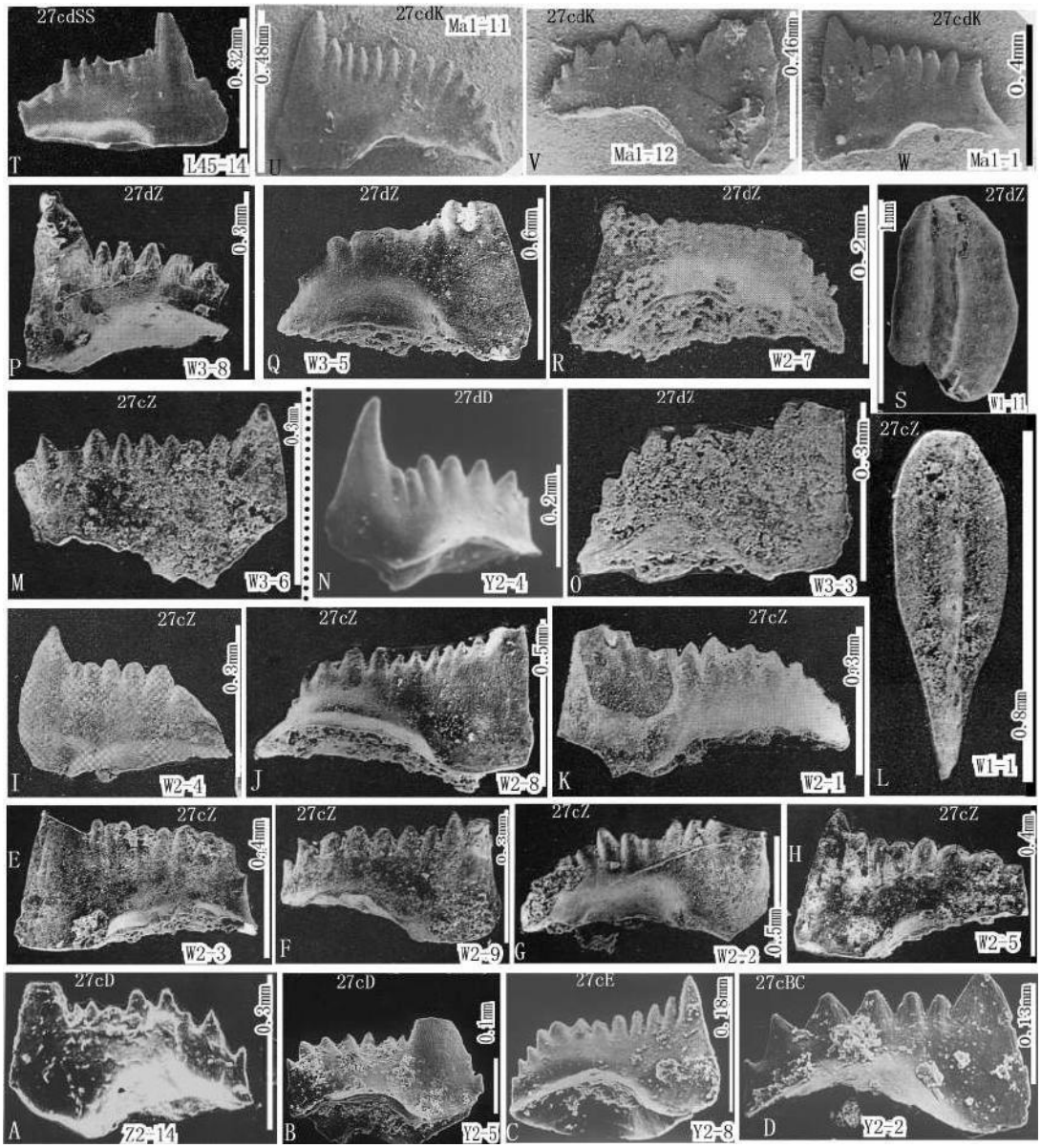

Fig. 1.4**A -W**. Conodonts from Beds 27c and 27d. (*C.* =*Clarkina*, *H.* =*Hindeodus*, *N.* =*Neospathodus*, D/27c=Bed 27c of Section D, others contractions in similar way). **A**, *H. irregularis* sp. nov. (Holotype), = *Isarcicella parva* (Kozur et Pjatakova) -Zhang et al., 1995, pl. 2, Fig. 14, from D/27c. **B**, *H. parvus*, = *H. parvus* -Zhang et al., 1996, pl. 2, fig. 5, from D/27c. **C**, *H. difformis* sp. nov. (Holotype), = *H. parvus* -Zhang et al., 1996, pl. 2, fig. 8, from E/27c. **D**, *H. scutatus* sp. nov. (Holotype), = *H. latidentatus* (Kozur, Mostler et Rahimi-Yazd) -Zhang et al., 1996, pl. 2, fig. 2, from a section between B and C/27c. **E**, *H.* cf. *parvus*, = *H.* cf. *turgidus* (Kozur Mostler et Rahimi-Yazd, 1975) -Wang, 1995, pl. 2, fig. 3, from Z/882-3 (=D/27d). **F**, *H. similes* sp. nov. (Holotype), = *H.* cf. *turgidus* (Kozur, Mostler et Rahimi-Yazd 1975) -Wang, 1995, pl. 2, fig. 9, from Z/882-3 (=D/27d). **G**, *H.* cf. *typicalis*, = *H. parvus* morphotype 2 -Wang, 1995, pl. 2, fig. 2, from Z/882-3 (=D/27d). **H**, *H. amblyodontus* sp. nov. (Holotype), = *H. latidentatus* (Kozur, Mostler

et Rahimi-Yazd, 1975) -Wang, 1995, pl. 2, fig. 5, from Z/882-3 (=D/27d). **I**, *H. proparvus* sp. nov. (Holotype), = *H. latidentatus* (Kozur, Mostler et Rahimi-Yazd, 1975) -Wang, 1995, pl. 2, fig. 4, from Z/882-3 (=D/27d). **J**, *H. difformis* sp. nov., = *H.* cf. *turgidus* (Kozur Mostler et Rahimi-Yazd, 1975) -Wang, 1995, pl. 2, fig. 8, from Z/882-3 (=D/27d). **K**, *H.* sp. 1, = *H. parvus* morphotype 2 -Wang, 1995, pl. 2, fig. 1, from Z/882-3 (=D/27d). **L**, *C. paradeflecta* sp. nov., = *C. changxingensis* (Wang et Wang, 1981) -Wang, 1995, pl. 1, fig. 1, from Z/882-3 (=D/27d). **M**, *H. scalaris* sp. nov., = *H. parvus* Mophotype1 -Wang, 1995, pl. 3, fig. 6, from Z/882-3 (=D/27d). **N**, *H. parvus*, = *H. parvus* -Zhang et al., 1996, pl. 2, fig. 4, from D/27d. **O**, *H*. *difformis* sp. nov., = *H. parvus* Mophotype 2 –Wang, 1995, pl. 3, fig. 3, from Z/882-4 (=D/27d). **P**, *H. scutatus* sp. nov., = *H. parvus* Mophotype1 –Wang, 1995, pl. 3, fig. 8, from Z/882-4 (=D/27d). **Q**, *H*. *coalitus* sp. nov. (Holotype), = *H. turgidus* (Kozur, Mostler et Rahimi-Yazd, 1975) -Wang, 1995, pl. 3, fig. 5, from Z/882-4 (=D/27d). **R**, *H. changxingensis rotundus* subsp. nov., = *H. typicalis* (Sweet, 1970) -Wang, 1995, pl. 2, fig. 7, from Z/882-4 (=D/27d). **S**, *C.* sp. 8, = *C.* sp. -Wang, 1995, pl. 1, fig. 11, from Z/882-4 (=D/27d). **T**, *N. anterodentata* (Dai et Tian, 1989), = *H. anterodentata* (Dai et Tian, 1989) -Li et al., 1989, pl. 45, fig. 14, from Shangsi/31~32 (=D/27d). **U**, *H. angustus* sp. nov. (Holotype), = *H. minutus* (Ellison, 1941) –Matsuda, 1981, pl. 1, fig. 11, from Kashmir/ 57 (=D/27d). **V**, *H. arcuatus* sp. nov. (Holotype), = *H. minutus* (Ellison, 1941) –Matsuda, 1981, pl. 1, fig. 12, from Kashmir/57 (=D/27d). **W**, *H. scalaris* sp. nov. (Holotype), = *H. minutus* (Ellison, 1941) -Matsuda, 1981, pl. 1, fig. 1, from Kashmir/57 (=D/27d).

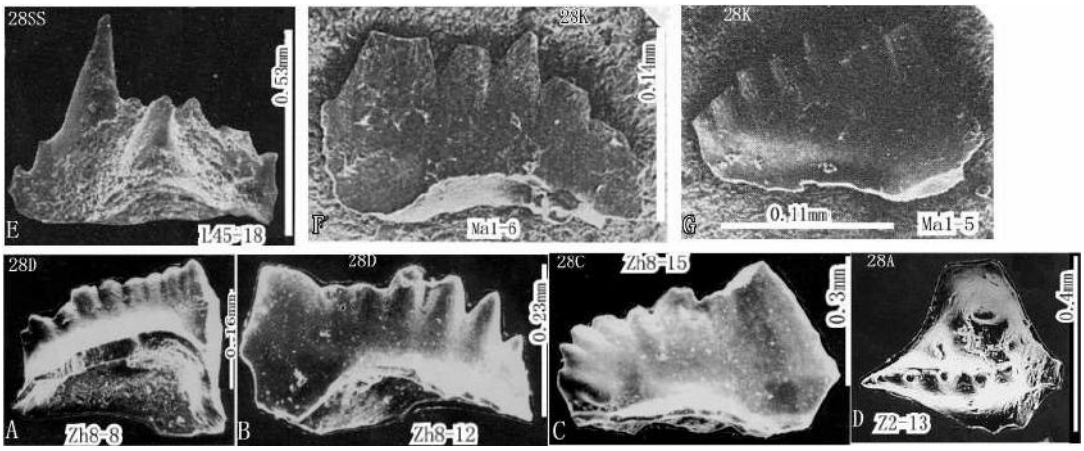

Fig. 1.5**A -G**. Conodonts from Bed 28. (*H. =Hindeodus*, *I. =Isarcicella, N. =Neospathodus*, D/28=Bed 28 of Section D, others contractions in similar way). **A**, *H.* sp. 2, = *Isarcicella* sp. -Zhang et al., 1996, pl. II.8, fig. 8, from D/28. **B**, *H.* cf. *parvus*, =*H. parvus* -Zhang et al., 1996, pl. II.8, fig. 12, from D/28. **C**, *H.* cf. *parvus*, = *H. parvus* -Zhang et al., 1996, pl. II.8, fig. 15, from C/28. **D**, *Isarcicella staeschei* Dai et Zhang, 1989, =*Isarcicella isarcica* (Huckriede) -Zhang et al., 1995, pl. 2, fig. 13, from A/28. **E**, *Isarcicella isarcica* (Huckriede), =*Isarcicella isarcica* (Huckriede) -Li et al., 1989, pl. 45, Fig. 18, from Shangsi/33 (=D/28？). **F**, *H.* sp. 3, =*H. minutus* (Ellison, 1941) –Matsuda, 1981, pl. 1, fig. 6, from Kashmir/61 (=D/28). **G**, *N.* sp. 1, =*H. minutus* (Ellison, 1941) –Matsuda, 1981, pl. 1, fig. 5, from Kashmir/61 (=D/28).

2 Permian-Triassic Evolution of Reefs : Extinctions

Abstract For each 400-by-400km square of Earth's surface, one reef representative is selected. The quantity of the reef representatives of a geological period is the approximate of the distribution area of reefs of that period. Comparison of the reef representative quantities of various periods of the Permian and Triassic Periods shows: (1) The Guadalupian (Pg) has the most numerous reef representatives, i.e., the largest distribution of reefs, (2)The reef representative quantities of the early Wuchiapingian and Early Triassic are zero, representing two gaps of reef development, (3) During the periods following each gap, reef representative quantities increase with time, (4) Three catastrophic events are reflected in Permian to Triassic history of reefs: end-Guadalupian, end-Changhsingian and end-Carnian events.

The results of the end-Guadalupian events include: 1) the death of the Guadalupian reefs, 2) the absence of reefs from the early Wuchiapingian, 3) the decline in the diversity of many carbonate-platform invertebrates. The end-Changhsingian catastrophic events caused: 1) the death of the Changhsingian reefs, 2) the absence of reefs from the Early Triassic, 3) the disappearance of nearly all carbonate-platform invertebrates, and 4) the very scarcity of marine organisms in the Early Triassic. Though microbial deposits and stromatolite are present in Early Triassic, their meanings are totally different from common metazoan reefs: the former represent poor environmental conditions, while the latter represent favorable conditions. "Real reefs" are absent from Early Triassic. The end-Carnian catastrophic events caused: 1) the death of Ladinian-Carnian reefs, 2) the disappearance of all Ladinian-Carnian reef-building organisms. Norian-Rhaetian reef-building organisms are all different from pre-Norian reef-building organisms.

2.1 Introduction

Two mass extinction events occurred in the Permian, one at the end of the Guadalupian and the other at the end of the Changxingian (=Changhsingian). The end-Changxingian extinction is of greater magnitude: more than 90% of the Changxingian marine species disappeared (Yang et al., 1991). Many researchers have dealt with the end-Changxingian extinction, on the basis of various invertebrate groups (e.g., Yang et al., 1991; Erwin & Pan, 1996; Sepkoski, 1990; Yin, 1985; Li, 1995). This section deals with the evolution and extinction of reefs during the Permian and Triassic.

2.1.1 Reefs and Catastrophic Events

Reefs are carbonate rock bodies built by in situ organisms and thicker than adjacent

correlative strata. The growth of most reefs needs special environmental conditions, e.g., a temperature range of 25~29^{o}C, salinity range of 3.4%~3.7%, small water-depth (photic zone), and clarity and moderate turbidity of the water. Essentially, reefs represent such an environment where the carbonate production by in situ organisms is substantially greater than those of the surrounding areas. Great carbonate productions are maintained by very favorable environmental conditions. If the environmental factors of a reef become less favorable, the carbonate production will decrease and some reef-building organisms may die out, and, consequently, less mature reef structure forms (we regard framestoneto bet mature, and bafflestone to be less mature). Finally, if the environmental factors of a reef become similar to those of the surrounding areas, the reef stops growth completely and gives rise to deposition of non-reef facies sediments.

So, it is understandable that reefs are very sensitive to changes in environmental conditions and will more drastically response in external features and internal structures to environmental changes. Because reefs have more sophisticated and substantial three-dimensional structures built by in situ organisms, they can more effectively record changes in environmental conditions. So, the study of ancient reefs can reveal more information about ancient environmental changes, especially drastic environmental changes (i.e., catastrophic events).

In this section the Permian and Triassic history of reefs, their spatial and temporal distribution and relationship with mass extinctions are dealt with.

2.1.2 Parameters Reflecting the Distribution and Size of Reefs

In this section, reefs of different periods of the Permian and Triassic Periods are compared in terms of distribution area, size and main reef-builders. Since the sizes of reefs vary greatly, it is not proper to compare just the numbers of reefs reported from different periods of Permian and Triassic. A large Permian barrier reef is near 1000 km long, while many reefs are only several meters across. So, “reef representatives” are selected and compared. A “reef representative” is a typical reef selected from the reefs in each square about 400 by 400 km in area. The amount of representative reefs of a period is an approximation to the distribution area of the reefs of that period. So, the amounts of reef representatives of different ages are compared. Since the thickness of some reefs is unknown, e.g., the Early Permian reef of Sicily (Senowbari-Daryan and Di Stefano, 1988), only the thicknesses of the thickest reefs of different periods are compared. The number of reef representatives (Nrr) and maximal thickness (Tmax) are the most important two parameters to characterize the development magnitude of reefs.

2.1.3 Chronostratigraphic division of the Permian and Triassic Systems

In this study the chronostratigraphic division of the Permian by Jin et al. (1997) is followed. According to this scheme, Lower Permian consists of Zisongian (=Asselian+Sakmarian,) and

Longlinian (=Artinskian) Stages, in ascending sequence. The Middle Permian (Guadalupian) consists of Qixiaian (=Kungurian), Xiangboian (=Roadian), Maokouian (=Wordian), and Lengwuian (=Capitanian) Stages. The Upper Permian (Lepingian) consists of Wuchiapingian and Changhsingian (=Changxingian) Stages (Table 2.1).

Table 2.1 Division of the Permian Period

Series	**Stages**	**Fusulinid zone**	**Correlation**
Upper Permian (=Lepingian)	Changhsingian (=Changxingian)	*Palaeofusulina sinensis* zone	Changhsingian
		Palaeofusulina minima zone *Gallowayinella meitienensis* zone *Codonofusiella kwangsiana* zone	
	Wuchiapingian		Wuchiapingian
		-	
Middle Permian (=Guadalupian)	Lengwuian	*Metadoliolina multivoluta* zone *Yabeina gubleri* zone	Capitanian
	Maokouian	*Neoschwagerina margaritae* zone *N. craticulifera* zone	Wordian
	Xiangboian	*N. simplex-Praesumatrina neosch-wagerinoids* zone *Cancellina elliptica* zone	Roadian
	Luodianian	*Misellina claudiae* zone *Brevaxina dyhrenfurthi* zone	Kungurian
Lower Permian (=Chuanshanian)	Longlinian	*Pamirina-Darvasites ordinatus* zone	Artinskian
	Zisongian	*Robustoschwagerina schellwieni-R. ziyunensis* zone *Sphaeroschwagerina moelleri* zone *Pseudoschwagerina fusiformis* zone	Sakmarian Asselian

The division of the Triassic by Chen et al. (2000) is followed. According to the scheme, the Lower Triassic consists of Griesbachian, Nammalian, and Spathian Stages, in ascending sequence. The Middle Triassic consists of Anisian and Ladinian Stages. The Upper Triassic consists of Carnian, Norian and Rhaetian Stages (Table 2.2).

Table 2.2 Division of the Triassic System

	Stage	Conodont zones
Upper Triassic	Rhaetian	*M. posthersteini* *M. hersteini*
	Norian	*E. bidendata* *E. postera* *E. multidentata* *E. abneptis* *N. primitia*
	Carnian	*N. polygnathiformis* *N. diebeli*
Middle Triassic	Ladinian	*Gladigondolella bed* *N. mombergensis*
	Anisian	*N. costricara-P. excelsa* *N. germanicus-N. kockeli* *N. regale*
Lower Triassic	Spathian	*N. timorensis* *N. jubata* *N. collinsoni* *N. costatus*
	Nammalilan	*N. milleri* *N. waageni* *N. pakistanensis* *N. cristagalli* *N. dieneri* *N. kummelli*
	Griesbachian	*N. carinata-N. planata* *I. staeschei* *H. parvus*

(After Chen et al., 2000)

2.2 Reefs in different periods of the Permian and Triassic Periods

2.2.1 Reefs in the Early Permian

Five types of reefs have been reported from Early Permian. Reefs mainly built by phylloid algae were reported from the Sakmarian and Artinskian in Slovenia (Ramovs, 1986; Cys, 1985; Toomey and Cys, 1979). Reefs mainly constructed by *Palaeoaplysina*, a problematical hydrozoan, were reported from the Asselian through Sakmarian in the Urals (Chuvashov, 1983), the Sakmarian or early Artinskian of Yukon (Davis, 1989), and the Virgilian through Sakmarian in east-central Idaho (Breuninger et al., 1989). Reefs mainly constructed by bryozoans were reported from the Artinskian and Sakmarian in southwestern Ellesmere Island (Beauchamp, 1989a, b). *Tubiphytes*-calcisponge reefs were reported from the Sakmarian of West Texas (Wahlman, 1985). Calcisponge-bryozoan reefs were reported from the Sakmarian of West Texas (Schatzinger, 1983). Phylloid algal-calcisponge reefs were reported from the Sakmarian of west Texas and southeastern New Mexico (Wahlman, 1988). Tetracoral-calcisponge reefs were reported from the Artinskian of Pishan County, Xinjiang, China (Yu, 1990). Boundstone built by blue-green algae dominated by *Girvanella* was reported from the Artinskian of south Qinling Mountains (Gong and Fan, 1999). Very thick calcisponge reefs occur in the Asselian –Artinskian of Ruoqiang, Xinjiang (Tian, Shugang, Personal comm.). *Palaeoaplysina* reefs of Early Permian age have been reported from Svalbard (Worsley, 1986; Skang et al., 1982), and from the island of Bjornoya on the western margin of the Barents Shelf (Lonoy, 1988).

From these reefs, 9 representatives are selected: Urals, Yugoslavia, Texas and New Mexico, Idaho, Yukon, Ellesmere Island, Bjornoya, Svalbard, Southern Alps. So, Nrr = 9.

Most of the Early Permian reefs are of small or very small size. But two of them are of great thickness: one from New Mexico and the other from Ellesmere Island, both 130 m thick maximally. So, for the Early Permian reefs, Tmax = 130.

The Early Permian reefs were mainly built by bryozoans, *Tubiphytes*, a problematicum probably including foraminifers and thalamid sponges, *Palaeoaplysina*, a sheetlike organism interpreted as a hydrozoan by some researchers (Davies, 1971; Davies and Nassichuk, 1973), phylloid algae, which functioned as bafflers, calcisponges (mainly thalamid sponges and inozoans), and non-calcareous sponges, which have never built into large reefs. Different from the cases of the Middle and Upper Permian reefs, in Early Permian reefs *Palaeoaplysina*, phylloid algae, bryozoans and *Tubiphytes* are relatively more common and more important reefbuilders. Calcisponges are less abundant and had lower diversity, compared to the cases in the Middle and Upper Permian reefs.

It is believed that a eustatic fall occurred at the end of the Artinskian Stage. Jiang and Qian (1986) stated that a subaerial exposure occurred in most places in South China at the end of

Carboniferous (=end of Artinskian), and evidence of erosion formed. A convincing evidence is the coal measure of the lowest part of the Middle Permian (= Kungurian-Capitanian) in China. Jin and Shang (2000) stated that the worldwide regression began at early Artinskian and reached its acme at the end of Artinskian. A disconformity occurs on the top of the Artinskian strata, while the contact between the Asselian strata and the underlying Mapingian (= Virgilian) strata is conformable in most places in China. Consequently Chinese geologists traditionally regarded Asselian-Artinskian strata as the uppermost unit of the Upper Carboniferous. In recent years, in order to keep in agreement with international stratigraphic division, most Chinese geologists assign Asselian-Artinskian strata to the Lower Permian. Even so, Asselian-Artinskian reefs resemble Carboniferous reefs more than Guadalupian reefs.

2.2.2 Reefs in the Middle Permian (Qixiaian and Maokouian)

Middle Permian reefs are widely distributed throughout the world. They have been reported from Slovenia, Oman, Texas-New Mexico, Greenland, Japan, England, Sicily, Zhejiang, Guangxi and Guizhou (Babcock and Yurewicz, 1989; Fan et al., 1990; Flügel, Kochansky-Devide, and Ramovs, 1984; Flügel, Di Stefano and Senowbari-Daryan, 1991; Garber, Grover, and Harris, 1989; Ramovs, 1986; Sano, Horibo, and Kumamoto, 1990; Toomey, 1991; Weidlich and Senowbari-Daryan, 1996; Wu, 1991). From these reefs, 10 representatives are selected: Slovenia, Oman, Texas-New Mexico, Greenland, Japan, England, Sicily, Zhejiang, Guangxi, Guizhou. So, for the Middle Permian, Nrr = 10.

Not only have wide distribution, Middle Permian reefs tend to have large scale, generally more than 100 m in thickness. For example, the reef core of the Middle Permian reef of Xiangbo, Guangxi Province, China is 167 m thick, being a part of a barrier reef about 1,000 km long. The core of the Capitan reef is maximally 183 m thick. The thickest reef is the Capitan reef. So, for the Middle Permian, Tmax = 183.

Most Middle Permian reefs were built by calcisponges (thalamid sponges, inozoans), sclerosponges, and hydrozoans. The encrustation of *Archaeolithoporella* is important to the construction of the reefs. Bryozoans, *Tubiphytes*, and the alga *Monostysisyrinx* (Wu, 1991) were local framebuilders.

In terms of dimension, distribution and internal structure, Middle Permian reefs are very developed. Since Middle Permian reefs were mainly constructed by calcisponges, it seems that the physico-chemical conditions of Middle Permian oceans were favorable to the life of typical reef-building organisms such as calcisponges.

2.2.3 Death of Middle Permian Reefs and Regressive Event

Although in some places Early Permian reefs lasted into the Middle Permian, all Middle Permian reefs ceased to grow at the end of the Middle Permian, and were generally covered by

regressive deposits. According to our studies, palaeokarsts occur in the top of the Middle Permian reefs of Ziyun, Guizhou Province, China, and fluvial deposits on the top of the Middle Permian reef in Tonglu, Zhejiang Province, China. The reefal facies of the Capitan reef of Guadalupe, New Mexico is covered by evaporite (Garber, et al., 1989). Such evidence probably indicates a global sea-level fall at the end of the Middle Permian, which might be related to the death of Middle Permian reefs. Jin et al. (1995) believed that a mass extinction caused by a worldwide regression occurred at the end of the Middle Permian. This conclusion is in agreement with the case of reefs.

2.2.4 Absence of Reefs from the Lower Wuchiapingian

No reefs have been found from the lower Wuchiapingian, although nonreefal carbonate deposits of the Wuchiapingian Stage have been reported from some places over the world (Zhao et al, 1981). Carbonates of the early Wuchiapingian are widely distributed in China (Sha et al., 1990). The absence of reefs from the lower Wuchiapingian may indicate that, after the marine ecological crisis at the end of the Middle Permian, a period of time was needed for normal oceanic conditions to restore.

2.2.5 Reefs in the Middle and Upper Wuchiapingian Stage

One calcisponge reef of middle Wuchiapingian age has been reported from Laibin, Guangxi Province, China (Yang, 1987; Sha et al., 1990). The main reefbuilders consist of calcisponges, sclerosponges, hydrozoans, *Archaeolithoporella*, *Tubiphytes*, similar to the cases of Middle Permian and Changxingian reefs. The maximal thickness of the reef is about 100 m. Besides, one sheetlike tetracoral reef was found in Ziyun, Guizhou Province, China, by Wang Shenghai and the present authors. It occurs in the upper part of the Wuchiapingian strata, maximally 3 m thick, consisting of framestone composed of only one fasciculate tetracoral species, *Pseudohuangia*.

The sparsity of reefs in the middle-upper Wuchiapingian indicates that the oceanic conditions were locally favorable to the growth of reef-building organisms such as calcisponges. The maximal thickness of the Laibin reef is about 100 m. So, for the middle-upper Wuchiapingian Stage, Nrr = 2, and Tmax = 100.

2.2.6 Reefs in the Changhsingian Stage

Changhsingian reefs are widely distributed in China. Other occurrences of Changhsingian reefs include Thailand (Senowbari-Daryan and Ingavat-Helmcke, 1994) and Greece (Flügel and Reinhardt, 1990). In China, Changhsingian reefs have been reported from Jiangsu, Zhejiang, Jiangxi, Hunan, Hubei, Guangxi, Guizhou, and Sichuan Provinces (Fan et al., 1990). From these reefs, 6 representatives are selected: Greece, and Jiangsu, Guizhou, Jiangxi, and Guangxi

Provinces of China. So, for the Changhsingian, Nrr = 6.

Most Changhsingian reefs are thick and of large scale. For example, the Changhsingian reef in Ziyun, Guizhou Province is 167 m thick maximally; the Changhsingian reef at Xiangbo, Guangxi Province, is 145 m maximally thick. The Changhsingian reef in Ziyun is the thickest. So, for the Changhsingian Stage, Tmax = 167.

Changhsingian reefs were mainly built by calcisponges, sclerosponges, hydrozoans, *Archaeolithoporella*, *Tubiphytes*, similar to middle-uuper Wuchiapingian reefs in composition. The more development of reefs in the Changhsingian Stage indicates that the oceanic conditions of that period were more favorable to reef growth.

2.2.7 End-Permian death of Changhsingian Reefs and Regressive Event

All Changhsingian reefs disappeared at the end of the Changhsingian Stage. Regressive deposits have been found on the top of many Changhsingian reefs. For example, the reef-core of the Changhsingian reef in Lichuan, Hubei Province, China is covered by back-reef lagoonal deposits, which and the top of the underlying reef-core deposits were severely dolomitized (Fan et al., 1982). The study by Fan et al. (1982) shows that the dolomitization was related to mixing of sea-water and fresh water. Our studies show that the dolostone on the top of the Changhsingian reefs in Ziyun are related to evaporation of tidal-flat environments, as indicated by desiccation cracks in the dolostone. These lines of evidence indicate that a sea-level fall occurred at the end of the Changhsingian Stage. It is probable that the end-Permian disappearance of reefs is probably caused by an event related to the regression.

2.2.8 Absence of Reefs from the Lower Triassic

Tidal-flat algal deposits were reported from the Griesbachian strata in Japan (Sano et al., 1997). Although Sano et al. assigned them as “microbial bindstone-cementstone facies,” they are not the reef in the sense we commonly mean. Reefs are carbonate bodies built by in situ organisms and thicker than the adjacent coeval strata. We persist that typical reefs represent oceanic conditions favorable to most marine organisms, especially stenotropic reef-building organisms such as calcisponges and compound corals; stromatolite bodies do not represent oceanic conditions favorable to stenotropic reef-building organisms, and do not belong to typical reefs. Tidal-flat algal deposits are common in strata. But, they do not belong to “real reefs”.

Thin (<1.5m) sheetlike stromatolite beds are reported from the upper Lower Triassic (~3-4 m.y. after the beginning of the Triassic) in Nevada, USA (Schubert and Bottjer, 1992). Without typical reefbuilding organisms and paleotopographic relief, they are not regarded as reefs. So, for the Lower Triassic, **Nrr** = 0, **Tmax** = 0.

The absence of reefs from the Lower Triassic suggests that the oceanic conditions in the Early Triassic were unfavorable to common reef-building organisms such as calcisponges and

tetracorals.

2.2.9 Reefs in the Anisian Stage

Anisian reefs have been reported from Italian Dolomites and Poland (Fois et al., 1984; Bodzioch, 1991). The reefs in Dolomite are maximally 15 m thick, mainly composed of calcisponges, sclerosponges, and encrusting algae, while those in Poland are mainly composed of siliceous sponges, maximally 1 m thick. In China, although scleractinians have been reported from Anisian strata (Qi, 1984), no Anisian reefs have been found. So, the Anisian is a period when oceanic conditions were locally favorable to reef growth. For the Anisian Stage, Nrr = 2, and Tmax = 15.

2.2.10 Reefs in the Ladinian and Carnian Stages

Ladinian and Carnian reefs have been reported from Sichuan Province of China, Nevada, Oregon, Alaska, Italian Dolomites, Yugoslavia, Turkey, and the Bavarian Alps (Wolff, 1973; Rigby, Wu, and Fan, 1998; Wu, 1984, 1989, 1990; Wu, 1994; Brandner, Flügel, and Senowbari-Daryan, 1991; Gaetani, Fois, Jadoul, and Nicora, 1981; Russo, Neri, Mastandrea, and Baracca, 1997;Turnsek, Buser, and Ogorelec, 1984; Russo, 1998). In some European and American reefs the boundary between the Ladinian and Carnian is difficult to determine. Compared to Anisian reefs, the distribution of Ladinian and Carnian reefs is much greater. From these reefs, 7 representatives are selected: Sichuan, Nevada, Oregon, Alaska, Italian Dolomite, northern Yugoslavia, and Turkey. So, for the Ladinian and Carnian Stages, Nrr = 7.

The thickest reef of Ladinian and Carnian age is in Dolomites, Italian, which is maximally 150 m thick (Gaetani et al., 1981). The reefs in Yugoslavia are maximally 130 m. So, for the Ladinian and Carnian Stages, Tmax = 150.

Ladinian and Carnian reefs were mainly built by calcisponges, sclerosponges, scleractinians, hydrozoans, and hexactinellid sponges. Although scleractinians were present in Ladinian and Carnian reefs, they were subordinate to calcisponges. Hexactinellid sponges are local reef-building organisms. In the Carnian reefs in Sichuan Province, Chain, Hexactinellid sponges are dominant reef-builders.

On the whole, Ladinian and Carnian reefs are more developed than Anisian reefs. This may indicate that the oceanic conditions in the Ladinian and Carnian Stages were much improved.

2.2.11 End-Carnian Death of Ladinian-Carnian Reefs

All Carnian reefs ceased to grow at the end of the Carnian Stage, which might be caused by a global regressive event (Stanley, 1988; Douzen and Ishiga, 1995; Assereto and Casati, 1965). We made a comparison between the thalamid sponges in pre-Norian reefs and those in

Norian-Rhaetian reefs and found that there are no common species between them. So, we agree that a catastrophic event occurred at the end of the Carnian Stage, which killed all of the reef-building organisms in Ladinian-Carnian reefs.

2.2.12 Reefs in the Norian and Rhaetian Stages

Norian and Rhaetian reefs have been reported from Peru, British Columbia, Greece, Austria, Sicily, India, and Oman (Bernecher, 1996; Bhargava and Bassi, 1985; Senowbari-Daryan et al., 1996; Stanley and Nelson, 1996; Senowbari-Daryan and Stanley, 1994; Di Stefano, Gullo, and Senowbari-Daryan, 1990). From these reefs, 7 representatives are selected: Peru, British Columbia, Greece, Austria, Sicily, India, and Oman. The reef in Sicily is the thickest, maximally 200 m thick. So, for the Norian and Rhaetian Stages, Nrr = 7, and Tmax = 200.

Norian-Rhaetian reefs were mainly built by scleractinians, calcisponges, sclerosponges, and hydrozoans. Although scleractinians appeared in Anisian, they did not become the primary reefbuilders until the Norian. In Norian-Rhaetian reefs the dominant framebuilders are scleractinians, which generally occur in more agitated outer part of reefs and could have large dimensions. On the contrary, calcisponges are more abundant in the protected places in reefs.

Flügel and Stanley (1984) assumed that there was a reorganization of reefbuilding organisms at the end of the Carnian. Some researchers proposed that the faunal change was related to the regressive event at the end of the Carnian (Stanley, 1988). It seems that a catastrophic event related to a regression caused the extinction of the reef-building organisms in the Carnian reefs.

2.3 Comparison of the Distributions, Sizes and Composition of the Reefs in Different Periods

Figure 2.1 shows the numbers of the reef representatives of different periods of the Permian and Triassic Periods. A reef representative is selected from the reefs in any district with an area of 400 by 400 km. So, the numbers of the reef representatives of a period is an approximate to the distribution area of the reefs in that period. As seen from figure 2.1, the Middle Permian has the most numerous reef representatives, i.e., the largest distribution area of reefs. The numbers of the reef representatives of the early Wuchiapingian Stage (P3w1) and that of the Early Triassic (T1) are both zero, representing two gaps of reef temporal distribution. These two gaps represent the periods following some catastrophic events devastating to reefs. During the period following each gap, the number of reef representatives increases with time (e.g., P3w2 through P3c: 2 to 5; T2a through T2L-3c: 2 to 6).

Figure 2.2 shows the maximal thickness of the reefs of different Permian and Triassic periods. It is obvious that the maximal reef thickness increases with time in each post-gap period (P3w2 to P3c; T2a to T3n). For example, the maximal thickness of the reefs in the Anisian Stage

is 15 m, while that of Ladinian-Carnian reefs increases to 150 m.

Figure 2.3 shows the taxonomic composition of the major reef-builders (including framebuilders, bafflers, prebafflers, covers, binders) of the reefs of different periods. The major reef-builders in Permian and Triassic reefs include calcisponges (including thalamid sponges, inozoans), sclerosponges, hydrozoans, scleractinians, tetracorals, *Tubiphytes*, bryozoans, phylloid algae, *Palaeoaplysina*, and hexactinellid sponges. In terms of the taxonomic composition of main reefbuilders, Permian and Triassic reefs can be classified as calcisponge reefs, calcisponge & scleractinian reefs, tetracoral reefs, *Tubiphytes* & bryozoan reefs, bryozoan reefs, *Tubiphytes* reefs, phylloid alga reefs, *Palaeoaplysina* reefs, and hexactinellid sponge reefs.

According to their paleoenvironmental properties, Permian and Triassic reefs are grouped as 5 types: group 1 (CC-type), including calcisponge reefs, calcisponge & scleractinian reefs, tetracoral reefs, all representing marine environments the most favorable to reef growth; group2 (TB-type), including *Tubiphytes* & bryozoan reefs, bryozoan reefs, *Tubiphytes* reefs, representing environments less favorable to reef-builders, probably of deeper water depth; group 3 (PH-type), including only phylloid alga reefs, representing a special environment; group 4 (PA-type), including only *Palaeoaplysina* reefs, representing another special environment; group 5 (HE), including hexactinellid sponge reefs, representing deep water environments. Stromatolite "reefs" are not included: they are not the reefs in the same sense we commonly used. As seen from Figure 2.3, the percentage of CC-type reefs increases with time during the post-gap periods. For example, CC-type reefs accounts for 50% of Anisian reefs, while they account for 89% of Ladinian-Carnian reefs. Such an increase may be related to the improvement of oceanic conditions.

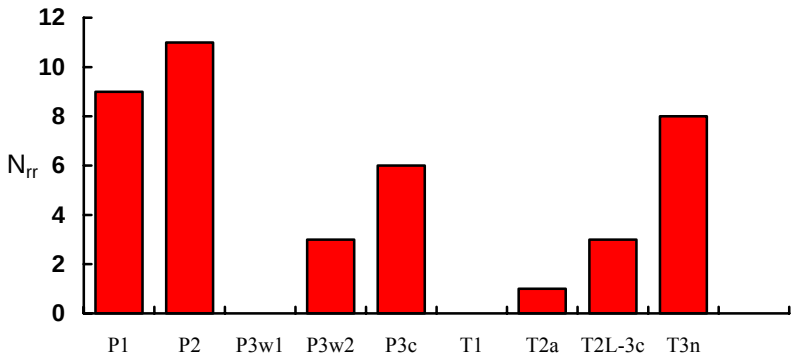

Fig. 2.1 Quantities of reef representatives (Nrr) of different periods, as approximates of reef distribution areas. P1=Lower Permian; P2=Middle Permian; P3w1=lower Wuchiapingian; P3w2=mid-upper Wuchiapingian; P3c=Changhsingian; T1=Early Triassic; T2a=Anisian; T2L-3c=Ladinian-Carnian; T3n = Norian- Rhaetian.

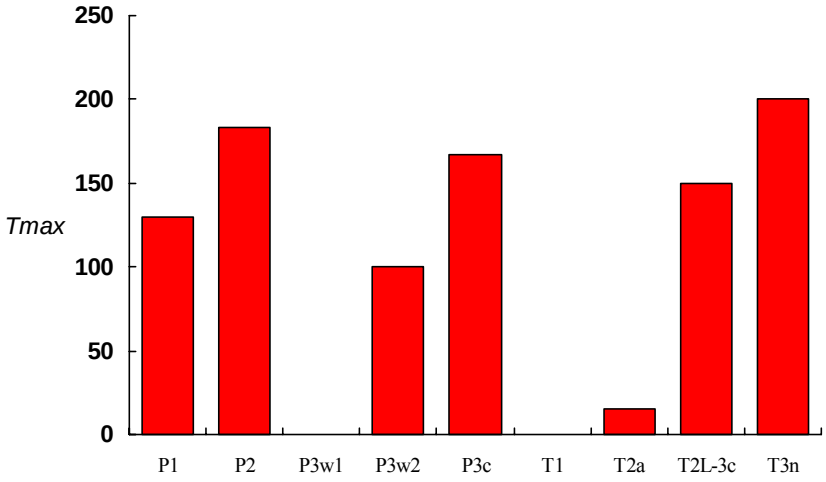

Fig. 2.2 Maximal thicknesses of reefs (Tmax) of different Permian and Triassic periods. P1=Lower Permian; P2=Middle Permian; P3w1=lower Wuchiapingian; P3w2=mid-upper Wuchiapingian; P3c=Changhsingian; T1=Lower Triassic; T2a = Anisian; T2L-3c = Ladinian-Carnian; T3n = Norian-Rhaetian.

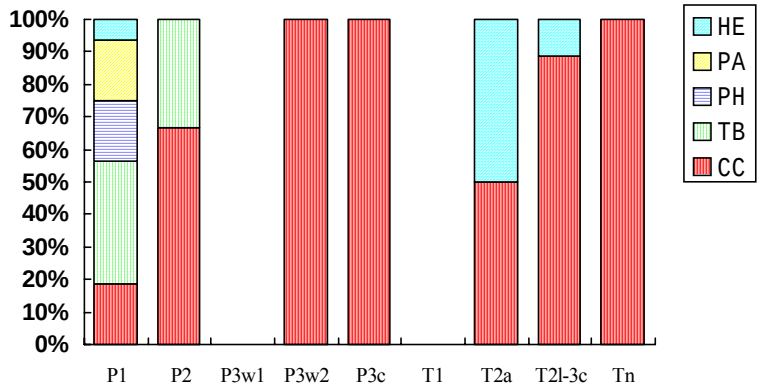

Fig. 2.3 Reef types of different Permian and Triassic periods. CC=calcisponge reefs, calcisponge-scleractinian reefs, tetracoral reefs; TB=Tubiphytes reefs, Tubiphytes-bryozoan reefs, bryozoan reefs; PH= phylloid algal reefs; PA=Palaeoaplysina reefs; HE=hexactinellid sponge reefs. P1=Lower Permian; P2=Middle Permian; P3w1=lower Wuchiapingian; P3w2=mid-upper Wuchiapingian; P3c=Changhsingian; T1=Lower Triassic; T2a=Anisian; T2l-3c=Ladinian-Carnian; Tn=Norian-Rhaetian.

2.4 Implications of P-T evolution of reefs: catastrophic events

Three catastrophic events are reflected in Permian-Triassic evolution of reefs: end-Guadalupian, end-Changhsingian and end-Carnian events.

The results of the end-Guadalupian event include: 1) the death of Guadalupian (=the Middle Permian) reefs, 2) the absence of reefs from the early Wuchiapingian, 3) the decline in the diversity of most non-reef invertebrates (e.g., Yang et al., 1991).

The end-Changhsingian catastrophic event caused: 1) the death of Changhsingian reefs, 2) the absence of reefs from the Early Triassic, 3) the disappearance of nearly all non-reef invertebrates (Yang et al., 1991), and 4) the sparsity of marine organisms in the Early Triassic.

The end-Carnian catastrophic event caused: 1) the death of Ladinian-Carnian reefs, 2) the disappearance of all Ladinian-Carnian reef-building organisms: Norian-Rhaetian reefbuilding organisms are all different from pre-Norian reefbuilding organisms. Norian-Rhaetian non-reef organisms are different from pre-Norian non-reef organisms, too.

In terms of magnitudes, however, the end-Guadalupian and end-Carnian extinctions are not compatible to the end-Changhsingian extinction. Though the reef ecosystems were destroyed at the end of the Guadalupian, non-reef ecosystems suffered much less. At the end of the Changhsingian Stage, however, not only reef ecosystems, but also non-reef ecosystems were destroyed by some catastrophic events.

3 Permian-Triassic Evolution of Reefal Thalamid Sponges: Extinctions

Abstract: Thalamid sponges, a Porifera group with calcareous skeleton, were one of the most important reef-building groups in the Permian. All reefs disappeared at the end of the Permian. Reefs did not appear until the Middle Triassic Anisian Stage. Reef-building organisms in Middle Triassic reefs contain thalamid sponges. Then, did any thalamid sponges in Permian reefs survive the end-Permian mass extinction and persist into the Middle Triassic reefs? Comparison between the thalamid sponges in Permian reefs and those in Triassic reefs at species level shows that no Permian reefal thalamid sponges persisted into the Triassic reefs.

3.1 Introduction

It has been found that reefal organisms are more sensitive to environmental changes than nonreefal organisms (Dodd and Stanton, 1981). For example, hermatypic corals can withstand temperatures of 16~29^{o}C, be the most abundant at 25~29^{o}C, while ahermatypic corals can live at -1~28^{o}C. So, when physico-chemical conditions of oceans changes, reefal organisms will response to the changes the earliest and the most drastically. The organisms with the narrowest ecological limits will die first. Further change in environmental conditions will lead to death of organisms with wider ecological limits, which will lead to change in the richness and diversity of reef biota. So, if catastrophic events occur in the Permian, or any other geological periods, they would lead to change in reefal biota, especially such features as richness and diversity. For this reason, detailed study of change in taxonomic composition of reef biota can reveal some valuable information about ancient environmental changes, especially about catastrophic events.

Many paleontologists have made studies on Permian catastrophic events on basis of nonreefal invertebrate groups (e.g., Yang et al., 1991; Erwin and Pan, 1996; Sepkoski, 1990; Yin, 1985; Li, 1995). Due to the incompleteness of the data of Permian and Triassic reefal calcisponges (a dominant group of reef-building organisms with calcareous skeleton as well as spicules), even the classic study by Sepkoski (1990) did not include calcisponges in his statistic study of invertebrate groups. Sepkoski's study includes foraminifers, corals, bryozoans, brachiopods, gastropods, bivalves, but not calcisponges. Our study is intended to deal with the evolution of a main group of reef-building calcisponges in the Permian and Triassic Periods, thalamid sponges.

The most important and abundant reef-building organisms in Permian and Triassic reefs are

calcisponges, including thalamid sponges and inozoans. Thalamid sponges have characteristic segmented skeletons, and are relatively easy to recognize and study, and are more thoroughly studied. Compared to thalamid sponges, inozoans are less studied. So, evolution of thalamid sponges in the Permian and Triassic is focused on in our study.

In this study, comparison of reefal thalamid sponges of different periods are conducted at specific level, since in our opinion, assignment of species to genera is somewhat subjective and comparison at generic or higher taxonomic level has less reliable base.

It is understandable that different researchers have different research styles, which would lead to substantial difference in results of their taxonomic studies. For example, different researchers can place the same specimen to different species. Such a problem, if not corrected, will lead to bias in evolution study based on taxonomic data. To avoid such a problem, all known reefal thalamid sponge species should be checked in terms of same taxonomic criteria, and those incorrectly assigned should be corrected. In this study, we firstly checked all known reefal thalamid sponge species and correct those incorrectly assigned. Based on this, comparison among the thalamid sponge species of different periods is made.

The chronostratigraphic division of the Permian System follows the scheme of Jin et al. (1997; see Section 2 of this work). According to this scheme, the Lower Permian consists of Asselian, Sakmarian and Artinskian. The Middle Permian consists of Kungurian, Roadian, Wordian, and Capitanian. The Upper Permian consists of Wuchiapingian and Changhsingian (= Changxingian).

The division of the Triassic System follows the scheme of Harland et al. (1989; see Section 2 of this work). According to this scheme, the Lower Triassic consists of Griesbachian, Nammalian and Spathian Stages. The Middle Triassic consists of Anisian and Ladinian Stages. The Upper Triassic consists of Carnian, Norian, and Rhaetian Stages.

3.2 Permian-Triassic evolution of reefal thalamid sponges

All previously described thalamid sponge fossils from Permian and Triassic reefs are included in the study, except for those without pictures, which makes it impossible for us to check their identification. The earliest document is by Waagen & Wentzel (1887), on the fossils from Salt Range. The latest document is by Rigby, Senowbari-Daryan and Liu (1998), on the Capitan reef of Guadalupe Mountains. Pictures of all described thalamid sponge fossils were compared to the pictures of their holotypes, and those incorrectly assigned were corrected.

Changhsingian reefs are mainly distributed in China. So the studies by Chinese researchers are critical to this study. We found that, however, in the past studies, medium-sized (diameter > 0.5 cm) and large-sized (diameter >1 cm) thalamid sponges caught more attention, while small thalamid sponges were generally not included in previous studies. In this study, small thalamid sponges from the Changhsingian reefs in Ziyun, Guizhou Province, China is included, in order to

reach a more reliable result about evolution of thalamid sponges.

In the following sections, the after-revision species names of reefal thalamid sponge of different periods are listed. Then, comparison among the thalamid sponge species of different periods is made.

3.2.1 Thalamid sponges in Early Permian reefs

Early Permian reefal thalamid sponges were reported from Sicily by Senowbari-Daryan and Di Stefano (1988). They include:

Amblysiphonella barroisi Steinmann (S)
Colospongia cf. *benjamini* (Girty) (S)
Discosiphonella lercarensis Senowbari-Daryan & Di Stefano (S)
Girtyocoelia beedei (Girty) (S)
Guadalupia cylindrica Girty (S)
Parauvanella paronai Senowbari-Daryan & Di Stefano (S)
Salzburgia sp. (S)
Sollasia ostiolata Steinmann (S)
Sollasia sp. (S)
Note: The letter in "()" indicates occurrence locality. (S): Sicily, Italy.

3.2.2 Thalamid sponges in Middle Permian reefs

According to the work by Aleotti, Dieci and Russo (1986), Flügel, Di Stefano and Senowbari-Daryan (1991), Parona (1933), Rigby, Fan and Zhang (1989), Rigby, Fan, Wang and Zhang (1994), Wu (1991), Rigby, Senowbari-Daryan and Liu (1998), Senowbari-Daryan and Rigby (1991), Senowbari-Daryan and Rigby (1988), Waagen & Wentzel (1887), Weidlich and Senowbari-Daryan (1996), and this study, the following thalamid sponge species (including 110 species and 1 subspecies) are present in Middle Permian reefs throughout the world:

Amblysiphonella ?*permosicula* (Parona) (S)
Amblysiphonella bancaoensis Zhang (O)
Amblysiphonella cf. *A. merlai* Parona (T)
Amblysiphonella cf. *merlai* Parona (G)
Amblysiphonella clathrata Parona (S)
Amblysiphonella merlai Parona (O) (S) (T)
Amblysiphonella multilamellosa Waagen & Wentzel (R)
Amblysiphonella nodulifera Girty (S)
Amblysiphonella obliqua Senowbari-Daryan & Rigby (T)
Amblysiphonella omanica Weidlich & Senowbari-Daryan (O)
Amblysiphonella ramosa Senowbari-Daryan & Rigby (T)

Amblysiphonella socialis Waagen & Wentzel (O) (R)
Amblysiphonella sp. (O)
Amblysiphonella sp. (X)
Amblysiphonella sp. A (G)
Amblysiphonella sp. B (G)
Amblysiphonella spinosa Rigby, Fan & Zhang (X)
Amblysiphonella vesiculosa (Koninck) (R) (S)
Amphorithalamia cateniformis Senowbari-Daryan & Rigby (T)
Bullicoelia columnaria (Weidlich & Senowbari-Daryan) (O)
Carterina gracilis Rigby, Fan & Zhang (T)
Carterina pyramidata Waagen & Wentzel (R)
Colospongia cf. *C. americana* (Girty) (O)
Colospongia cortexifera Senowbari-Daryan & Rigby (O) (S) (T)
Colospongia gemina (Waagen & Wentzel) (R) (S)
Colospongia sinensis Wu (Z)
Colospongia maxima Rigby, Fan & Zhang (O)
Colospongia paronae Aleotti, Dieci & Russo (S)
Colospongia salinaria (Waagen & Wentzel) (R)
Colospongia sp. (X)
Cystospongia guangxiensis Wu (X)
Cystothalamia adrianensis Senowbari-Daryan (S)
Cystothalamia conica (Termier & Termier) (T)
Cystothalamia distefanoi Senowbari-Daryan (S)
Cystothalamia guadalupensis (Girty) (G)
Cystothalamia nodulifera Girty (S)
Discosiphonella (= *Cystauletes*) *lercarensis* Senowbari-Daryan & Di Stefano (T)
Discosiphonella (= *Cystauletes*) *mammilosa* (King) (T) (G)
Discosiphonella (= *Cystauletes*) sp. (X)
Discosiphonella radicifera (Waagen & Wentzel) (R)
Enoplocoelia interchora Senowbari-Daryan & Rigby (T)
Exaulipora permica (Senowbari-Daryan) (G)
Follicatena sp. (X)
Girtyocoelia beedei (Girty) (T) (O) (G)
Girtyocoelia gracilis Weidlich & Senowbari-Daryan (O)
Graminospongia girtyi (Parona) (T) (S)
Guadalupia ? *cidarites* Parona (S)
Guadalupia cidarites Parona (S)
Guadalupia cylindrica Girty (S) (T)
Guadalupia digitata (Girty) (G)

Guadalupia minima Parona (S) (X)
Guangxispongia spinalis Wu (X) (Z)
Huibaoia exaulifera Rigby, Senowbari-Daryan and Liu (G)
Imbricatocoelia elongata Rigby, Fan & Zhang (O) (X) (S) (T)
Imbricatocoelia irregulara Rigby, Fan & Zhang (X)
Imbricatocoelia obconica Rigby, Fan & Zhang (X)
Imbricatocoelia paucipora Rigby, Fan & Zhang (X)
Imbricatocoelia ramosa Senowbari-Daryan & Rigby (X)
Imbricatocoelia sp. (Parona) (S)
Imperatoria (?) sp. (Z)
Intrasporeocoelia laxa Wu (X)
Intrasporeocoelia hubeiensis Fan & Zhang (S) (O) (X) (T)
Laccosiphonella merlai (Parona) (S)
Lemonea ? *polysiphonata* Senowbari-Daryan (?, Wu) (G)
Lemonea conica Senowbari-Daryan (G)
Pachyphleia typica Wu (Z)
Parauvanella sp. (X)
Parauvanella cylindrica Wu (Z)
Parauvanella minima Senowbari-Daryan (O) (X) (G)
Parauvanella paronai Senowbari-Daryan & Di Stefano (O) (T)
Pisothalamia spiculata Senowbari-Daryan & Rigby (T)
Planiguadalupia explanata (King) (G)
Platythalamiella ? sp. (G)
Platythalamiella newelli Senowbari-Daryan & Rigby (T)
Polycystocoelia cf. *P. huajiaopingensis* Zhang (T)
Polycystothalamia sinuolata Wu (X)
Polycystothalamia sp. (X)
Polyedra tebagaensis Senowbari-Daryan & Rigby (T)
Polyphymaspongia zitteliana (Girty) (G)
Preverticillites columnella Parona (O) (S) (T)
Preverticillites parva Rigby, Senowbari-Daryan and Liu (G)
Pseudoamblysiphonella polysiphonata Senowbari-Daryan & Rigby (T)
Pseudoguadalupia alveolaris (Parona) (S) (T)
Rahbahthalamia bullifera (Senowbari-Daryan & Rigby) (O) (T)
Reticulospongia reticulata Wu (Z) (X)
Rhabdactinia depressa Rigby, Fan & Zhang (X) (T)
Rhabdactinia squamata Rigby, Fan & Zhang (X)
Salzburgia ? *irregularis* Weidlich & Senowbari-Daryan (O)
Salzburgia ? *nana* Rigby, Fan & Zhang (X)

Solenolmia (= *Dictyocoelia*) *permica* Senowbari-Daryan & Rigby (T) (S)

Solidothalamia cylindrica (Girty) (G)

Solidothalamia lambdiformis Wu (X)

Solidothalamia? *micra* (Rigby, Senowbari-Daryan and Liu) (G)

Sollasia abista Rigby, Fan & Zhang (O) (X)

Sollasia ostiolata permica Parona (S)

Sollasia ostiolata Steinmann (S) (O) (T) (X) (G)

Sollasia spheroida Rigby, Fan & Zhang (O)(X)

Spica spica Termier & Termier (O) (T)

Stromatogloma typica Wu (X)

Stylocoelia circopora Wu (Z) (S) (X)

Stylothalamia elegant Rigby, Fan, Wang and Zhang (Z)

Subascosymplegma oussifensis (Termier & Termier) (T)

Tebagathalamia cylindrica Senowbari-Daryan & Rigby (T) (X)

Tebagathalamia diagonalis Wu (X)

Tebagathalamia granularis Wu (X)

Tebagathalamia lamella Wu (X) (Z)

Thaumastocoelia ? *irregularis* Weidlich & Senowbari-Daryan (O)

Thaumastocoelia sp. (O)

Tristratocoelia rhythmica Senowbari-Daryan & Rigby (T) (G)

Uvothalamia planiinvoluta Senowbari-Daryan (S)

Welteria ? *hawasinensis* Weidlich & Senowbari-Daryan (O)

Note: (R): Salt Range, Pakistan, (S): Sicily, Italy; (T): Tebaga, Tunisia; (X): Xiangbo, Guangxi Province, China; (Z): Ziyun, Guizhou Province, China; (O): Oman Mountains.

3.2.3 Thalamid sponges in Upper Permian Changhsingian reefs

According to the studies of Fan and Zhang (1985), Rigby, Fan and Zhang (1989), Rigby, Fan, Wang and Zhang (1994), Senowbari-Daryan and Ingavat-Helmcke (1994), Zhang (1983), and this study, the following thalamid sponges (including 83 species) are present in the Changhsingian reefs throughout the world:

Ambithalamia permica Senowbari-Daryan and Ingavat-Helmcke (Th)

Amblysiphonella bancaoensis Zhang (L)

Amblysiphonella merlai? Parona (X)

Amblysiphonella obliquisepta Zhang (L)

Amblysiphonella omanica Weidlich & Senowbari-Daryan (Z)

Amblysiphonella regularis Zhang (L)

Amblysiphonella sp. A (X)

Amblysiphonella sp. B (X)

Amblysiphonella specialis Rigby, Fan and Zhang (LA)
Amblysiphonella vesiculosa minima Zhang (L)
Amblysiphonella yini Fan & Zhang (L)
Baryspongia beedei Wu (Z)
Belyaevaspongia insolita (Belyaeva) (Th)
Carterina gracilis Rigby, Fan & Zhang (J) (Z) (LA)
Carterina pyramidata Waagen & Wentzel (LA)
Colospongia cf. *dubia* Laube (L)
Colospongia cortexifera Senowbari-Daryan & Rigby (?, Wu) (J) (Z)
Colospongia gemina (Waagen & Wentzel)) (Z) (L)
Colospongia maxima Rigby, Fan & Zhang (X)
Colospongia sp. 1 (Th)
Colospongia sp. 2 (Z)
Colospongia spheroida Wu (Z)
Colospongia tubiformis Wu (Z)
Diecithalamia permica Wu (Z)
Discosiphonella asiatica (Fan & Zhang) (L) (X)
Discosiphonella heteroideus Wu (Z)
Discosiphonella lepida (Zhang) (L)
Discosiphonella orientalis (Fan & Zhang) (L)
Discosiphonella ostiolata Wu (Z)
Discosiphonella spongioformis Wu (Z)
Discosiphonella typica (Zhang) (L) (X)
Discosiphonella variabilis (Zhang) (L)
Drupinella irregulara Wu (Z)
?*Girtyocoelia beedei* (Girty) (?, Wu) (Th)
Girtyocoelia fibrilata Wu (Z)
Girtyocoelia sp. (L)
Guadalupia cylindrica Girty (Z)
Guadalupia irregulara Wu (Z)
Guadalupia minima Parona (Z)
Huayingia glomerata Rigby, Fan, Wang and Zhang (J)
Imbricatocoelia elongata Rigby, Fan & Zhang (X)
Intrasporeocoelia hubeiensis Fan & Zhang (Z) (L) (Th)
Monocoelia flata Wu (Z)
Neoguadalupia explanata Rigby, Fan & Zhang (X)
Pachycoelia siphonella Wu (Z)
Parauvanella cylindrica Wu (Z)
Parauvanella irregulara Wu (Z)

Parauvanella maxima Wu (Z)

Parauvanella minima Senowbari-Daryan (?, Wu) (LA) (L)

Parauvanella paronai Senowbari-Daryan & Di Stefano (?, Wu) (J) (Z)

Parauvanella sp. Senowbari-Daryan) (L)

Parauvanella spinosa Wu (Z)

Phraethalamia tubulara Senowbari-Daryan and Ingavat-Helmcke (Th)

Pinacophyllum orthocera Wu (Z)

Pinacophyllum parallela Wu (Z)

Polycystocoelia asiatica (Fan & Zhang) (L) (X)

Polycystocoelia huajiaopingensis Zhang (X) (Z) (J)

Polycystocoelia sinica Zhang (L)

Polycystocoelia sp. (Z)

Polytholosia tubifera Wu (Z)

Preverticillites columnella Parona (?, Wu) (X)

Pseudodeningeria pachyphloeus Wu (Z)

Rahbahthalamia bullifera (Senowbari-Daryan & Rigby) (Z)

Rhabdactinia columnaria Yabe & Sugiyama (X) (Z)

Rhabdactinia irregulara Rigby, Fan & Zhang (Z)

Rhabdactinia regulara Wu (Z)

Salzburgia irregulara Wu (Z)

Salzburgia permica Wu (Z)

Solenolmia ? sp. (Z)

Sollasia angulara Wu (Z)

Sollasia irregulara Wu (Z)

Sollasia minima Wu (Z)

Sollasia ostiolata Steinmann (J) (Z) (Th)

Sollasia sp. (L)

Sollasia spheroida ? Rigby, Fan and Zhang (?, Wu) (Th)

Sollasia tubiformis Wu (Z)

Spinocoelia spinosa Wu (Z)

Stromatogloma typica Wu (Z)

Subascosymplegma ? *paracatenulata* Rigby, Fan & Zhang (X)

Subascosymplegma sp. (Z)

Tebagathalamia minima Wu (Z)

Tristratocoelia rhythmica Senowbari-Daryan and Rigby (Th)

Uvanella micritica Wu (Z)

Note: (L): Lichuan, Hubei Province, China; (LA): Laolongdong, Beipei, Sichuan Province, China; (Th): Thailand; (X): Xiangbo, Guangxi Province, China; (J): Jianshuigou, Sichuan Province, China; (Z): Ziyun, Guizhou Province, China.

3.2.4 Thalamid sponges in Middle Triassic Anisian and Ladinian reefs

According to the work of Fois et al. (1984), Scholz (1972), Brandner, Flügel and Senowbari -Daryan (1991), Ott (1967), and Senowbari-Daryan et al. (1993), the following thalamid sponge species (20 species and 2 subspecies) are present in the Anisian and Ladinian reefs throughout the world.

Alpinothalamia bavarica (Ott) (A)
Anisothalamia minima Senowbari-Daryan et al. (ID)
Celyphia ? *minima* Senowbari-Daryan et al. (ID)
Celyphia zoldana Ott, Pisa & Farabegoli, 1980 (ID)
Colospongia catenulata (D)
Colospongia catenulata catenulata Ott (A)
Colospongia catenulata macrocatenulata Scholz (H)
Colospongia sp. (ID)
Cryptocoelia manon manon (Munster) (A)
Cryptocoelia zitteli Steinmann(D)
Deningeria crassireticulata Senowbari-Daryan et al. (ID)
Deningeria tenuireticulata Senowbari-Daryan et al. (ID)
Diecithalamia polysiphonata Dieci, Antonacci & Zardini (A)
Follicatena cautica Ott (A) (D)
Girtyocoelia oenipontana Ott (D)
Olangocoelia otti Bechstadt & Brandner (ID)
Sestrocatena alpinus (Ott) (D) (A)
Solenolmia (= *Dictyocoelia*) *manon* (D)
Thaumastocoelia ? *dolomitica* Senowbari-Daryan et al. (?, Wu) (ID)
Uvanella irregularis Ott (D) (A)
Uvanella norica Senowbari-Daryan 1990 (ID)
Vesicocaulis depressus Ott (A) (D)
Note: (A): Northern Alps; (D): Western Dolomite; (ID): Italian Dolomites; (H): Hungary.

3.2.5 Thalamid sponges in Late Triassic Carnian reefs

According to the works of Bernecker (1996), Dieci et al (1968), Fois and Gaetani (1984), Fursich and Wendt (1977), and Senowbari-Daryan and Shafer (1983), the following thalamid sponges (42 species and 2 subspecies) are present in the Carnian reefs throughout the world.

Amblysiphonella cf. *A. lorentheyi* Vinassa De Regny (G)
Amblysiphonella lorentheyi Vinassa (D)
Amblysiphonella minima Senowbari-Daryan and Shafer (G)
Amblysiphonella strobiliformis Dieci, Antonacci & Zardini (D)

Amblysiphonella timorca Vinassa (D)
Aplinothalamia bavarica Ott (D)
Aplinothalamia slovenica (Senowbari-Daryan) (O)
Ascosymplegma expansum Seilacher (D)
Celyphia submarginata (Munster) (D)
Ceotinella mirunae Pantic (G) (O)
Colospongia andrusovi Jablonsky (G)
Colospongia catenulata catenulata Ott (G)
Colospongia cf. *C. elongata* (Wilckens) (G)
Colospongia dubia (Munster) (D) (G)
Colospongia sp.1 (G)
Colospongia sp.2 (G)
Cryptocoelia lata Senowbari-Daryan and Shafer (G)
Cryptocoelia zitteli Steinmann (D) (G) (O)
Enoplocoelia armata (Klipstein) (D)
Follicatena cautica Ott (G)
Girtyocoelia ostiaesaccus Senowbari-Daryan (G)
Prosiphonella amplectens Dieci, Antonacci & Zardini (D)
Sestrocatena alpinus Ott (G)
Solenolmia (= *Dictyocoelia*) *manon* (Munster) (G) (D)
Solenolmia (= *Dictyocoelia*) *manon manon* (Munster) (C) (O)
?Solenolmia (= *Dictyocoelia*) *manon* (Munster) (G)
Stylothalamia dehmi Ott (G)
Thaumastocoelia cassiana Steinmann (D)
Uvanella ? *lamellata* Senowbari-Daryan (O)
Uvanella irregularis Ott (C) (G)
Verticillites ? sp.1 (G)
Verticillites cf. *V. cretaceus* Defrance (G)
Vesicocaulis carinthiacus Ott (G)
Vesicocaulis depress Ott (D)
Vesicocaulis multisiphonatus Kovacs (G)
Vesicocaulis polysiphonata Dieci, Antonacci & Zardini (D)
Vesicocaulis reticuliformis Jablonsky (G)
Zardinia ? sp.2 (G)
Zardinia cf. *Z. perisulcata* Dieci et al. (G)
Zardinia cf. *Z. platithalamica* Dieci et al. (G)
Zardinia perisulcata Dieci, Antonacci & Zardini (D)
Zardinia platithalamica Dieci, Antonacci & Zardini (D)
Zardinia cylindrica Senowbari-Daryan and Shafer (G)

Zardinia sp. 1 (G)

Note: (G): Greek island; (O): Oman Mountains; (C): Civetta, Dolomites; (D): Dolomites.

3.2.6 Thalamid sponges in Late Triassic Norian and Rhaetian reefs

According to the works of Senowbari-Daryan (1994), Senowbari-Daryan and Reid (1987), Senowbari-Daryan and Schafer (1979), Senowbari-Daryan and Schafer (1986), Senowbari -Darytan and Stanley (1992), Senowbari-Daryan et al. (1996), Stanley and Nelson (1995), and Stanley et al. (1994), the following thalamid sponges (63 species) are present in the Norian and Rhaetian reefs throughout the world.

? *Cryptocoelia zitteli* Steinmann (Y)

Alpinothalamia minima (Senowbari-Daryan & Schafer) (S)

Amblysiphonella ? *polyformis* Senowbari-Daryan & Schafer (S)

Amblysiphonella sp. 1 (S)

Amblysiphonella sp. 2 (S)

Amblysiphonella sp. 3 (S)

Annaecoelia interiecta Senowbari-Daryan & Schafer (A)

Annaecoelia mirabilis Senowbari-Daryan & Schafer (A)

Antalythalamia riedeli Senowbari-Daryan (T)

Ascosymplegma expansum Seilacher (Y)

Battaglia major Senowbari-Daryan & Schafer (S)

Battaglia minor Senowbari-Daryan & Schafer (S)

Celyphia ? *norica* Senowbari-Daryan & Schafer (S)

Cheilosporites tirolensis Wahner (S) (G)

Cinnabaria expansa (Seilacher) (N)

Cinnabaria minima Senowbari-Daryan (G)

Colospongia bimuralis Senowbari-Daryan (Y)

Colospongia cf. *C. menulensis* Senowbari-Daryan & Schafer (Y)

Colospongia dubia ? (Munster) (?, Wu) (Y)

Colospongia mennulensis Senowbari-Daryan & Schafer (S)

Cribrothalamia madoniensis Senowbari-Daryan (S)

Cryptocoelia crassiparietalis Senowbari-Daryan & Schafer (S)

Cryptocoelia lupensis Senowbari-Daryan (S)

Cryptocoelia tenuiparietalis Senowbari-Daryan (S)

Discosiphonella ? sp. (S)

Follicatena irregularis Senowbari-Daryan & Schafer (S) (Y)

Gigantothalamia ovoidalis Senowbari-Daryan (T)

Henricellum cf. *H. insigne* Wilckens (Y)

Madonia conica Senowbari-Daryan & Schafer (S)

Neoguadalupia ? *norica* Senowbari-Darytan and Stanley (N)
Nevadathalamia cylindrica (Seilacher) (N)
Panormida priscae Senowbari-Daryan (S)
Paradeningeria alpina Senowbari-Daryan & Schafer (A) (Y)
Paradeningeria gruberensis Senowbari-Daryan & Schafer (A)
Paradeningeria sp. (S)
Paradeningeria weyli Senowbari-Daryan & Schafer (A)
Paravesicocaulis multiosculatus Kovacs (S)
Platythalamiella siciliana Senowbari-Daryan (S)
Polycystocoelia norica Senowbari-Daryan & Reid (Y)
Polycystocoelia sp. 1 (Y)
Polysiphospongia collesanensis Senowbari-Daryan & Schafer (S)
Polysiphospongia fluegeli Senowbari-Daryan & Schafer (S)
Polytholosia sp. 1 (S)
Polytholosia sp. 2 (S)
Polytholosia sp. 3 (S)
Pseudouvanella parallela Senowbari-Daryan (T)
Salzburgia ? sp. (Y)
Salzburgia variabilis Senowbari-Daryan & Schafer (A)
Solenolmia (= *Dictyocoelia*) ? sp. (S)
Solenolmia cf. *manon* (Munste) (Y)
Sollasia ? aff. *baloghi* Kovacs (S)
Sphaerothalamia vesiculifera Senowbari-Daryan (T)
Stylothalamia polysiphonata Senowbari-Daryan (T)
Thaumastocoelia ovoidalis Senowbari-Daryan (T)
Thaumastocoelia ? *sphaeroida* Senowbari-Daryan (?, Wu) (T)
Uvanella ? *irregularis* Ott (Y)
Uvanella ? *tegimentopora* Senowbari-Daryan & Schafer (S)
Uvanella cf. *irregularis* Ott (S)
Verticillites conicus Senowbari-Daryan & Schafer (S)
Weidlichia cylindrica (Senowbari-Daryan) (S)
Weidlichia siciliana (Senowbari-Daryan) (S)
Welteria ? sp. (S)
Yukonella rigbyi Senowbari-Daryan & Reid (Y)

Note: (S): Sicily; (A): Northern Calcareous Alps; (N): Nevada, USA; (T): Turkey; (Y): Yukon, Canada; (G): Greece.

3.3 Comparison of the reefal thalamid sponge faunas of different periods

The thalamid sponges of different Permian and Triassic periods are compared and the following results are obtained.

(1) Extinction rates of reefal thalamid sponge species at the end of the Middle Permian, Changhsingian Stage, and Carnian Stage were 83.6%, 100%, and 100%, respectively

The thalamid sponges in Early Permian reefs have lower diversity, including 9 species, of which 5 species lasted into Middle Permian reefs. The extinction rate (=ratio of the number of extinct species to that of total species) is 44.4%.

The thalamid sponges in the Middle Permian were very diverse, including 110 species, of which 92 species disappeared at the end of this period, with an extinction of 83.6%.

No reefs of early Wuchiapingian age have been reported. Only one calcisponge reef of middle-upper Wuchiapingian age has been reported from China. However, its thalamid sponges have not been described. The thalamid sponges in upper Permian Changhsingian reefs include 83 species, with the second high diversity of the Permian and Triassic Periods. All of the 83 species disappeared at the end of the Changhsingian Stage, with an extinction rate of 100%.

There were no reefs and reefal thalamid sponges in the Early Triassic. Real reefs ("real reefs" exclude "stromatolite reefs" and microbial deposits) reoccurred in the Middle Triassic Anisian Stage. The thalamid sponges in Middle Triassic Anisian and Ladinian reefs had lower diversity, including 20 species, no one of which came from Permian reefs. Seven of the 20 species lasted into Late Triassic Carnian reefs, with an extinction rate of 65% at the end of the Ladinian Stage.

The thalamid sponges in Late Triassic Carnian reefs had higher diversity than in Anisian and Ladinian reefs, including 42 species. All of the 42 species disappeared at the end of the Carnian Stage, with an extinction rate of 100%.

The thalamid sponges in Late Triassic Norian and Rhaetian reefs had the highest diversity of the Triassic, including 63 species.

(2) Extinctions of thalamid sponges in the Permian and Triassic indicate three mass extinction events, which occurred at the end of the Middle Permian, Changhsingian Stage, and Carnian Stage

The extinction of reefal thalamid sponges at the end of the Carnian Stage has no comparable event in non-reefal marine organisms.

Figure 3.1 shows the difference in the numbers of total species, new species of the different periods of the Permian and Triassic Periods, and the species lasting into the next period. In Figure 3.2, the percentages of the thalamid sponge species of different periods that lasted into the next period are shown.

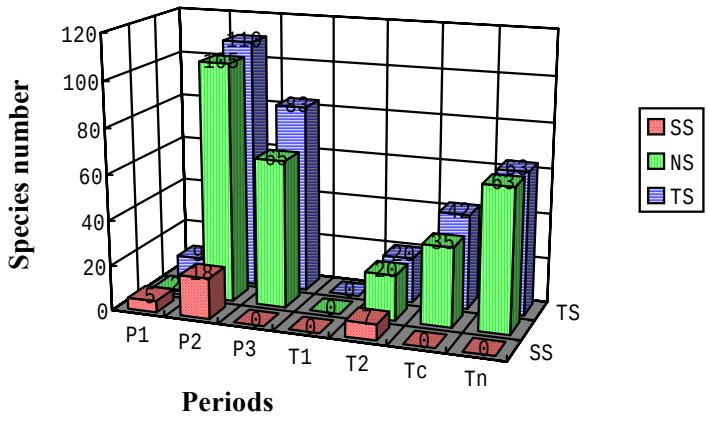

Fig. 3.1 Thalamid sponge species numbers of different periods of Permian and Triassic. TS: Total species. NS: New species; SS: the species that lasted into the next period. P1=the Early Permian; P2=the Middle Permian; P3=the Changhsingian (late Late Permian); T1=the Early Triassic; T2=the Anisian and Ladinian Stages; Tc=the Carnian Stage (early Late Triassic); Tn=the Norian and Rhaetian Stages (late Late Triassic).

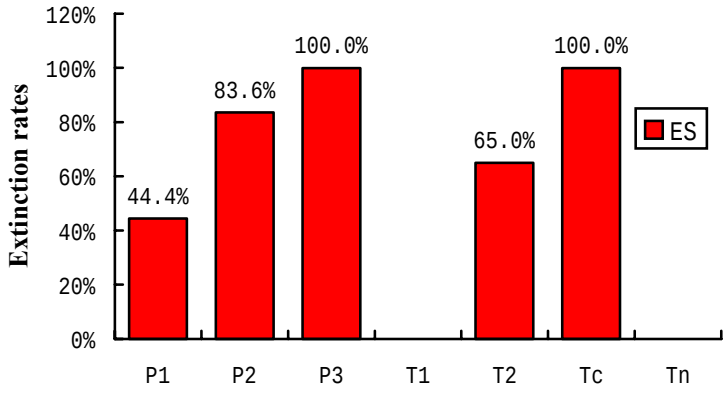

Fig. 3.2 Extinction rates of reefal thalamid sponge species at the end of different periods of the Peremian and Triassic. P1=the Early Permian; P2=the Middle Permian; P3=the Changhsingian Stage; T1=the Early Triassic; T2=the Anisian and Ladinian Stages; Tc=the Carnian Stage (early Late Triassic); Tn=the Norian and Rhaetian Stages (late Late Triassic).

4 Ecological Selection and Cause of End-Permian Mass Extinction

Various hypotheses have been proposed for the cause of the end-Permian mass extinction, e.g., extraterrestrial impact, cosmic radiation, global warming, global cooling, oceanic anoxia, volcanism, etc. Though global warming and oceanic anoxia seem to have more supporters, actually they conflict with the biotic selection in the extinction. The authors of global cooling failed to present solid evidence, and this viewpoint has no supporters up to now. A critical issue about the end-Permian extinction is the sea-level change across the P-T boundary. Some researchers believed in a regression at the end of the Permian, while others argued for a transgression. The change in $\delta^{18}O$ of sea water across the P-T transition is also in dispute. Most data indicate a decrease in the $\delta^{18}O$ of seawater. But, the opposite results are present, too.

As to the various hypotheses are concerned, we believe that any hypothesis, if it cannot give a mechanism accounting for the extinctions of both marine and terrestrial organisms, it would be unacceptable. From this reason, transgression, regression, and oceanic anoxia are all unacceptable. Considering evidence, we propose that global cooling, a mechanism impacting both terrestrial and marine ecosystems, is the most possible mechanism accounting for the end-Permian extinction. The main evidence includes the followings.

4.1 Glacier distribution

Lasting global warming can cause decrease in glacier distribution and even its total disappearance, as well as formation of glacial till. On the contrary, long-term global cooling will cause expansion of glacier volume and distribution, but no glacial till to form. Up to now, no glacial till has been found from P-T boundary deposits.

4.2 Sea-level change

Long-term global warming will result in global sea-level rise. On the contrary, lasting global cooling will cause global sea-level drop. Evidence for a global sea-level drop at the end of the Permian has been found (Wu, 2003).

4.3 Change in $\delta^{18}O$ of seawater

Zhang et al. (1991) analyzed the $\delta^{18}O$ of the carbonates from the P-T boundary sections at Huaying and Liangfengya, Sichuan Province, and those in Jiangxi and Hubei Provinces. These studies used whole-rock samples, which may include diagenetic components that would reduce the reliability of the $\delta^{18}O$ results. To improve the reliability of the test results, we took several single-component (micrite) samples from the 1.1-m-thick latest Permian deposits on the top of the Ziyun reef, Guizhou Province, southwestern China. X-ray diffraction tests show that they do not contain dolomite component. The oxygen isotopic compositions of these samples are shown in Fig. 4.1.

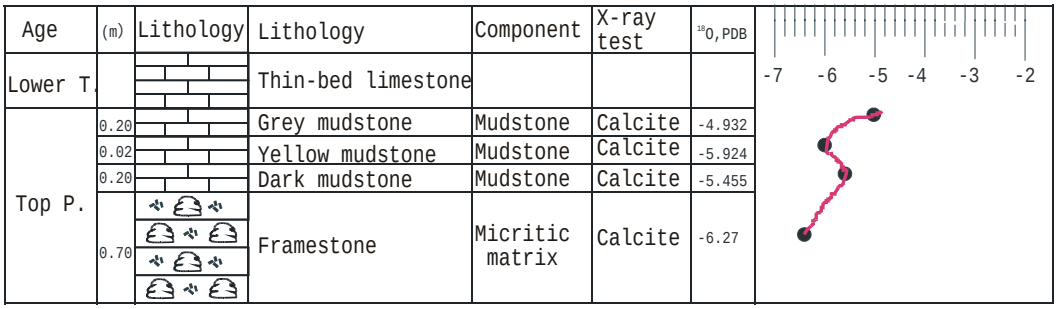

Fig. 4.1 Oxygen isotopic curve of the latest Permian in Ziyun, Guizhou, China

As seen from Fig. 4.1, $\delta^{18}O$ (‰, PDB) increased at the end of the Permian. Increase in $\delta^{18}O$ of sea water is probably related to climatic cooling.

4.4 Ecological selection in the end-Permian mass extinction

If the end-Permian mass extinction was caused by a global warming, the tropical and subtropical organisms in low-latitude areas would have expanded their distribution to high-latitude areas to replace the organisms adapted to cool-cold climates. If the end-Permian extinction was caused by a global cooling, the organisms in low-latitude areas would have disappeared, while those in high-latitude areas would have expanded their distribution to the low-latitude areas.

The ecological selection in the end-Permian mass extinction is in agreement with a global cooling.

4.4.1 Extinction of reefs and reefal organisms

Modern reefs are distributed in low-latitude, warm, shallow seas. Paleozoic reefs are believed to have similar geographic distribution, as they have similar formation mechanism.

Reefs in Late Permian Changhsingian Stage were worldwide distributed. They have been reported from Greece, Thailand, and southern China (including Jiangsu, Jiangxi, Hunan, Hubei, Guizhou, Sichuan, Guangxi Provinces). Many of them have large scale and typical structure.

Unfortunately, all Changhsingian reefs disappeared at the end of the Permian. The Lower Triassic is a gap of reef temporal distribution. Real reefs (not including "stromatolite reefs" and microbial deposits) did not occur until the Middle Triassic Anisian Stage. In the Anisian Stage, reefs were moderately developed.

The Changhsingian reefs were mainly constructed by calcisponges, sclerosponges, and calcareous algae. The calcisponges include inozoans and thalamid sponges, all with calcareous skeletons. Did any Changhsingian reef builder survive the end-Permian crisis?

Some researchers (Flügel and Stanley, 1984) once claimed that some Permian thalamid sponges, such as *Girtyocoelia* lasted into the Early Triassic. But Flügel (1994) himself denied it later. He believed that the similarity between the Early Triassic thalamid sponges and Permian thalamid sponges was actually morphological and they are virtually different organisms. We have examined all Permian and Triassic reefal thalamid sponge species and found that all Changhsingian thalamid sponge species disappeared at the end of the Permian. The thalamid sponges in the Middle Triassic Anisian reefs are all new species.

Up to now, at least one species of tetracoral, *Waagenophyllum,* has been reported from Changhsingian reefs (Fan et al., 1990; Xu et al., 1997; Liu et al., 1997). Like the coeval nonreefal tetracorals (Yang et al., 1991), this reefal tetracoral disappeared at the end of the Permian. Consequently, there are no tetracoral reefs in post-Permian strata.

4.4.2 Foraminifers

According to shell composition and structure the Late Permian Changhsingian foraminifers can be classified as 4 groups: the first one has calcareous microgranular test, mainly including fusulinids and endothyrids; the second one has agglutinated test composed of sand and other particles cemented by organic glue; the third group has porcelaneous test; the fourth group has hyaline (calcareous, perforated, transparent or translucent) test.

In the Changhsingian Stage, microgranular foraminifers were the most important, agglutinated foraminifers the secondary, and the other two groups the least abundant (Yang et al., 1991).

The end-Permian extinction of Changhsingian foraminifers has high taxonomic selection. Nearly all microgranular foraminifers disappeared at the end of the Permian. In south China, of the 66 species of Changhsingian microgranular foraminifers, all but one disappeared at the end of the Permian (Tong, 1993). At generic level, 98.6% of Changhsingian microgranular foraminifers disappeared, with only one genus left (Yang et al., 1991).

Compared to microgranular foraminifers, agglutinated foraminifers were very fortunate: only 15 of the Changhsingian agglutinated foraminifer genera disappeared at the end of the Permian (Yang et al., 1991). Hyaline foraminifers and porcelaneous foraminifers suffered no major extinction: only 14.3% of Changhsingian hyaline foraminifers disappeared at the end of the Permian (Yang et al., 1991).

The selective extinction of foraminifers at the end of the Permian was probably controlled by climatic change. Since modern and ancient agglutinated foraminifers live in both warm water and cold water, any changes in climate will never kill them all. If the climate becomes too hot, the foraminifers in cold water will be killed, while those in warm water will survive it by migration to cold water; if the climate becomes too cold, the foraminifers in the warm water will be killed, while those in the cold water will survive it through migration to warm water.

Since Paleozoic microgranular foraminifers lived in warm water, their extinction at the end of the Permian, as well as the surviving of most agglutinated foraminifers indicate that the selective extinction of foraminifers at the end of the Permian was probably related to climatic cooling.

4.4.3 Bivalves

Changhsingian bivalves had the same provinciality as Wuchiapingian bivalves. In the Wuchiapingian Stage, there were five bivalve geographic regions. They are: (1) the cool-water Boreal region (including Siberia, Arctic Canada), (2) the cool-water Meridional region (including New Zealand, New Caledonia, E. Australia), (3) the transitional Southern Tethys including Kashmir, the Salt Range, Western Australia, Himalaya), (4) the transitional Northern Pacific region (including Japan, Nevada of USA, Fareast of Russian), and (5) the Tropical Tethys region (including South China, South Alps, Northern Caucasia, Pamirs). In the Boreal and Meridional regions, cool-water bivalve fauna characterized by *Atomodesma* or/and *Kolymia* were developed. In the Tropical Tethys region, the typical cool-water bivalves were lacking, while pectinaceans were dominant. At the intermediate latitudes the bivalve faunas were transitional.

The same provinciality remained in the Changhsingian Stage. However, Changhsingian bivalves reported are limited to low-latitude regions including South China, South Alps, Greece, Iran, Pamirs and Japan. Total 59 genera of Changhsingian bivalves have been reported (Yang et al., 1987), which are mostly from South China. The Changhsingian bivalves in South China include 50 genera and 112 species (Yin, 1985), which is dominated by pectinaceans. According to Yin (1985), Changhsingian pectinaceans in South China include 21 genera and 56 species, which were characterized by *Hunanopecten exilis* and *H. quijiangensis*. With round, small, and thin shells, weak ornaments, and widespread occurrence in siliceous deep-water facies, these species are regarded as nektons (Yang et al., 1991). Changhsingian bivalves in Japan include 18 genera and 18 species, sharing no common species with South China and belonging to a separate region. Other occurrences of Changhsingian bivalves include Italy, Greece, and Julfa of Iran.

The only reported cool-water Changhsingian bivalve fauna are from Kashmir (Nakazama et al., 1975). It includes 11 genera and 13 species, with a typical component *Claraia stachei*.

The stratigraphic level with this species grades upward into the bed yielding *Otoceras*, a cool-water ammonoid (Yin, 1983).

During the end-Permian crisis almost all Changhsingian bivalve species disappeared (Yang et al., 1987). Only a few cool-water bivalves, such as *Claraia stachei, Leptochondria, Entolium, Pseudoclaraia*, survived the crisis. Though including some Changhsingian survivors, the post-extinction bivalves were dominated by newborn species, such as *Claraia griesbachi, Eumorphotis venetiana, Pseudoclaraia wangi*. This fauna was cosmopolitan. For example, *Claraia stachei* occurred in both the Boreal region (within the Changhsingian Boreal region) and Northern Tethys (within the Changhsingian Tropical region); the *Claraia griesbachi* occurred in both Himalaya (within the Changhsingian cool-water South Tethys region) and South China (within the Changhsingian Tropical Tethys). Since *Claraia stachei* was a cool-water species in Changhsingian, its survival of the end-Permian crisis indicates that the crisis might be a climate cooling (since climate warming will decrease cool-water areas, while climate cooling increase coo-water areas). The worldwide distribution of the cool-water species in the post-extinction period indicates that the cool-water conditions were worldwide developed at that time. Or, in other words, the Earth then was totally a "cool ball" and no climate zonation developed.

In late Changhsingian Stage, *Claraia stachei* occurred at, and only at Kashmir, but totally absent from low-latitude areas. At the end of the Permian, this species disappeared from Kashmir and never occur again at this locality. During early Griesbachian Stage, however, this species occurred at Greenland. It disappeared from Greenland at the close of the Griesbachian. Since the end of early Griesbachian it occurred at eastern Australia. It disappeared from eastern Australia at the end of late Griesbachian. From middle late Griesbachian, it occurred at South China and persisted to the end of the Smithian. Its disappearance from western American is also at the end of Smithian. It seems that this species is a stenotropic organism adapted to cool water. As the climate globally became cooler and cooler since the end of the Permian, it migrated from high-latitude areas to low-latitude areas to escape too cold water of high latitudes. The Changhsingian-Smithian migration of this species indicates that the global climate became cooler and cooler during this period.

An interesting phenomenon is that the species of *Claraia* in the post-extinction period had only concentric growth lines, while those in Changhsingian and late Griesbachian are ribbed. Nicol (1967) pointed out that the Arctic bivalves generally have small, thin shells, with little or no ornamentation but growth lines, while the tropical forms generally have larger and thicker shells and more ornamentation. The change in the shell features of *Claraia* may indicate that the post-extinction species of *Claraia* were adapted to cool waters, while the Changhsingian or late Griesbachian species were adapted to warm-water conditions.

Yang et al. (1991) believed that the affection of the end-Permian crisis on bivalves is selective: the epifaunal and nektonic bivalves were severely affected by the crisis, while the infaunal were hardly affected. Thorson (1957) pointed out that the proportion of infaunal

bivalves to epifaunal types is generally higher in cold water than in warm waters. Then, the bivalves that disappeared in the end-Permian crisis are mostly warm water types, while those that survived the crisis are mostly cold-water types. The selective extinction of Changhsingian bivalves indicates that the end Permian mass extinction might be caused by climate cooling.

4.4.4 Ammonoids

The ammonoids in Changhsingian were diverse and abundant. According to Yang et al. (1991), Changhsingian ammonoids include 39 genera and 153 species. The ammonoids in late Changhsingian include 105 species (Yang and Wang, 1999).

The ammonoids in late Changhsingian generally have large evolute discoidal shells with carinate venter and ventral keel, ornamented with strong ribs and nodes, and with ceratitic suture chiefly (Yang and Wang, 1999). They were not only diverse but also abundant.

Most Changhsingian ammonoids disappeared in the end-Permian crisis. According to Yang et al. (1991), only 1 species of 1 genus, *Pseudogastrioceras*, persisted into post-extinction period (early Griesbachian). But, Yang and Wang (1999) stated that three genera, *Pseudogastrioceras*, *Episgeceras*, and *Nodosageceras*, survived the end-Permian crisis.

The three surviving genera have these common features: small-shelled, with weak or no ornamentations. Nicol (1964, 1967) and others found that there are some relationships between morphology of mollusk shells and water temperature: the Arctic forms are usually small, simple, having little or no ornamentation, while the tropical forms can be quite large, ornate, and heavy-shelled. Mollusks shell morphology indicates that the surviving ammonoids were adapted to cold waters, while the extinct genera were adapted to warm waters.

In the post-extinction oceans the sparse survived Changhsingian ammonoids were accompanied by some newborn disaster ammonoids including *Hypophiceras, Tompophiceras, Metophiceras*, and *Otoceras*. The post-extinction ammonoids had small shells with weak ornamentation. Their diversity and abundance were low. But, their distribution was worldwide. These features indicate that they were adapted to cool to cold waters.

Contrary to ammonoids, Changhsingian nautiloids suffered no extinction in the end -Permian crisis (Teichert, 1990). But their abundance was very low in post-extinction seas. Why the nautiloids could survive the crisis? Modern nautiloids mostly live in shallow waters. But, they can move to and live in deep water, too. For example, *Nautilus* can be found in water as deep as 4,000 m deep, although it generally stays in shallow water. Paleozoic nautiloids were strong swimmers and should have similar ability to move to and live in deep water (generally cold water). This seems to be why they can survive the end-Permian crisis, which was probably caused by climatic cooling. Since most organisms nautiloids preyed on in the Changhsingian Stage were absent in the post-extinction oceans, the abundance of nautiloids was limited.

4.4.5 Gastropods

Abundant Changhsingian gastropods were reported from South China, including 35 genera and 53 species (Pan and Yu, 1993). Other occurrences of Changhsingian gastropods include Japan, Alps, Turkey and Kashmir.

Changhsingian gastropods in South China include 3 assemblages. The first assemblage occurred in clastic coastal and estuary deposits, represented by *Acteonina solida*. The second assemblage occurred in carbonate platform deposits, represented by *Porcellia lingshuiensis* and *P. magninodosa*. The last assemblage was distributed in deep-water siliceous deposits, represented by *Extendilabrum alticarinatum* (Pan and Yu, 1993). Evidence from other groups such as bivalves and plants indicates that during the Changhsingian Stage South China was within low-latitude, warm-water biotic province.

Changhsingian gastropods reported from Kashmir include 5 species belonging to 3 genera. During the Changhsingian Stage, Kashmir belonged to cool-water biotic zone.

At the end of the Permian, nearly all gastropods disappeared, either the warm water types in South China or the cool-water types in Kashmir. At generic level some gastropods survived the crisis. They include *Bellerophon*, *Retispira*, *Warthia*, and *Stachella*. The three Changhsingian gastropod genera in Kashmir include *Bellerophon* and *Retispira*, which indicates that these two genera were adapted to cool waters or low-latitude deep waters. *Warthia* occurred in the lowest Triassic of Kashmir, too. So, we believe that the Changhsingian genera that survived the end-Permian crisis are those that were adapted to cool waters.

An excellent statistic study on the end-Permian selective extinction of gastropods was made by Erwin (1989). He found that the gastropods that survived the end-Permian crisis have these attributes: (1) broad geographic distribution, (2) long geological range, and (3) more species in a single genus. Virtually, all these are the attributes of eurytropic taxa. It is eurytropic animals that have broad geographic distribution and long geological range. Ecology of modern gastropods may give us some inspiration. Modern gastropods differ greatly in ecology and distribution: some are adapted to broad temperature range and have wide distribution; some others are adapted to narrow temperature range and have very limited distribution. Erwin's study and the case of modern gastropods tell us that the survived Changhsingian gastropods are eurytropic types.

A curious phenomenon is that abundant tiny (<2mm) gastropods, generally one to several millimeters large, occurred worldwide in post-extinction earliest Triassic deposits (Yang et al., 1987; Hallam and Wignall, 1997). Hallam and Wignall (1997) stated that "microgastropod grainstones composed of millimeter-sized species are found throughout all equatorial Tethyan sections and extend into the Perigondwanan sections of Pakistan". One may ask, "Are these small gastropods juveniles killed by catastrophes?" Study by Batten and Stokes (1987) shows that the tiny gastropods are adults.

It is known that modern gastropods change their shell-size to adapt to unusual environ-

mental conditions. Observations by modern biologists show that the growth rate of modern gastropods is influenced or controlled by environmental conditions. The growth rate of some gastropods under favorable conditions is about 12 times greater than those under unfavorable conditions. In addition, under unfavorable conditions, life length of gastropods decreased by 5~6 times. This means that the shell size of the adult gastropods in unfavorable conditions will greatly decrease. Nicol (1967) claimed that the shells of mollusks in Arctic water are small, thin, with weak or without ornamentations, while those in warm waters are generally larger, thick, and with strong ornamentations. This rule is true of earliest Triassic bivalves, ammonoids, and probably gastropods. So, we believe that the small-sized gastropods in the earliest Triassic were adapted to cool-water conditions.

4.4.6 Brachiopods

Brachiopods in Late Changhsingian were diverse, including more than 89 genera and 146 species, and were mainly distributed in South China. In the late Changhsingian, brachiopods in South China include more than 62 genera and 119 species (Xu and Grant, 1994). Late Changhsingian brachiopods in the Salt Range, Pakistan include more than 21 genera and 22 species (Grant, 1970), and those from Kashmir include more than 11 genera and 11 species (Shimizu, 1981). Some other places, such as Southern Alps (Waterhouse, 1967), Pancaucasia (Teichert et al., 1973), and Iran (Iranian-Japanese Research Group, 1981) yield brachiopods probably belonging to early Changhsingian rather than late Changhsingian (Xu and Grant, 1994).

Paleobiogeographic provinciality was developed for Late Permian brachiopods. According to Nakamura et al. (1985), there were two paleogeographic provinces in the Tethyan Realm: Middle Tethyan and Gondwana Tethyan. The Middle Tethyan was divided as two subprovinces: Cathaysia Tethyan (including the South China, Iran, Trancaucasia) and West Tethyan (which extends from Kashmir and Pakistan in the east to the Southern Alps in the west) (Xu and Grant, 1994).

Almost all late Changhsingian brachiopods disappeared in the end-Permian crisis. According to Erwin (1994), 90% of the late Changhsingian brachiopod genera disappeared in the end-Permian crisis. At specific level, the extinction rates are slightly different between different places. According to Xu and Grant (1994), of the 119 species of the late Changhsingian brachiopods only 15 survived the end-Permian crisis and lasted into the early Griesbachian. The extinction rate is 87%. Of the late Changhsingian brachiopods in the Salt Range, 3 genera and 3 species persisted into the early Griesbachian, and the extinction rate is 90%. Of the late Changhsingian brachiopods in Kashmir, 1~2 species lasted into the early Griesbachian and the extinction rate is 86%.

The brachiopods in early Griesbachian were almost all late Changhsingian survivors, except some species of *Lingula*. Brachiopods of this period were characterized by small and

thin shells, and very broad distribution. As to the late Changhsingian brachiopod survivors were concerned, Zhao et al. (1981) stated: “most of them are thin-shelled and probably are neustons. They have great adaptability to various lithofacies and have wide geographic distribution: you could encounter them in almost all shallow marine deposits in South China. Probably thanks to their greater adaptability to environments, they could survive the crisis at the transition of the Paleozoic and Mesozoic”.

The brachiopods that survived the end-Permian crisis in Kashmir were also small, and because of this, Shimizu (1981) called them “dwarf”.

It is obvious that the brachiopods that survived the end-Permian crisis were eurytopic. A common characteristic among the survivors is that they have small and thin shells. Dodd and Stanton (1981) pointed out that, “the brachiopods living in cold water in the Antarctic region have thinner shells and fewer spicules in their tissue than do those from warmer areas. This may be related to the greater solubility of $CaCO_3$ and to the physiologic difficulty in secreting the shell in cold water”. A known rule for mollusks is that the mollusks in cold water are generally small and thin-shelled (Nicol, 1967). For this reason, I believe that the brachiopods that survived the end-Permian crisis were adapted to cold water or both warm-temperature water and cold water.

Early Griesbachian brachiopods show no paleobiogeographic provinciality. But, their distribution was worldwide (Xu and Grant, 1994). Compared to their distribution in late Changhsingian, their distribution really expended. For example, in Salt Range, *Crusithyris* and *Lingula* were absent from the Upper Changhsingian but occurred in the lower Griesbachian. So, we propose that in the early Griesbachian cool-cold waters were globally distributed and there were no climatic zonation.

Of the early Griebachian brachiopods, *Lingula* is a typical disaster genus, which has a long geologic history from Ordovician to Recent. During the long geologic history, several catastrophic events have occurred. But, *Lingula* have survived all of them. Which talent it has enabled it to do so? *Lingula* has a talent in digging deep burrows. Dodd and Stanton (1981) stated that, “the animal is able to retreat within its burrow to avoid contact with low-salinity water at surface”. Probably it also has adaptation to extreme changes in temperature. When the environmental conditions were unfavorable, it retreated within its deep burrow to avoid them. This may be the secret of *Lingula’*s survival of all catastrophes.

4.4.7 Plants

In Late Permian there were four floral kingdoms: the Angara kingdom, Atlantic kingdom, Cathaysian kingdom, and Gondwana Kingdom (Dobruskina, 1987). The first flora was distributed in Siberia, representing North Temperate mid-latitude climates; the second flora was distributed in North American (Oregon) and Urals, representing paleo-equator and lower latitude climate; the third flora was distributed in China, India, southern Sumatra，representing

paleo-equator and low latitude climate, too. The forth flora was distributed on the Gondwana, representing south temperate to cold, high-latitude climate.

During the end-Permian extinctions all components of the four floras disappeared except for some *Glossopteris*. *Glossopteris* was the dominant components of the Gondwana kingdom. But its distribution was by no means limited to the Gondwana. It occurred in the Cool Temperate Zone (Ziegler, 1990), Warm Temperate Zone, Mid-latitude desert, North Boreal Zone, and Cold Temperate Zone, showing very wide adaptability to climates (Asama, 1985; Archangelsky, 1990). Perhaps thanks to its great climate adaptability, some glossopteris survived the end-Permian catastrophes and lasted into the post-extinction flora (Pant, 1987; Pant and Pant, 1987).

Other plants that had survived the end-Permian catastrophes include some small weedy isoetales such as *Isoetes*, some seed ferns such as *Dicroidium* (Retallack, 1995), and some conifers including *Voltzia*. The post-extinction earliest Triassic flora had some dominant trees, including conifer *Voltzia*, seed fern *Dicroidium*, and lycopod *Pleuromeia*. All of them were cosmopolitan in distribution (Meyen, 1973; Schopf, 1973; Dobruskina, 1987). *Voltzia* and *Dicroidium* were encountered at all paleo-latitudes (Dobruskina, 1987; Veevers et al., 1994; Retallack, 1995) and *Pleuromeia* was encountered virtually in all coastal habitats (Wang, 1996).

The removal of low-latitude plants and the survival of the cold-climate *Glossopteris* at the end of the Permian suggest that the end-Permian extinction was probably caused by climate cooling.

4.5 Conclusion

Evidence of global sea-level changes, oxygen isotopic changes of sea water, as well as biotic selection in the extinction indicates that the end-Permian mass extinction was probably caused by drastic climatic cooling.

Reference

Aleotti, G., Dieci, G., and Russo, F., 1986. Eponges Permiennes de la Vallee de Sosio (Sicile); Revision systematique des sphinctozoaires. Ann. Paleont., 72(3), 211-246.

Alvarez, L., Alvarez, W., Asaro, F., Michel, H., 1980. Extraterrestrial cause for the Cretaceous-Tertiary extinction. Sciences 208, 1095-1180.

Assereto, R., Casati, P., 1965. Revisione della stratigrafia permo-triassica della val Camonica meridionale (Lombardia). Rivista Italiana di Paleontologia e Stratigrafia. 71(4), 999-1097.

Babcock, J.A., Yurewicz, D.A., 1989. The massive facies of the Capitan limestone, Guadalupe Mountains, Texas and New Mexico. In: Harris, P.M., and Grover, G.A., Subsurface and outcrop examination of the Capitan shelf margin, northern Delaware Basin. SEPM Core Workshop 13, 365-372.

Beauchamp, B., 1989. Lower Permian (Sakmarian) *Tubiphytes*-bryozoan buildup, southwestern Ellesmere Island Canadian Arctic Archipelago. In: Geldsetzer, James and Tebbutt, (Eds.), Reefs, Canada and Adjacent areas. 585-589.

Bernecker, M., 1996. Upper Triassic reefs of the Oman Mountains: data from the south Tethyan margin. Facies, 34, 41-76.

Brandner, R., Flugel, E., Senowbari-Daryan, B., 1991. Microfacies of carbonate slope boulders: indicator of the source area (Middle Triassic: Mahlknecht Cliff, western Dolomites). Facies, 25, 279-296.

Cao, C. Q., Shang, Q. H., 1998. Microstratigraphy of Permo-Triassic sequence of the Meishan section, Zhejiang, China. Palaeoworld 9, 147-152.

Chen, C. Z., He, G. X., Chen, J. H., Sun, D. L., Wang, Z. H., 2000. Marine Triassic. In: Stratgraphical Studies in China (1979-1999), 241-259.

Chuvashov, B. I., 1983. Permian reefs of the Urals. Facies 8, 191-212.

Clark, D. L., 1959. Conodonts from the Triassic of Nevada and Utah. Journal of Paleontology 33 (2), 305-312.

Clark, D.L, Wang, C. Y., Orth C.J, Gilmore, J.S. 1986. Conodont survival and low iridium abundances across the Permian-Triassic boundary in South China. Science 233, 984-986.

Dai, J. Y., Zhang, J. H., 1989. Conodonts. In, Li, Z. S., Zhan, L. P., Dai, J. Y., Jin, R. G., Zhu, X. F., Zhang, J. H., Huang, H. Q., Xu, D. Y., Yan, Z., Li, H. M., (Eds.), 1989. Study on the Permian–Triassic biostratigraphy and event stratigraphy of northern Sichuan and southern Shaanxi. Ministry of Geology and Mineral Resources, Geological Memoirs, Series 2, No.9, 220-238.

Davies, G. R., Richards, B. C., Beauchamp, B., Nassichuk, W. W., 1989. Carboniferous and Permian reefs in Canada and adjacent areas. In: Geldsetzer, James and Tebbutt, (eds.), Reefs, Canada and Adjacent areas. 565-574.

Deng, Z. Q., 1981. Upper Permian sponges from Laibin of Guangxi. Acta Paleont. Sinica, 20/5, 418-424.

Di Stefano, P., Gullo, M., Senowbari-Daryan, B., 1990. The Upper Triassic reef of Monte Genuardo (southwestern Sicily). Boll. Soc. Geol. It., 109, 103-114.

Dieci, G., Antonacci, A., Zardini, R., 1968. Le Spugne cassiane (Trias mediosuperiore) della regione dolomitica attorno a Cortina'Ampezzo. Bull. Soc. Paleont. Ital., 7(2), 94-155.

Ding, M. H., 1983. Early Triassic conodonts from Majiashan, Chao County, Anhui, China and the stratigraphy. Earth Science-Journal of Wuhan College of Geology 20 (2), 37-48.

Ding, M. H., 1992. Conodont sequences in the Upper Permian and Lower Triassic of South China and the nature of conodont faunal changes at the systemic boundary. In: W. C. Sweet, Z. Yang, J. M. Dickens, H. Yin, (eds.), Permo-Triassic Events in the Eastern Tethys. Cambridge University Press, Cambridge (1992). 109–119.

Dodd, J. R., Stanton, R. J., Jr., 1981. Paleoecology, concepts and application. John Wiley & Sons, Inc., New York, 559p.

Douzen, K., Ishiga, H., 1995. Sea-level change deduced from rhythmicity of Middle Triassic to Lower Jurassic bedded cherts of Southwest Japan. Journal of the Geological Society of Japan 101(5), 354-366.

Ellison, S., 1941. Revision of the Pennsylvanian conodonts. Journal of Paleontology 15 (2), 107-143.

Erwin, D. H., 1993. The great Paleozoic crisis. Columbia University Press, New York. 327pp.

Erwin, D. H., P. Hua-Zhang, 1996. Recoveries and radiations: gastropods after the Permo-Triassic mass extinction. In: Hart, M.B., (ed.), 1996, Biotic recovery from mass extinction events. Geological Society Special Publication No. 102, 223-229.

Fagerstrom, J. A., 1994. The history of Devonian-Carboniferous reef communities: extinction, effects, recovery. Facies 30, 177-192.

Fan, J. S., Ma, X., Zhang, Y. B., Zhang, W., 1982. The Upper Permian reefs in west Hubei, China. Facies 6, 1-44.

Fan, J. S., Qi, J. W., Zhou, T. M., Zhang, X. L., Zhang, W., 1990. Permian reefs in Longlin, Guangxi. Geological Publishing House. 128pp.

Fan, J. S., Wu, Y. S., 2002. Sedimentology of the Middle Triassic Poduan Formation in Guanling, Guizhou Province, China. Journal of Palaeogeography, 4(2), 67-74.

Fan, J. S., Wu, Y. S., 2002. Restudy of the Permian reefs in eastern Sichuan Province, China. Oil and Gas Geology, 23(1): 12-18.

Fan, J. S., Wu, Y. S., 2002. Calcareous algae in the Permian reefs in Guangxi, Guizhou, and Sichuan Procinces and their paleoecology. Journal of Micropaleontology, 19(4), 337-347

Fan, J. S.g, Zhang, W., 1985. Sphinctozoans from Late Permian of Lichuan, West Hubei, China. Facies, 13, 1-44.

Flügel, E., Reinhardt, J., 1989. Uppermost Permian reefs in Skyros (Greece) and Sichuan (China): implications for the Late Permian extinction event. Palaios 4, 502-518.

Flügel, E., Di Stefano, Senowbari-Daryan, B., 1991. Microfacies and depositional structure of allochthonous carbonate base-of-slope deposits: the late Permian Pietra di Salomone Megablock, Sosio Valley (western Sicily). Facies 25, 147-186.

Flügel, E., Kochansky-Devide, V., Ramovs, A., 1984. A middle Permian calcisponge /algal/cement reef: Straza near Bled, Slovenia. Facies, 10, 179-256.

Fois, E., Gaetani, M., 1984. The recovery of reef-building communities and role of cnidarians in carbonate sequences of the Middle Triassic (Anisian) in the Italian Dolomites. Palaeontographica Americana, 54, 191-200.

Fursich, F. T., Wendt, J., 1977. Biostratinomy and palaeoecology of the Cassian Formation (Triassic) of the Southern Alps. Palaeogeogr. Palaeoclimat. Palaeoecol., 22(4), 257-324.

Gaetani, M., Fois, E., Jadoul, F., Nicora, A., 1981. Nature and evolution of Middle Triassic carbonate buildups in the Dolomites (Italy). Marine Geology, 44, 25-57.

Garber, R. A., Grover, G. A., Harris, P. M., 1989. Geology of the Capitan shelf margin-subsurface data from the northern Delawere Basin. SEPM Core Workshop 13, 3-272.

Hallam, A., Wignall, P.B., 1997. Mass extinctions and their aftermath. Oxford University Press. p. 98-116.

Harland, W. B., Armstrong, R. L., Cox, A. V., Craig, L. E., Smith, A. G., Smith, D. G., 1989. A geologic time scale. Cambridge University Press. 263pp.

Harris, P. M., Grover, G. A., 1989. Subsurface and outcrop examination of the Capitan shelf margin, northern Delaware Basin. SEPM Core Workshop 13.

Henderson, C. M., Baud, A., 1996. Correlation of the Permian-Triassic boundary in Arctic Canada and comparison with Meishan, China. Proceedings, 30th International Geological Congress 11, 143-152.

Isozaki, Y., 1997. Permo-Triassic boundary superanoxia and stratified superocean: records from lost deep sea. Science, 276, 235-238.

Jin, Y. G., 1994. Two phases of the end-Permian mass extinction. Annual Convention of Canadian Society of Petroleum Geologists, Program and Abstract. p.152.

Jin, Y. G., Mei, S. L., Wang, W., Wang, X. D., Shen, S. Z., Shang, Q. H., Chen, Z. Q., 1998. On the Lopingian Series of the Permian System. Palaeoworld 9, 1-18.

Jin, Y. G., Shen, S. Z., Zhu, Z. L., Mei, S. L., Wang, W., 1996. The Selong Section, candidate of theglobal stratotype section and point of the Permian-Triassic boundary. In: Yin, H. F., (ed.), 1996. The Palaeozoic-Mesozoic boundary candidates of the global stratotype section and point of the Permian-Triassic boundary. China University of Geosciences Press, Wuhan.

Jin, Y. G., Wang, Y., Wang, W., Shang, Q. H., Cao, C. Q., Erwin, D. H., 2000. Pattern of marine mass extinction near the Permian–Triassic boundary in South China. Science 289 (2000), 432–436.

Jin, Y. G., Wardlaw, B. R., Glenister, B. F., Kotlyar, G.V ., 1997. Permian chronostratigraphic subdivision. Episodes 20(1), 10-15.

Jin, Y. G., Zhang J., Shang, Q. H., 1995. Pre-Lopinggian catastrophic event of marine faunas. Acta Palaeontologica Sinica 34(3), 410-427.

Johnson, A. L. A., 1986. Triassic scallop extinctions. Palaeontological Association (Great Britain) Annual Conference Abstract, 15.

Kershaw, S., Guo, L., Swift, A., Fan, J., 2002. ?Microbialites in the Permian-Triassic boundary interval in central China: structure, age and distruction. Facies 47, 83–90.

Kershaw, S., Zhang, T., Lan, G., 1999. A ?microbiolite carbonate crust at the Permian-Triassic boundary in South China, and its paleoenvironemntal significance. Paleogeography, Paleoclimatology, Paleoecology 146, 1-18.

Knoll, A. H., Bambach, R. K., Canfield, D. E., Grotzinger, J. P., 1996. Comparative earth history and Late Permian mass extinction. Science 273, 452-457.

Kozur, H., 1975. Beiträge zur Conodontenfauna des Perm. Geol. Paläont. Mitt. Innsbruck 5 (4), 1-44.

Kozur, H., 1977. Revision der Conodontengattung Anchignathodus und ihrer Typusart. Z. Geol. Wiss. Berlin. 5 (9), 1113-1127.

Kozur, H., 1996. The conodonts Hindeodus, Isarcicella and Sweetohindeodus in the Uppermost Permian and Lowermost Triassic. Geologia Croatica 49 (1), 81-115.

Kozur, H., Mostler, H., Rahimi-Yazd, A., 1975. Beiträge zur Mikropalaontologie permotriadischer Schichtfolgen. Teil II, Neue Conodonten aus dem Oberperm und der basalen Trias von Nord- und Zentral Iran. Geol. Paläont. Mitt. Innsbruck 5 (3), 1-23.

Lai, X. L., Mei, S. L., 2000. On zonation and evolution of Permian and Triassic conodonts. In: H. Yin, J. M. Dickins, G. R. Shi and J. Tong, eds., Permian-Triassic Evolution of Tethys and Western Circum-Pacific. Elsevier Science. 371-392.

Lai, X. L., Wignall, P., Zhang, K. X., 2001. Palaeoecology of the conodonts Hindeodus and Clarkina during the Permian –Triassic transitional period. Palaeogeography, Palaeoclimatology, Palaeoecology 171, 63–72.

Lehrmann, D. J., Yan, W., Wei, J. Y., Yu, Y. Y., Xiao, J. F., 2001. Lower Triassic peritidal cyclic limestone; an example of anachronistic carbonate facies from the Great Bank of Guizhou, Nanpanjiang Basin, Guizhou Province, South China. Palaeogeography, Palaeoclimatology, Palaeoecology, 173(3-4), 103–123.

Li, L., 1995. Evolutionary change of bivalves from Changhsingian to Griesbachian in south China. Acta Palaeontologica Sinica, 34(3), 350-369.

Li, Z. S., Zhan, L. P., Dai, J. Y., et al. 1989. Study on the Permian-Triassic biostratigraphy and event stratigraphy of northern Sichuan and southern Shaanxi. Geological Publishing House.

Li, Z. S., Zhan, L. P., Yao, J. X., Zhou, Y. Q., 1991. On the Permian-Triassic events in South China; probe into the end Permian abrupt extinction and its possible causes. In: Kotaka, T., Dickins, J. M, McKenzie, K. G, Mori, K., Ogasawara, K., Stanley, G. D Jr. (Eds.), Shallow tethys 3. Proceedings of the International Symposium on Shallow Tethys 3, 371-385.

Liu, Z. H., et al., 1997. Upper Permian reefs in Hunan and Chenxi. Science and Technological Publisher of Yunnan Province.

Matsuda, T., 1981. Early Triassic conodonts from Kashmir, India, Part 1, Hindeodus and Isarcicella. Journal of Geosciences, Osaka City University 24 (3), 75-108.

Mei, S. L., 1996. Restudy of conodonts from the Permian–Triassic boundary beds at Selong and Meishan and the natural Permian–Triassic boundary. In Centennial Memorial Volume of Prof. Sun Yunshu, Palaeontology and Stratigraphy, H. Wang and X. Wang, eds., China University of Geosciences Press, Beijing (1996), 141-148.

Mei, S. L., Zhang, K. X., Wardlaw, B. R., 1998. A refined succession of Changhsingian and Griesbachian neogondolellid conodonts from the Meishan section, candidate of the global stratotype section and point of the Permian-Triassic boundary. Palaeogeography, paleoclimatology, Paleoecology 143, 213-226.

Murata, M., 1981. Late Permian and Early Triassic conodonts from Guryul Ravine. Memoirs of the Geological Survey of India, Palaeontologia Indica, New Series XLVI, 181-184.

Nestell, M. K., Wardlaw, B. R., 1987. Upper Permian conodonts from Hydra, Greece. Journal of Paleontology 61 (4), 758-772.

Nicoll, R. S., Metcalfe, I., Wang, C. Y., 2002. New species of the conodont Genus Hindeodus and the conodont biostratigraphy of Permian-Triassic boundary interval. Journal of Asian Earth Sciences 20, 609-631.

Noe, S. U., 1987. Facies and paleogeography of the marine Upper Permian and of the Permian-Triassic boundary

in the Southern Alps (Bellerophon Formation, Tesero Horizon). Facies 16, 89-142.

Orchard, M. J., Nassichuk, W. W., Rui, L., 1994. Conodonts from the Lower Griesbachian *Otoceras latilobatum* Bed of Selong, Tibet and the position of the Permian-Triassic boundary. Canadaian Society of Petrolum Geologists, Mem. 17, 823-843.

Ott, E., 1967. Segmentierte Kalkschwamme (Sphinctozoa) aus der alpinen Mitteltrias und ihre Bedeutung als Riffbildner im Wettersteinkalk. Bayer. Akad. Wiss., Math.-naturwiss. Kl., Abh., N. F., 131, 1-96.

Paull, R. K., Paull, R. A., 1994. H*indeodus parvus*-proposed index fossil for the Permian-Triassic boundary. Lethaia 27, 271-272.

Perri, M. C., Farabegoli, E., 2003. Conodonts across the Permian-Triassic boundary in the Southern Alps. Cour. Forsch.-Inst. Senckenberg 245, 281-313.

Perri, M. C., 1991. Conodont biostratigraphy of the Werfen Formation (Lower Triassic), Southern Alps, Italy. Bollettino della Società Paleontologica Italiana 30 (1), 23–46.

Perri, M. C., Molloy, P. D., Talent, J. A., 2004. Earliest Triasasic conodonts from Chitral, Northernmost Pakistan. Rivista Italiana di Paleontolologia Stratigrafia 110(2), 467-478.

Qi, W. T., 2002. Evolution of reef ecosystems and global environmental change history. Peking University Press, p.168.

Ramovs, A., 1986. Reef building organisms and reefs in the Permian of Slovenia, NW Yugoslavia. Mem. Soc. Geol. It., 34, 189-193.

Raup, D. M., 1979. Size of the Permian-Triassic bottleneck and its evolutionary implications. Science 206, 217-218.

Riedel, P., 1988. Facies and development of the 'Wilde Kirche' reef complex (Rhaetian, Upper Triassic, Karwendelgebirge, Austria). Facies, 18, 205-218..

Rigby, J. K., Senowbari-Daryan, B., 1996. Gigantospongia, new genus, the largest known Permian sponge, Capitan Limestone, Guadalupe Mountains, New Mexico. J. Paleont., 70(3), 347-355.

Rigby, J. K., Fan, J. S., Zhang, W., 1989. Sphinctozoan sponges from the Permian reefs of South China. J. Paleont., 63/4, 404-439.

Rigby, J. K., Fan, J. S., Wang, S. H., Zhang, X. L., 1994. Sphinctozoan and inozoan sponges from Permian reefs of South China. Brigham Young University Geology Studies, 40, 43-109.

Rigby, J. K., Senowbari-Daryan, B., Liu, H. B., 1998. Sponges of the Permian upper Capitan Limestone Guadalupe Mountains, New Mexico and Texas. Brigham Young University Geology Studies 43, 19-101.

Rigby, J. K., Wu, X. C., Fan, J. S., 1998.Triassic hexactinellid sponges from patch reefs in north-central Sichuan, People's Republic of China. Brigham Young University Geology Studies 43, 119-165.

Russo, F., Neri, C., Mastandrea, A., Baracca, A., 1997. The mud mound nature of the Cassian Platform margins of the Dolomites; a case history: the Cipit boulders from Punta Grohmann (Sasso Piatto Massif, Northern Italy). Facies, 36, 25-36.

Sano, H., Horibo, K., Kumamoto, Y., 1990. *Tubiphytes-Girvanella* reefal facies in Permian buildup, Mino terrane, central Japan. Sedimentary Geology, 68, 293-306.

Scholz, G., 1972. An Anisian Wetterstein limestone reef in North Hungary. Acta. Miner.-Petrogr., Szeged, 20(2), 337-362.

Schönlaub, H. P., 1991. The Permian-Triassic of the Gartnerkofel-1 Core (Carnic Alps, Austria), Conodont biostratigraphy. Abh. Geol. B.-A. 45, 79-98.

Schubert, J. K., Bottjer, D.J., 1992. Early Triassic stromatolites as post-mass extinction disaster forms. Geology, 20, 883-886.

Senowbari-Daryan, B., 1994. Segmentierte Schwamme ("Sphinctozoen") aus der Obertrias (Nor) des Taurus-Gebirges (S-Turkei). Abh. Geol. B.-A., 50, 415-446.

Senowbari-Daryan, B., Di Stefano, 1988. Microfacies and sphinctozoan assemblage of some Lower Permian breccias from the Lercara Formation (Sicily). Riv. Ital. Paleont. Stratigr., 94(1), 3-34.

Senowbari-Daryan, B., Ingavat-Helmcke, R., 1994. Sponge assemblage of some Upper Permian reef limestones from Phrae province (Northern Thailand). Geologija, 36, 5-59.

Senowbari-Daryan, B., Reid, R. P., 1987. Upper Triassic sponges (sphinctozoa from southern Yukon, Stikinia terrane. Can. J. Earth Sci., 24, 882-902.

Senowbari-Daryan, B., Rigby, J. K., 1988. Upper Permian segmented sponges from Djebel Tebaga, Tunisia. Facies 19, 171-250.

Senowbari-Daryan, B., Rigby, J. K., 1991. Three additional thalamid sponges from Djebel Tebaga (Tunisia). J. Paleont., 65, 623-629.

Senowbari-Daryan, B., Schafer, P., 1979. Neue Kalkschwamme und ein Problematikum (*Radiomura cautica* n.g., n. sp.) aus Oberrhat-Riffen sudlich von Salzburg (Nordliche Kalkalpen). Mitt. Osterr. Geol. Ges., 70, 17-42.

Senowbari-Daryan, B., Schafer, P., 1986. Sphinctozoen (Kalkschwamme) aus den norischen Riffen von Sizilien. Facies, 14, 235-284.

Senowbari-Daryan, B., Shafer, P., 1983. Zur Sphinctozoen-Fauna der obertriadischen Riffkalke (Pantokratokalke) von Hydra, Griechenland. Geol. et Palaeont., 17, 179-205.

Senowbari-Daryan, B., Stanley, G.D., Jr., 1992. Late Triassic thalamid sponges from Nevada. J. Paleont., 66(2), 183-193.

Senowbari-Daryan, B., Matarangas, D., Vartis-Matarangas, M., 1996. Norian-Rhaetian reefs in Argolis Peninsula, Greece. Facies 34, 19-20.

Senowbari-Daryan, B., Zuhlke, R., Bechstadt, T., Flugel, E., 1993. Anisian (Middle Triassic) buildups of the Northern Dolomites (Italy): the recovery of reef communities after the Permian/Triassic Crisis. Facies 28, 181-256.

Sepkoski, J. J., Jr., 1990. The taxonomic structure of periodic extinction. In: Sharpton, V. L., and Ward, P. D., eds., Global catastrophes in Earth history; an interdisciplinary conference on impacts, volcanism, and mass mortality. Geological Society of America Special Paper 247.

Sha, Q. A., Wu, W. S., Fu, J. M., 1990. Comprehensive study on the Permian in Dianqiangui area. Science Press. 215p.

Stanley, G. D., Jr., 1988. The history of early Mesozoic reef communities: a three-step process. Palaios, 3, 170-183.

Stanley, G. D., Jr., Nelson, J.L., 1995. New investigations on Eaglenest Mountain, northern Quesnel terrane: an Upper Triassic reef facies in the Takla Group, central British Columbia (93N/11E). Geological Fieldwork

1995, paper 1996-1.

Stanley, G. D., Jr., Gonzalez-Leon, C., Sandy, M. R., Senowbari-Daryan, B., Doyle, P., Tamura, M., Erwin, D. H., 1994. Upper Triassic invertebrates from Antimonio Formation, Sonora, Mexico. J. Paleont. 68, Supplement to No. 4, 1-33.

Stanley, S. M., Yang, X., 1994. A double mass extinction at the end of the Paleozoic Era. Science 266, 1340-1344.

Stanley, S.M., 1988. Paleozoic mass extinctions: shared patterns suggesting global cooling as a common cause. American Journal of Sciences, 288, 334-352.

Stepanov, D. L., Golshani, F., Stöcklin, J., 1969. Upper Permian and Permian-Triassic boundary in North Iran. Geological Survey of Iran, Report 12, 1-67.

Sun, Y. Y., Chai, Z. F., Ma, S. L., Mao, X. Y., Xu, D. Y., et al., 1984. The discovery of iridium anomaly in the Permian-Triassic boundary clay in Changxing, Zhejiang, China and its significance. In: Su, Z. W., (Ed.), Developments in geoscience; contribution to the 27th international geological congress. P.235-245. Science Press.

Sweet, W. C., 1970a. Permian and Triassic Conodonts from Guryul Ravine, Vihi District, Kashmir. Paleont. Contrib. Kansas Univ. 49, 1-10.

Sweet, W. C., 1970b. Uppermost Permian and Lower Triassic conodonts of the Salt Range and Trans-Indus Ranges, West Pakistan. In：KUMMEL, B. AND TEICHERT, C. (edits.), Stratigraphic Boundary Problems, Permian and Triassic of West Pakistan. Spec. Publ. Kansas Univ., Dept. Geol. 4, 207-275. Lawrence.

Sweet, W. C., 1973. Contodontophorida Eichenberg, 1930. In Permian–Triassic Strata, Kuh-e-Ali Bashi, Northwest Iran, Teichert, C., Kummel, B., Sweet, W. C., eds., Bulletin Musseum of Comparative Zoology 145 (8), 423-472.

Sweet, W. C., 1973. Late Permian and Early Triassic conodonts faunas. In The Permian and Triassic systems and their mutual boundary, Logan, A., and Hill, L.V., eds., Canadian Society of Petroleum Geologists, 630-646.

Teichert, C., Kummel, B., Kapoor, H. M., 1970. Mixed Permian and Triassic Fauna, Guryul Ravine, Kashmir. Science 167, 174-175.

Teichert, C., Kummel, B., Sweet, W. C., 1973. Permian-Triassic strata, Kuh-E-Ali Bashi, Northwest Iran. Bulletin Musseum of Comparative Zoology 145 (8), 359-472.

Tian, S. G., 1993. The Permo–Triassic boundary and conodont zones in northwestern Hunan Province (in Chinese with English abstract). Bulletin of Chinese Academy of Geological Sciences 26, 133-150.

Tian, S. G., Fan, J. S., 2001. Early-Middle Permian reef frameworks and reef-building models in the eastern kunlun Mountains, Acta Geologica sinica (English Edition), 75(2), 115-125.

Toomey, D. F., 1991. Late Permian reefs of southern Tunisia: facies patterns and composition with the Capitan reef, southwestern United States. Facies, 25, 119-146.

Turnsek, D., Buser, S., Ogorelec, B., 1984. The role of corals in Ladinian-Carnian reef communities of Slovenia, Yugoslavia. Palaeontographica Americana, 54, 201-209.

Twitchett, R. J., Looy, C. V., Morante, R., Visscher, H., Wignall, P.B., 2001. Rapid and synchronous collapse of marine and terrestrial ecosystems during the end-Permian biotic crisis. Geology 29, 351-354

Waagen, W., Wentzel, J., 1887. Salt-Fossil. 1. Productus-Limestone fossils, 7. Coelenterata- Amorphozoa-Protozoa. Mem. Geol. Surv. India, Palaeont. Indica, 925-988.

Wahlman, G. P., 1988. Subsurface Wolfcampian (Lower Permian) shelf-margin reefs in the Permian Basin of west Texas and southeastern New Mexico. Midcontinent SEPM Special Publication, 1, 177-204.

Wang, C. Y., 1994. Permian-Triassic Eventostratigraphy and biostratigraphy of South China. Journal of Stratigraphy 18 (2), 110-118.

Wang, C. Y., 1995. Conodonts of Permian–Triassic boundary beds and biostratigraphic boundary (in Chinese with English abstract). Acta Palaeontologica Sinica 34 (2), 129-151.

Wang, C. Y., Wang, Z. H., 1981. The conodonts from the Permian Longtan and Changxing Formations in Changxing area, Zhejiang, paleoecology and stratigraphy. In Proceedings the 1st symposium of China Society of Micropaleontology, Science Press, Beijing, 114-120.

Wang, H. Z., Liu, B. P., (eds.), 1980. Course of Earth history. Geological Publishing House, 201-219.

Wang, Y. B., Zhang, K. X., Gong, Y. M., et al., 1998. The discovery of early Permian reef belt in east Kunlun and its significance. Chinese Science Bulletin, 1998, 43(11), 947～950.

Wang, Z. H., 1978. Permian-Early Triassic conodonts from Hanzhong, Shanxi, China. Acta Palaeontologica Sinica 17 (2), 213-227.

Wang, Z. H., Dai, J. Y., 1981. Triassic conodonts fron Jiangyou and Beichuan, Sichuan, China. Acta Palaontologica Sinica 20 (2), 138-150.

Weidlich, O., Fagerstrom, J.A., 1998. Evolution of Upper Capitan-massive (Permian), Guadalupe Mountains, New Mexico. Brigham Young University Geology Studies, 43, 167-179.

Weidlich, O., Senowbari-Daryan, B., 1996. Late Permian “sphinctozoans” from reefal blocks of the Ba’id area, Oman Mountains. J. Paleont., 70(1), 27-46.

Weidlich, O., Kiessling, W., Flugel, E., 2003. Permian-Triassic boundary interval as a model for forcing marine ecosystem collapse by long-term atmospheric oxygen drop. Geology 31(11), 961-964.

Wendt, J., Wu Xichun, Reinhardt, J.W., 1989. Deep-water hexactinellid sponge mounds from the Upper Triassic of northern Sichuan (China). Palaeogeogr., Palaeoclimat., Palaeoecol. 76, 17-29.

Wignall, P. B., Hallam, A., 1996. Facies change and the end-Permian mass extinction in S.E. Sichuan, China. Palaios 11, 587-596.

Wolff, H., 1973. Fazies-Gliederung und Palaogeographie des Ladins in den bayerischen Kalkaipen zwischen Wendelstein und Kampenwand. N. Jb. Geol. Palaont. Abh. 143(2), 246-274.

Wood, R., 1999. Reef evolution. Oxford University Press.

Wood, R., 1995. The changing biology of reef-building. Palaios 10, 517-529.

Wood, R., Dickson, J. D., Kirkland-George, B., 1996. New observations on the ecology of the Permian Capitan reef, Texas and New Mexico. Palaeontology, 39, 733-762.

Wu, X. C., 1990. Late Triassic lychniscosa fauna in northwestern Sichuan. Acta Palaeontologica Sinica 29(3), 349-363.

Wu, Y. S., 1991. Organisms and communities of Permian reef of Xiangbo, China; calcisponges, hydrozoans, bryozoans, algae, microproblematica. International Academic Publishers. 192pp.

Wu, Y. S., 1994a. Paleoecology of Permian reefs in Guizhou and Guangxi. Oil & Gas Geology 15(3), 201-207.

Wu, Y. S., 1994b. Community facies of reefs. Acta Petrologica Sinica 10(2), 218-222.

Wu, Y. S., 1995. Paleoecologic study of reefs. Bulletin of Institute of Geology, Academia Sinica 8, 248-262.

Wu, Y. S., 1998. Development model of the Middle Permian reef in Lengwu, Tonglu, Zhejiang Province, China. Marine Petroleum Geology, 3(2), 11-15.

Wu, Y. S., Jin, Y. G., and Fan, J. S., 2000. End-Permian regression: evidence from Permian reefs. 31st International Congress, Rio de Janeiro, Brazil, Abstract Volume, CD-ROM, Session 1-9.

Wu, Y. S., Fan, J. S., 2004. Revisions on some Permian-Triassic thalamid sponges (Sphinctozoans). Acta Palaeontologica Sinica, 43(4), 602-608.

Wu, Y. S., Fan, J. S., Jin, Y. G., 2003. Emergence of reefs at the end of the Late Permian and its significance. Acta Geologica Sinica, 77(3), 289-296.

Xu, D. Y., Ma, S. L., Chai, Z. F., Mao, X. Y., Sun, Y. Y., Zhang, Q. W., Yang, Z. Z.g, 1985. Abundance variation of iridium and trace elements at the Permian/Triassic boundary at Shangsi in China. Nature 314, 154-156.

Xu, D. Y., Yan, Z.,1993. Carbon isotope and iridium event markers near the Permian/ Triassic boundary in the Meishan section, Zhejiang Province, China. In: Geldsetzer, H. H. J and Nowlan, G. S. (Eds.), Event markers in Earth history. Palaeogeography, Palaeoclimatology, Palaeoecology 104, 171-175.

Xu, G. R., Luo, X. M., Wang, Y. B., Zhou, L. Y., Xiao, S. Y., 1997. On a building model of Late Permian reefs in central Yangtze River area. China University of Geosciences Press.

Yang, S. R., Hao, W. C., Wang, X. P., 1999. Conodont evolutionary lineages, zonation and P-T boundary at P-T boundary beds in Guangxi, China. In Biotic and geological development of the Paleo-Tethys in China, Beijing, 81-95.

Yang, S. R., Wang, X. P., Hao, W. C., 1993. Permian conodonts from the *Hypophiceras* bed in Zhenjiang, Jiangsu Province, China. Chinese Science Bulletin 38 (16), 1493-1497.

Yang, W. R., 1987. Bioherm of Wujiaping formation in Laibin, Guangxi. Oil and Gas Geology 8(4), 424-428.

Yang, Z. Y., Sheng, J. Z., Yin, H. F., 1995. The Permian-Triassic boundary,the global stratotype section and point (GSSP). Episodes 18 (1-2), 49-53.

Yang, Z. Y., Wu, S. B., Yin, H. F., Xu, G. R., Zhang, K. X., 1991. Geological Events of Permo-Triassic transitional period in South China. Geological Publishing Houses. 190pp.

Yang, Z. Y., Yin, H. F., Wu, S. B., Yang, F. Q., Ding, M. H., Xu, G. R., 1987. Permian–Triassic boundary stratigraphy and fauna of South China. Geological Special Report of China Ministry of Geology and Mineral Resources, Series 2, No.6, 70-76. Geological Publishing House, Beijing.

Yao, J. X., Li, Z. S., 1987. Permo-Triassic conodonts and the Permian-Triassic boundary of Selong, Nielamu County, Tibet, China. Chinese Science Bulletin 32 (1), 45-51.

Yin, H. F., 1985. Bivalves near Permian-Triassic boundary in south China. J. Paleont., 59(3), 575-600.

Yin, H. F., Dickins, J. M., Shi, G. R., and Tong, J., (eds.), 2000. Permian-Triassic Evolution of Tethys and western Circum-Pacific. Amsterdam, Elsevier.

Yin, H. F., Sweet, W. C., Glenister, B. F., Kotlyar, G., Kozur, H., Newell, N. D., Sheng, J., Yang Z., Zakharov, Y. D., 1996. Recommendation of the Meishan section as Global Stratotype Section and Point for basal boundary of Triassic System. Newsletters on Stratigraphy 34 (2), 81-108.

Yin, H. F., Tong, J. N., 1998. Multidisciplinary high-resolution correlation of the Permian-Triassic boundary.

Palaeogeography, Palaeoclimatology, Palaeoecology 143, 199-212.

Yin, H. F., Zhang, K. X., Tong, J. N., Yang, Z. Y., Wu, S. B., 2001. The Global Stratotype Section and Point (GSSP) of the Permian-Triassic Boundary. Episodes 24 (2), 102-114.

Zhang, J. H., Dai, J. Y., Tian, S. G., 1984. Late Permian-Early Triassic conodont biostratigraphy of Shangsi, Guangyuan, Sichuan, China. In Papers for the 27th International Geological Congress, 163-176.

Zhang, K. X., 1987. The conodont fauna of the Permian-Triassic transition in Changxing, Zhejiang Province, China and its stratigraphy. Earth Science-Journal of Wuhan College Geology 12 (2), 193-199.

Zhang, K. X., Ding, M. H., Lai, X. L., Liu, J. H., 1996. Conodont sequence of the Permian–Triassic boundary strata at Meishan section, South China. In The Palaeozoic–Mesozoic Boundary Candidates of Global Stratotype Section and Point of the Permian–Triassic Boundary, Yin, H., ed., China University of Geosciences Press, Wuhan, 57-64.

Zhang, K. X., Lai, X. L., Ding, M. H., Wu, S. B., Liu, J. H., 1995. Conodont sequence and its global correlation of Permian–Triassic boundary in the Meishan section, Changxing, Zhejiang Province (in Chinese with English abstract). Earth Science-Journal of China University of Geosciences 20 (6), 669-676.

Zhang, W., 1983. Study on the sphinctozoans of Upper Permian Changxing Formation from Lichuan area, west Hubei, China. In: A collection of theses for master's degree 1983. Inst. Geol. Acad. Sinica.

Zhao, J. K., Sheng, J. Z., Yao, Z. Q., Liang, X. L., Chen, C. Z., Rui, L., Liao, Z. T., 1981. The Changhsingian and Permian-Triassic boundary of south China. Bulletin of the Nanjing Institute of Geology and Paleontology, Academia Sinica. 2, 1-112.

Zhu, T. X., Huang, Z. Y., Hui, L., 1999. The geology of Late Permian Period biohermal facies in upper Yangtze Tableland. Geological Publishing House.

Introduction to the author

Wu, Ya Sheng at Texas A & M University in 2003, as a visiting scholar to outstanding geochemical geologist Professor Ethan Grossman

Ya-Sheng Wu graduated from Nanjing University in 1984, and received his Master of Science degree and PhD degree from the Graduate School, Chinese Academy of Science.

His thesis during Nanjing University deals with the paleoecology of fusulinids using the method of microfacies analysis, and the ecostratigraphy of Middle Permian Maokouian Stage.

Based on his observation on distribution pattern of different deposits in modern coral reefs in South China Sea, as well as his survey on some Permian and Devonian reefs in southwestern China, he proposed that a reef can be divided as different fabric-facies. Fabric facies have larger scale that microfacies, but smaller scale than traditional sedimentary facies such as reef-front, reef-core. As a complement to the classical classification of reef rocks by Embry et al., he proposed an intermediate type of reef-rock between bafflestone and non-reef rock, prebafflestone.

During 1985 to 1989, he made a systematic study on the organisms and communities in a typical Middle Permian reef in Longlin, Guangxi Province, southwestern China, described 121 species of sclerosponges, inozoans, sphinctozoans, hydrozoans, bryozoans, algae, and microproblematica, established 44 new genera and 68 new species and 20 new families, and recognized 6 types of guilds and 11 types of communities. These results were published as monograph in English in 1991.

According to his study on the distribution pattern of diagenetic products in reefs, he proposed (1993) the concept of diagenetic facies of reefs. Division of diagenetic facies in reefs is a useful tool in reservoir characterization in petroleum geology.

After making a detailed study on a Late Triassic reef in Sichuan Province, he proposed (1994) that a reef can be divided as various community facies, which means the distribution of reef rock with a special community.

During 1994-1995, he established an artificial intelligent identification system of thalamid sponges. With application of computer in analysis, he studied the evolutionary trends of major morphological characters in thalamid sponges and their taxonomic implications.

Previous researchers believed that the Middle Permian reef in Lengwu, Zhejiang Province, southeastern China is a deep-water lime-mud mound. His study (1998) shows that it is a baffled reef mainly constructed by calcisponges (including inozoans and thalamid sponges) and sclerosponges. The top of this reef is composed of overturned calcisponge skeletons, which was covered by tidal-flat stromatolite. So, this is a shallow-water fringe reef. He defined the rock consisting of overturned reef builders as bioliestone.

To determine amplitudes of pre-Cenozoic global sea-level changes is a difficult problem to geologists. In a

recently finished project from National Natural Foundation of China (NNFC), he established some new methods quantitatively calculate amplitudes of pre-Cenozoic eustatic sea-level changes.

In recent years, his studies focus on associated biotic and environmental changes during the Permian-Triassic transition, especially those in reef-bearing PTB sections. One of his ongoing project from NNFC focuses on biotic evolution and environmental changes during P-T transition in reef district.

One of his main recent results is finding of evidence for sea-level drop during P-T transition. His studies also involve oceanic anoxia, procedure of mass extinctions, and geochemistry of ancient oceans.

Selected publications

Wu, Y. S., Fan, J. S., 2004. Revisions on some Permian-Triassic thalamid sponges (Sphinctozoans). Acta Palaeontologica Sinica, 43(4), 602-608.

Wu, Y. S., Fan, J. S., Jin, Y. G., 2003. Emergence of reefs at the end of the Late Permian and its significance. Acta Geologica Sinica, 77(3), 289-296.

Wu, Y. S., Fan, J. S., 2003. Quantitative evaluation of the sea-level drop at the end-Permian: based on reefs. Acta Geologica Sinica, 77(1): 95-102.

Wu, Y. S., Fan, J. S., 2002. Calculating eustatic amplitude of Middle Permian from reefs. Science in China, Series D, 45(3): 221-232.

Wu, Y. S., Fan, J. S., 2000. Paleoecology of calcisponges. Acta Palaeontologica Sinica, 39(4), 544-547.

Wu, Y. S., Jin, Y. G., and Fan, J. S., 2000. End-Permian regression: evidence from Permian reefs. 31st International Congress, Rio de Janeiro, Brazil, 2000, Abstract Volume, CD-ROM, Session 1-9.

Wu, Y. S., 1998. Development model of the Middle Permian reef in Lengwu, Tonglu, Zhejiang Province, China. Marine Petroleum Geology, 3(2), 11-15.

Wu, Y. S., 1997. Classification of reef rocks. Geological Review, 43(3), 281-289.

Wu, Y. S., Yang, W. Q., 1996. Evolution of thalamid sponges. Acta Palaeontologica Sinica, 35(4), 500-508.

Wu, Y. S., 1995. Paleontology and paleoecology of reefs. Collection of Institute of Geology, Chinese Academy of Science, 8, 248-262.

Wu, Y. S., 1995. Classification of thalamid sponges. Acta Palaeontologica Sinica, 34(3), 381-392.

Wu, Y. S., 1994. Paleoecology of the Permian reefs in Guizhou and Guangxi Province. Oil and Gas Geology, 15/3, 201-207.

Wu, Y. S., 1994. Community-facies of reefs. Acta Petrologica Sinica, 10/2, 218-222.

Wu, Y. S., 1993. Models of China reefs. Carboniferous to Jurassic--Pangea: Program and Abstracts. GSGP & CSPG.

Wu, Y. S., 1993. Diagenetic facies of reefs. Scientia Geologica Sinica, 2(3): 349-355.

Wu, Y. S., et al., 1992. Fusulinid ecostratigraphy of the Maokouian Stage in Tongling, Anhui Province, China. Journal of Nanjing University (Earth Science Series), 4(1), 75-81.

Wu, Y. S., 1992. Fabric-facies and fabric-rock-types of reefs. Science in China (Series B), 35/12: 1503-1511.

Wu, Y. S., 1992. About reef studies in China. Oil and Gas Geology, 13(4).

Wu, Y. S., Fan, J. S., 1991. About the classification of reefs. Oil and Gas Geology, 12(3).

Wu, Y. S., 1991. Calcareous algae in the Middle Permian reefs in Longlin, Guangxi Province, China. Acta Palaeontologica Sinica, 30(6).

Wu, Y. S., 1991. Organisms and communities of the Permian reef of Xiangbo, China.-calcisponges, hydrozoans, algae, microproblematica. International Academic Publisher. 192p.